CONCENTRATIONS OF COMBUSTION DERIVED CONTAMINANTS IN REMOTE LAKES: RECENT TRENDS AND IMPLICATIONS FOR SITE ASSESSMENT

By

ANDREW ALLAN BENSON, B.Sc. Hon

A Thesis

Submitted to the School of Graduate Studies

In Partial Fulfillment of the Requirements

For the degree

Master of Science

McMaster University

MASTER OF SCIENCE (2009) **McMaster University**

(Geochemistry) **Hamilton, Ontario**

TITLE: **Concentrations of combustion derived contaminants in remote lakes: Recent trends and implications for site assessment**

AUTHOR: **Andrew Allan Benson, B.Sc. (McMaster University)**

SUPERVISOR: Dr. Gregory F. Slater

NUMBER OF PAGES: 87

ABSTRACT

Environmental quality and emissions guidelines are implemented due to their expected benefit for human and environmental health. However, implementation of such legislation requires knowledge of the behaviour and fate of the contaminants to be controlled. This thesis contributed to the overall understanding of atmospheric PAH deposition to remote lakes and the role atmospherically deposited contaminants play in site assessments which account for environmental pollution due to industry. In chapter 2, atmospheric PAH deposition derived from regional energy generation or industrial sources was found to be decreasing in recent sediments from Siskiwit Lake, Michigan, U.S.A. Considering that Siskiwit Lake is isolated from traffic and development, this supports recent theories which suggest that regional PAH deposition is being overprinting by local traffic sources in sub-urban or urban areas. This study also contributed to the understanding of perylene production in sediments by conclusively demonstrating increases in sedimentary perylene concentrations over a 20 year period. Moreover, kinetic modeling using 1^{st} and 2^{nd} order rate laws failed to accurately predict the concentration changes observed despite rate constants that were similar. This strongly suggested that perylene does not follow a simple concentration dependant kinetic reaction and is more likely controlled by complex kinetics perhaps involving biology. In chapter 3, the superiority of contaminant profiles in sediment cores over current dredge or grab sampling techniques was demonstrated. This was shown by successfully apportioning the

source of contaminants to a northern lake as atmospheric deposition rather than point source release from the adjacent industrial facility. Contaminant profiles are able to constrain concentration changes with time and thus atmospheric deposition and point source contributions can be recognized. This is essential as chapter 3 also demonstrated that atmospheric deposition has the potential to produce sediment concentrations at or above current federal guidelines using standard dredge sampling techniques. Without the use of contaminant profiles these exceedences may be attributed incorrectly to industry which may face remediation costs or other fines associated with environmental contamination. This has implications for redefining sediment quality guidelines or currently accepted sampling methods. Moreover, remediation efforts for atmospherically deposited contaminants must differ from a point source release. Site remediation would be effective for a single release of contaminants however with a continuous source, as is the case with atmospheric deposition, remediation efforts must be focussed on the atmospheric contaminant emissions which can be a large distance from the site.

ACKNOWLEDGEMENTS

There are so many who have a place in this section that I'm afraid I won't be able to mention them all; but I'm going to try! The first and foremost acknowledgement goes to my academic supervisor Dr. Greg Slater who provided excellent support and feedback at all points through this thesis as well as encouraged me to develop and improve several skills which will be integral to my future career. I would also like to thank the members of my committee Dr. Jim Smith and Dr. Brian McCarry. Thanks also to Jennie Kirby, who taught me pretty much all I know about analytical chemistry and instrumental analysis as well as my peers in the Environmental Organic Geochemistry Laboratory who provided excellent feedback and were also people to whom I could vent to and know they understand all too well. I would also like to thank my co-authors from Environment Canada Dr. Derek Muir, Dr. Chris Marvin and Fan Yang as well as my collaborators from Environ (EC) Canada Consulting Steve Desrocher, Tara Nelson and Matt Johnston. Also thanks to Dr. Bridget Bergquist for both guidance and the use of the instrumentation for mercury analysis as well as Dr. Sanghamitra Ghosh for guidance with the mercury analysis methodology. Finally thanks to Kevin Ferguson for his assistance in running the ICPMS.

My family and friends are very important to me and so I also would like to thank my Mom, Dad and brother for providing an environment very conducive to learning and for supporting my every decision throughout life. My current educational career would not have been possible if not for my family. All the

friends that I've met through undergraduate and graduate school have been an excellent support and a necessary distraction. It feels great to be part of a close group of friends and know that if I really needed to go to the Phoenix for a beer (or 5) there were always people willing to come along. I'd like to mention a few people specifically who have been with me through the whole thing, Duncan your talent for music and general running commentary is always entertaining, Lisa your ability to make Kingston blush is astounding (an elbow what??), Kingston frog legs are gross but the random nights following are hilarious, Holly, you're one of the most genuine people I know-don't ever lose that, Liane you're intelligent and caring two characteristics I regard highly, thanks for your patience and Gloria- thanks for introducing me to Greg sometimes these things result in a Masters.

Table of Contents

List of Figures

List of tables

Preface

This thesis is the culmination of research carried out by the author under the supervision of Dr. Greg Slater and in partial fulfillment of the requirements for the degree Master of Science (M.Sc.). All laboratory preparation, instrumental analysis, literature review and manuscript preparation was carried out solely by the author with the exception of ^{210}Pb analysis which was performed by Fan Yang at the National Water Research Institute (NWRI) for chapter 2 and by Dr. Bassam Ghaleb at the University of Quebec at Montreal for chapter 3. It should be noted however that the subsequent sedimentation rate and date calculations based on ^{210}Pb analysis for chapter 3 were performed by the author.

Samples from Siskiwit Lake for chapter 2 of this thesis were retrieved by Dr. Greg Slater in conjunction with Environment Canada however were prepared for analysis by the author. Samples from the Thunder Bay District for chapter 3 of this thesis were collected by the author with the assistance of Tara Nelson at Environ (EC) Canada Consulting.

Chapter 1 of this thesis is a literature review summarizing the relevant research regarding combustion derived PAH in the environment. Chapter 2 is the assessment of recent PAH deposition and perylene production in Siskiwit Lake, Michigan, U.S.A. and was prepared for submission to a peer-reviewed scientific journal. Chapter 3 demonstrates the efficacy of sediment core contaminant profiling for site assessments in the consulting industry and was also prepared for submission to a peer-reviewed scientific journal. Chapter 4 is a summary of the

major findings and conclusions from the research and subsequent manuscript preparation carried out by the author.

CHAPTER 1

Literature Review:

Polycyclic aromatic hydrocarbons (PAH) in the Environment

1. Introduction

The combustion of organic material is necessary for numerous anthropogenic processes including power generation, transportation and manufacturing. Impurities in fuels and incomplete combustion introduce many contaminants into the environment including polycyclic aromatic hydrocarbons (PAH), lead (Pb) and mercury (Hg). Several PAH, such as benzo(a)pyrene and dibenz(a,h)anthracene, are known carcinogens and the neurological and toxic effects of Pb and Hg are well documented [1-4]. Typically PAH are associated with particulate matter in the atmosphere which is closely linked to air quality [5, 6]. Several studies have found that inhalation of PAH bearing particulate can increase the probability of lung cancer or the development of respiratory conditions [7-9].

Long-range atmospheric transport and point source industrial releases of these contaminants to isolated areas can have negative effects on the biodiversity or reproductive health of sensitive ecosystems [10-13]. The ability to differentiate between these potential sources is essential when delineating the effects of industrial activity on local environments. This is even more pertinent when planning potential remediation strategies as remediation will not be

effective if the source of contaminants cannot be mitigated. In the case of atmospheric deposition it is not likely that any one industry is responsible for the contamination thus the focus of remediation efforts should be directed towards emission reductions rather than remediation of impacted sites.

2. PAH properties and Terminology

Parent PAH are large planar molecules consisting of 2 or more fused benzene rings (figure 1-1). Alkylated PAH have substitutent groups such as methyl- or ethyl- groups attached to these rings. Generally the solubility and vapour pressure of PAH decreases with increasing molecular weight. Thus naphthalene, the smallest PAH consisting of two benzene rings, is slightly soluble in water while larger PAH consisting of five or six benzene rings are virtually insoluble in water [14]. Similarly, vapour pressure increases with decreasing molecular weight, thus small PAH are generally more volatile than large PAH.

There are a large number of PAH; however the following two studies will focus primarily on the 16 PAH which are included on the Environmental Protection Agency (EPA) priority pollutant list as well as in the Canadian Environmental Protection Act (CEPA) [15, 16]; with the notable addition of perylene which is of interest as it is thought to be produced by natural processes. The PAH to be discussed in this thesis, along with the abbreviations used for each, are listed below: Naphthalene= Napth, acenapthene=Ace, acenapthylene= acey, fluorene=flo, phenanthrene=phen, anthracene=anth, fluoranthene=flua, pyrene=py, benzo(a)anthracene=B(a)A, benzo(b)fluoranthene=B(b)F,

benzo(k)fluoranthene=B(k)F, benzo(a)pyrene=B(a)P, perylene=pery, benzo(g,h,i)perylene=B(ghi)P, dibenz(a,h)anthracene=D(ah)A and ideno(1,2,3-cd)pyrene=ideno.

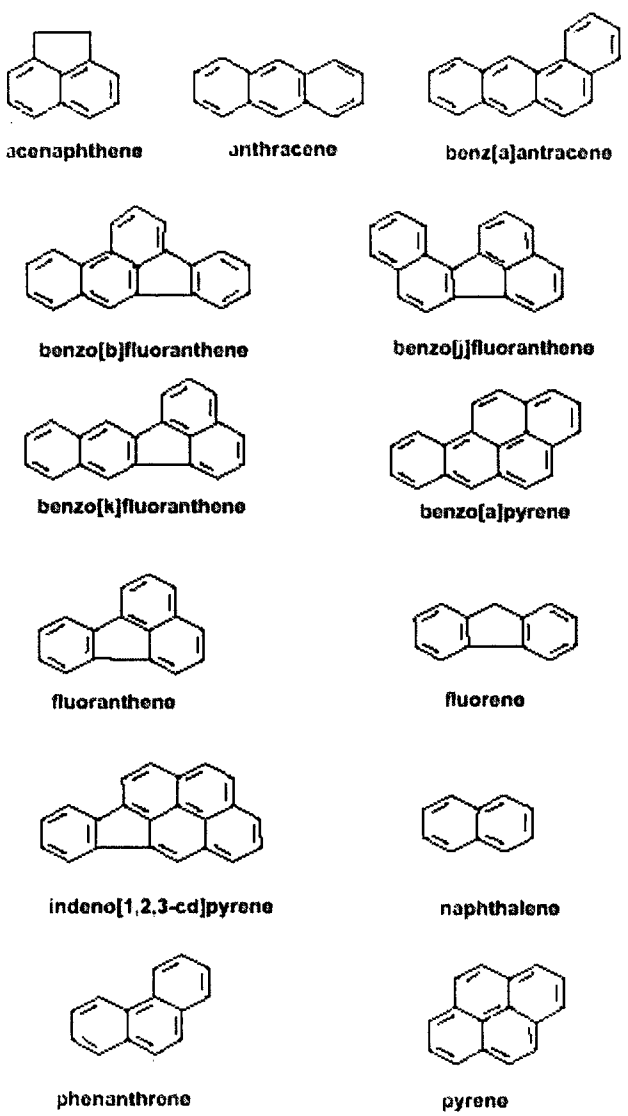

Figure 1-1: Structures of select PAH.
(Lima et al, 2003)

3. PAH formation

PAH in the environment can be grouped into 3 broad categories that have both natural and anthropogenic sources. The vast majority of PAH are pyrogenic and released into the environment via both anthropogenic (e.g. coal combustion) and natural processes (e.g. forest fires). Petrogenic PAH are found naturally in unburned thermogenic petroleum products such as coal and crude oil and can be released in anthropogenic spills as well as natural petroleum seeps. The third category consists of compounds suspected to be produced in abiotic diagenetic reactions or biologically mediated processes. The processes and reactions associated with this third category are generally not well constrained [17, 18]. The general focus of this thesis is towards pyrogenic PAH as well as a PAH produced in digenetic or biological reactions.

3.1 PAH Formation in Combustion Reactions

The relative proportion of PAH produced during combustion is affected primarily by 3 factors: type of fuel, amount of oxygen and temperature of combustion [19-22]. However, the wide variations in these factors make it very difficult to predict the relative proportions of PAH that will be in combustion emissions. Nonetheless, much effort has been devoted to the study of PAH formation in combustion reactions as this is the primary source of PAH in the environment (e.g. [22, 23]). Richter and Howard [22] described the potential formation of the first aromatic ring via multiple reactions of free radicals

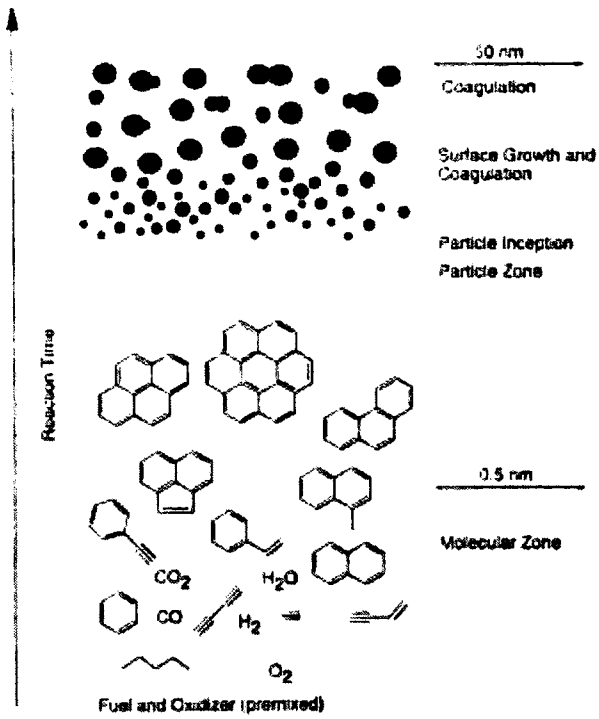

Figure 1-2: A reaction pathway for the formation of PAH and associated soot particles. From: Richter and Hower, 2000

and subsequent reactions of this ring with small hydrocarbon molecules such as acetylene as well as other free radicals to produce multi-aromatic structures (figure 1-2). Large PAH molecules can be the precursor for soot particles and in general an inverse relationship is seen where PAH concentrations in flames decrease with increasing soot production [22, 24]. PAH production can also be affected by the re-combustion of aromatic compounds to CO or CO_2 and water; a process termed pyrolytic oxidation [22]. The exact reaction pathway of this process is dependant on combustion conditions but is almost exclusively performed by either OH radicals or O_2 [22]. This PAH production pathway affects

the PAH assemblages produced by combustion as generally large PAH molecules are associated with soot production or are destroyed because they are easier to fragment and oxidize [21, 22]. Thus, PAH emissions chiefly consist of smaller and more stable 3,4 and 5 ring PAH molecules which are more likely to survive the combustion process [22]. The following is a more detailed discussion about reaction conditions and their effect on PAH formation.

3.1.1 Type of fuel

Under similar reaction conditions it was found that aromatic fuels produce significantly more PAH than aliphatic fuels [22]. This was supported by several studies which found correlations between the amounts of PAH in fuel and the amount of PAH emitted by the combustion of that fuel [25-27]. However, the relative proportion of different PAH in the fuels is not preserved suggesting that a significant fraction of the PAH originally present in the fuel are broken down and reformed into other PAH molecules and thus PAH in emissions are not necessarily representative of the type of fuel combusted [25, 26]. For instance, Schauer et al [28] combusted fuel with high amounts of the 5 ringed PAH perylene however the resulting emissions contained virtually none of this compound.

Mobile PAH emission sources such as vehicular traffic have also been implicated as a significant PAH source [29, 30]. PAH emissions specifically from automobiles are a mixture derived from PAH in the fuel and crankcase oil which are primarily fragmented and recombined as well as PAH formed during

combustion via the free-radical reaction pathway and those retained in the exhaust system on soot or other carbon deposits [22, 27, 31]. Ignition conditions such as spark plug ignition or glow plug ignition, vehicle age, temperature of start as well as the presence of a catalytic converter will also effect PAH concentrations and assemblages in automobile emissions [22, 25, 32]. Several studies have found that heavy diesel engines produce more PAH than conventional gasoline engines [27, 32] and older vehicles without catalytic converters produce significantly more PAH than newer vehicles with the now mandatory catalytic converters [25, 27, 33].

Combustion of fuels for heating can also produce significant amounts of PAH. Incomplete combustion is common in residential woods stoves due to the low oxygen environment and low temperature of combustion [34]. Harkov and Greenberg [35] suggest that 98% of benzo(a)pyrene found in the New Jersey atmosphere in the winter months is derived from wood combustion. Wood combustion can produce 6 times more benzo(a)pyrene per BTU than coal combustion, 400 times more than gasoline combustion and 9,000 times more than residential oil furnace combustion [35]. Furthermore, Jenkins et al [19] found that PAH emissions from biomass combustion can vary by up to two orders of magnitude. Similarly, combustion conditions ranging from biomass moisture content to the configuration of wood stacking can produce varying amounts of PAH emissions [19].

3.1.2 Excess air

Often in combustion processes limited oxygen is the main cause of incomplete combustion. The amount of oxygen in combustion processes is described using air to fuel ratios (A/F). Lean conditions (high A/F ratio) supplies the reaction with more excess air, while rich conditions (low A/F ratio) decreases the amount of excess air. Several studies show that small changes in A/F can cause large changes in PAH and/or soot emissions. Prado and Lahaye [24] demonstrated that decreasing excess air in residential oil burners increased PAH emissions up to 100 fold. While Mastral et al [36] demonstrated that PAH production decreased when excess air was increased from 5% to 20% during fluidized bed coal combustion; however, when excess air was increased again to 40% PAH production increased presumably due to fuel dilution [36]. A similar trend was observed for internal combustion engines, PAH emissions decrease with increasing excess air until the fuel is too dilute to efficiently burn at which point PAH emissions increase again [25].

3.1.3 Temperature of reaction

Temperature of reaction primarily affects the amount of PAH produced as well as the ratio of alkylated to parent PAH homologues. Colmsjo et al [37] showed that PAH concentrations increased 1000 fold at a municipal incinerator during a cold start. Mastral et al [36] showed that varying temperatures during coal combustion affected PAH emissions by up to two orders of magnitude. Typically, low temperature reactions produce more alkylated PAH homologues

while higher temperatures produces parent PAH [17]. This has been demonstrated in diesel engines where lower exhaust temperatures increased the amount of alkylated PAH relative to parent PAH [38]. This is also the reason for the high relative abundance of alkylated PAH found in petrogenic sources such as crude oil as these products tend to mature at relatively low temperatures [34]. Thus a general trend is seen where decreasing alkylated/parent PAH ratios correspond with increasing temperature [18].

3.2 Diagenetic or biologically produced PAH

Perylene is a 5 ring PAH whose presence in the environment is somewhat enigmatic. Perylene is structurally unstable at high temperatures [39] and thus has been found only in small quantities in emissions [40]. However, natural abundance radiocarbon analysis has shown that perylene in some sediments is derived from predominantly ancient sources and is thus likely to be derived from combustion of fossil fuels [41]. While in other areas perylene is shown to have considerable contributions from modern sources [42]. Profiles of perylene in sediment cores have shown disproportionately high concentrations of perylene with respect to pyrogenic PAH; and typically concentrations are low in surface sediments and increase with depth in a sediment core [39, 43, 44]. This prompted the hypothesis that perylene is produced in-situ under anoxic conditions [44]. However, the specific reaction mechanism and precursor compound remain unknown [39, 43]. Considerable effort has gone into finding the precursor and its source [39], and several compounds from both aquatic sources and terrestrial

sources have been suggested [44-46]. Some speculate that perylene does not have a specific precursor but production is controlled by the rate of microbial activity as well the amount of oxygen in the sediments [47]. It is hypothesized that in oxic situations perylene producing microbes are unable to compete for the organic carbon pool and thus perylene production begins below the sediment-water interface when anoxia sets in [47]. Some effort has been directed toward estimating the rate of production. Gschwend et al [44] estimated rate constants and precursor concentrations by curve fitting the sedimentary profile to 1st and 2nd order kinetic models. While these curves fit very well, the variability of perylene concentrations in sediments indicates that rates are likely location specific.

4. PAH in the natural environment

4.1 Transport and Deposition

Figure 1-3 summarizes the emission, transport and deposition of pyrogenic PAH in the environment. Pyrogenic PAH are emitted to the atmosphere as a gas or adsorbed to particulate [48]. Less volatile 5 and 6 ringed PAH typically partition to the particulate phase while the more volatile 3 and 4 ringed PAH remain in the gas phase [48]. Ambient temperature and particulate concentrations are also a factor, with higher temperatures and less particulate resulting in more PAH in the gas phase and vice-versa [48-50]. Particulate bound PAH in the atmosphere are transported as a function of the size of particulate [51, 52]. Windsor and Hites [51] calculated that PAH associated with the particulate fraction <10um in size could potentially be transported 1300 km while

larger particulate is typically deposited on a local scale. Atmospheric scavenging of PAH is more efficient with decreasing volatility of compounds [53] and can occur via two pathways. Wet deposition typically consists of gaseous or fine particulate bound PAH partitioning into water droplets or ice crystals and being washed out of the atmosphere via precipitation [53]. Larger particulate are more resistant to this and tend to directly fallout of the atmosphere via dry deposition as a function of environmental conditions such as wind speed and humidity [54]. Dry deposition is the more important PAH removal mechanism with ratios of dry to wet deposition as high as 9:1 [55].

4.2 Degradation

PAH in the atmosphere can be oxidized by ambient compounds such as ozone, nitrogen oxides and sulphur oxides [56]. Exposure to sunlight will also degrade PAH, and is perhaps an even more important factor than the presence of oxidizers [57]. These processes change the relative proportions of PAH in the atmosphere after emission, thus making it extremely difficult to correlate PAH assemblages in the environment to PAH emission assemblages [57]. PAH from all environmental compartments eventually end up in sediments and soils (see figure 3). At this point, chemical oxidation and/or exposure to sunlight play a very minor role and biodegradation becomes the primary pathway for PAH

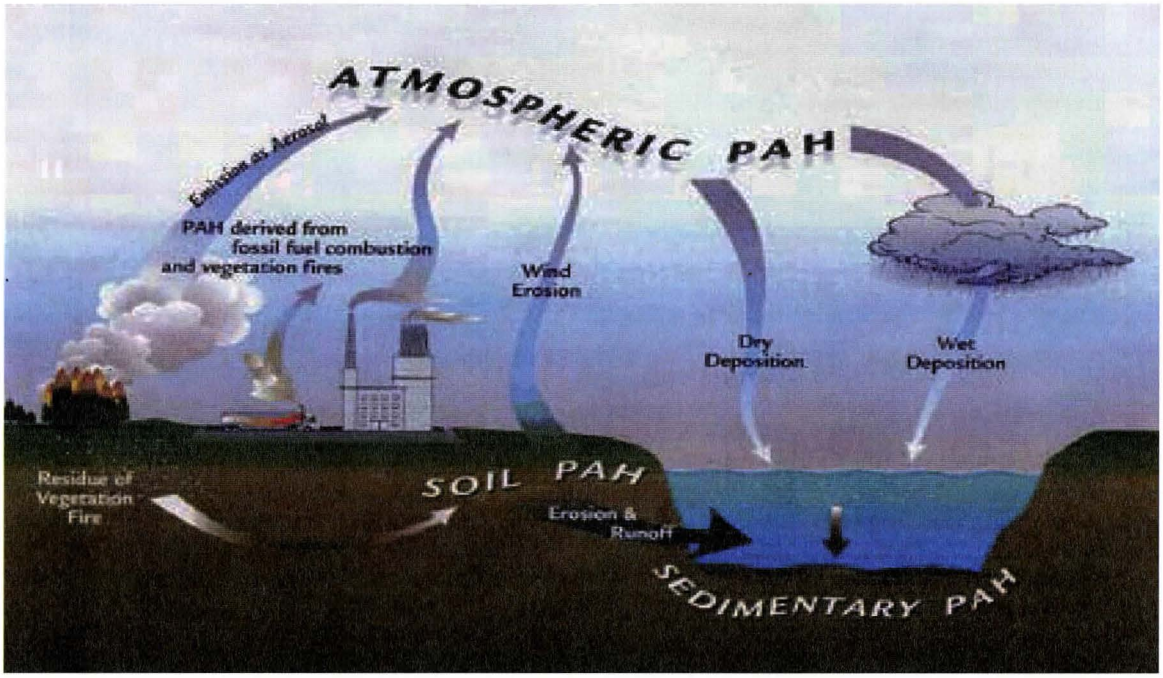

Figure 1-3: A diagram describing the sources, transport and deposition of atmospheric PAH [81]

degradation [58]. Studies have primarily focused their efforts on aerobic biodegradation and it is generally accepted that smaller PAH degrade faster than larger PAH and that parent PAH degrade faster than alkylated PAH [58, 59]. Furthermore, Jones et al [60] noted that PAH species bound to organic particulate are less available for biodegradation thus some types of PAH are preferentially degraded over others. For instance, PAH derived from combustion are typically associated with highly organic particulate such as ash or black carbon and exhibit far less degradation in aquatic environments than PAH associated with silt or clay particles [61]. It has also been noted that microbes with previous exposure to PAH tend to degrade them faster suggesting some adaptability of the microbes involved [62, 63]

In anoxic sedimentary environments, PAH are more persistent however are still susceptible to degradation particularly in denitrifying and sulphate reducing conditions [62]. Similar to aerobic degradation, smaller molecules are the first to be degraded, however a further trend was also noticed where the more soluble PAH were degraded preferentially as well [62]. For instance phenanthrene was degraded before anthracene despite being the same molecular weight [62].

4.3 Post depositional diffusion of PAH in sediments

Due to their large hydrophobic nature, PAH movement in cores is limited in comparison to other more soluble contaminants. Nonetheless, studies have shown Napth and Phen can be subject to some vertical diffusion in sediment cores [64]. This is related primarily to the organic carbon content of the sediment as well as, and perhaps more importantly, the concentrations of organic colloids in porewaters which have been shown to increase the solubility of organic compounds such as PAH [64, 65]. Larger PAH are more hydrophobic and tend to stay sorbed to organic carbon in the sediment thus requiring a process such as bioturbation to be transported any meaningful distance [64]. White [64] suggested that only napth would be susceptible to diffusion out of the sediment column into the overlying water. Moreover, it was suggested the magnitude of this effect would vary in different environments (e.g. salt marsh sediments versus lacustrine sediments) [64, 66]. Vertical movement of PAH was assumed to be negligible in this thesis as it is expected that the slow diffusion of 1 or 2 PAH out of the 16

analyzed will not play a significant role in the overall shape of the total PAH profiles.

4.4 Source apportionment

Muller et al [67] used sediment core profiling to constrain the sources of several heavy metals as well as PAH in the mid-1970s and produced a curve that demonstrated increasing PAH deposition until circa 1960 after which PAH deposition began to decrease. They hypothesized that this curve described atmospheric deposition and that coal consumption, which decreased simultaneously to PAH deposition, may be linked to the contamination [67]. Lee et al [68] further supported these findings after determining that the combustion of different materials under identical conditions produced varying amounts of alkylated and parent PAH. The subsequent comparison of these lab experiments to the environmental PAH from Indianapolis and Boston revealed that coal combustion was the most likely source of PAH contamination in Indianapolis while wood or kerosene combustion was more likely for Boston. Attempts to characterize global PAH distributions using soil and sediment cores found that concentrations varied widely between sites with maximum concentrations occuring in urban areas [17]. PAH profiling in sediment cores has since been extensively used and has produced similar curves globally (e.g. [10, 11, 29, 30, 55, 69, 70]). It was assumed that decreasing coal consumption and the advancement of combustion technology would lead to a continued decrease of PAH in sediment cores after peak deposition circa 1960 [18, 67]. Several

studies, however, have since found that PAH deposition through the 1990s began increasing at many urban and sub-urban sites [29, 30, 70, 71]. This was correlated in many cases to increasing use of passenger vehicles [30] and/or increasing consumption of diesel fuel [29] suggesting that this elevated PAH deposition may be a local phenomenon related to urban sprawl [30].

Attempts to delineate the PAH source or relative proportion of sources have yielded some promising results. As mentioned above, the profiling of sediment cores provided the first rough source apportionment when curves representing atmospheric deposition were recognized [17, 18, 55]. Correlation with coal consumption, then later with transportation emissions provided excellent evidence that PAH are atmospherically deposited and derived from combustion processes [29, 30, 55]. Furthermore, the use of ratios of alkylated to parent PAH have been able to distinguish between petrogenic and pyrogenic sources as there are proportionally more alkylated PAH in petrogenic sources [17, 72]. More recently, the ratio of methylphenanthrenes to phen has become predominant for the same purpose [73]. Similarly, there has been limited success of using parent PAH ratios such as flua to flua+py, phen to anth and Ideno to Ideno+B(ghi)P to distinguish between fuel type such as gasoline or wood combustion [73]. This is due to their relative abundance of the compounds in the emissions from these sources. However as mentioned earlier PAH assemblages are very difficult to predict since the reaction conditions and transport can significantly change them. Thus, it was noted that these methods generally decrease in efficacy with

increasing distance from urban centers [72-74]. In general, caution is usually suggested when source diagnostic ratios [29].

It was demonstrated that while long-range transport may change the relative proportions of PAH from combustion to deposition, the stable carbon isotope composition of PAH was not affected [75]. The isotopic similarity of wood soot and PAH in Conception Bay, Newfoundland was used to determine that wood burning was the dominant source of PAH [76]. O'Malley et al [76] also used the relative proportions of 4 and 5 ringed PAH and their respective isotopic compositions to determine that 20 to 50% of PAH may be derived from crankcase oil and 50 to 80% from wood burning. In these low temperature reactions source apportionment was relatively successful, however McRae et al [77] later showed that isotopic composition was not necessarily retained in high-temperature processes such as coal gasification thus highlighting the need to consider process when apportioning sources of PAH using stable carbon isotopes. Due to the overall similarity of the isotopic composition of fuels and the subsequent PAH, it is often difficult to distinguish between sources and thus isotopic methods are usually used in conjunction with source diagnostic ratios [29].

Statistical methods such as principal component analysis (PCA) have also been used to determine PAH source [78, 79]. This method is somewhat more advantageous than source ratios as it does not require the emission characterization of all sources [78]. PCA was able to model the relative contributions of PAH sources to the total PAH in suspended sediments at several

sites in Hamilton Harbour [78]. The proportions were consistent with the relative configuration of sources around the Harbour and thus the results are rather persuasive. Other methods such as multiple linear analysis and mass balance models have also been used in the past with some success [55, 80].

5. Research Objectives

The primary objective of the first study (chapter 2) was to investigate the recent trends in pyrogenic PAH deposition to Siskiwit Lake. A profile by McVeety and Hites [55] from the same site in the early 1980s demonstrated the atmospheric deposition curve controlled mainly by energy production and industrialization that has been found at many other sites. This study focuses on recent atmospheric deposition to determine whether the increasing PAH deposition seen at sub-urban and urban sites (e.g. [29, 30]) is also seen at this remote site. The secondary focus of this study was perylene production in Siskiwit Lake sediments. A previous study attempted to model perylene production using the perylene curve found in lake sediments [44]. This study presents a kinetic model for production similar to the previous model by Gschwend et al [44]. However, data from McVeety and Hites [55] is also modeled in this manner in order to evaluate whether the kinetic models can predict any observed increases in perylene production which may have occurred over the 20 year time period between the data sets.

The objective of the second study (chapter 3) was to determine whether PAH, Pb and Hg observed in sediments proximal to an industrial site at a remote

location were the result of the industrial site being a point source, or whether the observed contaminants were related to atmospheric deposition. This study compared sediment core profiles of Pb, Hg, and PAH from two lakes in northern Ontario. One of these lakes had an industrial site on its shoreline, while the other was chosen as a comparison site that had the same general characteristics but no industrial site. A comparison of these sites as well as other sites from the literature was used to investigate whether the observed contaminants were due to atmospheric versus point source. This study further characterized the extent to which atmospheric deposition could result in concentrations exceeding federal sediment quality guidelines and the implications that this could have in contaminated site assessment.

Citations

1. Baird, W. M.; Hooven, L. A.; Mahadevan, B., Carcinogenic polycyclic aromatic hydrocarbon-DNA adducts and mechanism of action. *Environmental and Molecular Mutagenesis* **2005,** *45*, (2-3), 106-114.
2. de Kok, T. M.; Hogervorst, J. G.; Briede, J. J.; van Herwijnen, M. H.; Maas, L. M.; Moonen, E. J.; Driece, H. A.; Kleinjans, J. C., Genotoxicity and physicochemical characteristics of traffic-related ambient particulate matter. *Environmental and Molecular Mutagenesis* **2005,** *46*, (2), 71-80.
3. Banks, E. C.; Ferretti, L. E.; Shucard, D. W., Effects of low level lead exposure on cognitive function in children: a review of behavioral, neuropsychological and biological evidence. *Neurotoxicology* **1997,** *18*, (1), 237-281.
4. Ratcliffe, H. E.; Swanson, G. M.; Fischer, L. J., Human exposure to mercury: A critical assessment of the evidence of adverse health effects. *Journal of Toxicology and Environmental Health* **1996,** *49*, 221-270.
5. Brown, J. R.; Field, R. A.; Goldstone, M. E.; Lester, J. N.; Perry, R., Polycyclic aromatic hydrocarbons in central London air during 1991 and 1992. *Science of the Total Environment* **1996,** *177*, 73-84.
6. Cui, W. X.; Eatough, D. J.; Eatough, N. L., Fine particulate organic material in the Los Angeles basin - I: Assessment of the high-volume Brigham Young University Organic Sampling System, BIG BOSS. *Journal of the Air & Waste Management Association* **1998,** *48*, (11), 1024-1037.
7. Armstrong, B.; Hutchinson, E.; Unwin, J.; Fletcher, T., Lung cancer risk after exposure to polycyclic aromatic hydrocarbons: A review and meta-analysis. *Environmental Health Perspectives* **2004,** *112*, (9), 970-978.
8. Cheng, J. P.; Yuan, T.; Wu, Q.; Zhao, W. C.; Xie, H. Y.; Ma, Y. G.; Ma, J.; Wang, W. H., PM10-bound polycyclic aromatic hydrocarbons (PAHs) and cancer risk estimation in the atmosphere surrounding an industrial area of Shanghai, China. *Water Air and Soil Pollution* **2007,** *183*, (1-4), 437-446.
9. Ma, J. Y. C.; Ma, J. K. H., The dual effect of the particulate and organic components of diesel exhaust particles on the alteration of pulmonary immune/inflammatory responses and metabolic enzymes. *Journal of Environmental Science and Health Part C-Environmental Carcinogenesis & Ecotoxicology Reviews* **2002,** *20*, (2), 117-147.
10. Kawamura, K.; Suzuki, I.; Fuji, Y.; Watanabe, O., Ice core record of polycyclic aromatic hydrocarbons over the past 400 years. *Naturwissenschaften* **1994,** *81*, (11), 502-505.
11. Fernandez, P.; Vilanova, R. M.; Grimalt, J. O., Sediment fluxes of polycyclic aromatic hydrocarbons in European high altitude mountain lakes. *Environmental Science & Technology* **1999,** *33*, (21), 3716-3722.
12. Poissant, L.; Koprivnjak, J. F.; Matthieu, R., Some persistent organic pollutants and heavy metals in the atmosphere over a St Lawrence River valley site (Villeroy) in 1992. *Chemosphere* **1997,** *34*, (3), 567-585.
13. Outridge, P. M.; Hermanson, M. H.; Lockhart, W. L., Regional variations in atmospheric deposition and sources of anthropogenic lead in lake sediments across the Canadian Arctic. *Geochimica Et Cosmochimica Acta* **2002,** *66*, (20), 3521-3531.

14. Solomons, T. W. G.; Fryhle, C. B., *Organic Chemistry*. 9th ed.; Wiley: London, 2007.
15. Agency, E. P. Clean Air Act. (May 26th),
16. Liu, D.; Maguire, R. J.; Pacepavicius, G. J.; Nagy, E., Microbial degradation of PAH and PAH nitrogen heterocyclics. *Environmental Toxicology and Water Quality* **1992,** *7*, (4), 355-372.
17. Laflamme, R. E.; Hites, R. A., Global distribution of PAH in recent sediments. *Geochimica Et Cosmochimica Acta* **1978,** *42*, (3), 289-303.
18. Gschwend, P. M.; Hites, R. A., Fluxes of PAH to marine and lacustrine sediments in the northeastern United States. *Geochimica Et Cosmochimica Acta* **1981,** *45*, (12), 2359-2367.
19. Jenkins, B. M.; Jones, A. D.; Turn, S. Q.; Williams, R. B., Emission factors for polycyclic aromatic hydrocarbons from biomass burning. *Environmental Science & Technology* **1996,** *30*, (8), 2462-2469.
20. Masclet, P.; Bresson, M. A.; Mouvier, G., PAH emitted by power stations and influence of combustion conditions. *Fuel* **1987,** *66*, (4), 556-562.
21. Ramdahl, T.; Bjorseth, A.; Lokensgard, D. M.; Pitts, J. N., Nitration of PAH adsorbed to different carriers in a fluidized bed reactor. *Chemosphere* **1984,** *13*, (4), 527-534.
22. Richter, H.; Howard, J. B., Formation of polycyclic aromatic hydrocarbons and their growth to soot- a review of chemical reaction pathways. *Progress in Energy and Combustion Science* **2000,** *26*, 565-608.
23. Frenklach, M., Production of PAH in chlorine containing environments. *Combustion Science and Technology* **1990,** *74*, (1-6), 283-296.
24. Pineiro-Iglesias, M.; Lopez-Mahia, P.; Vazquez-Blanco, E.; Muniategui-Lorenzo, S.; Prado-Rodriguez, D., Comparison between Soxhlet, ultrasonic and microwave assisted extraction of polycyclic aromatic hydrocarbons from atmospheric particulate matter. *Fresenius Environmental Bulletin* **2000,** *9*, (1-2), 17-22.
25. Pedersen, P. S.; Ingwersen, J.; Nielsen, T.; Larsen, E., Effects of fuel, lubricant and engine operating parameters on the emission of PAH. *Environmental Science & Technology* **1980,** *14*, (1), 71-79.
26. Westerholm, R. N.; Alsberg, T. E.; Frommelin, A. B.; Strandell, M. E.; Rannug, U.; Winquist, L.; Grigoriadis, V.; Egeback, K. E., Effect of fuel PAH content on the emissions of PAH and other mutagenic substances from a gsoline fueled automobile. *Environmental Science & Technology* **1988,** *22*, (8), 925-930.
27. Marr, L. C.; Kirchstetter, T. W.; Harley, R. A.; Miguel, A. H.; Hering, S. V.; Hammond, S. K., Characterization of Polycyclic Aromatic Hydrocarbons in Motor Vehicle Fuels and Exhaust Emissions. *Environmental Science and Technology* **1999,** *33*, (18), 3091-3099.
28. Schauer, J. J.; Kleeman, M. J.; Cass, G. R.; Simoneit, B. R. T., Measurement of emissions from air pollution sources. 5. C-1-C-32 organic compounds from gasoline-powered motor vehicles. *Environmental Science & Technology* **2002,** *36*, (6), 1169-1180.
29. Lima, A. L.; Eglinton, T. I.; Reddy, C. M., High-resolution record of pyrogenic polycyclic aromatic hydrocarbon deposition during the 20th century. *Environmental Science and Technology* **2003,** *37*, 53-61.

30. Van Metre, P. C.; Mahler, B. J.; Furlong, E. T., Urban Sprawl Leaves Its PAH Signature. *Environmental Science and Technology* **2000,** *34*, (19), 4064-4070.
31. Pruell, R. J.; Quinn, J. G., PAH in surface sediments held in experimental mesocosms. *Toxicological and Environmental Chemistry* **1985,** *10*, (3), 183-200.
32. Rogge, W. F.; Hildemann, L. M.; Mazurek, M. A.; Cass, G. R.; Simoneit, B. R. T., Sources of fine organic aerosol. 2. Noncatalyst and catalyst-equipped automobiles and heavy-duty diesel trucks. *Environ. Sci. Technol.* **1993,** *27*, (4), 636-651.
33. Garrigues, P.; Budzinski, H.; Manitz, M. P.; Wise, S. A., Pyrolytic and Petrogenic Inputs in Recent Sediments: A Definitive Signature Through Phenanthrene and Chrysene Compound Distribution. *Polycyclic Aromatic Compounds* **1995,** *7*, (4), 275 - 284.
34. Lima, A. L.; Farrington, J. W.; Reddy, C. M., Combustion-derived Polycyclic Aromatic Hydrocarbons in the environment- a review. *Environmental Forensics* **2005,** *6*, 109-131.
35. Greenberg, A.; Darack, F.; Harkov, R.; Lioy, P.; Daisey, J., PAH in New Jersey- A comparison of winter and summer concentrations over a 2 year period. *Atmospheric Environment* **1985,** *19*, (8), 1325-1339.
36. Mastral, A. M.; Callen, M.; Mayoral, C.; Galban, J., Polycyclic aromatic hydrocarbon emissions from fluidized bed combustion of coal. *Fuel* **1995,** *74*, (12), 1762-1766.
37. Colmsjo, A.; Zebuhr, Y.; Ostman, C., Polynuclear aromatic compounds in flue gases and ambient air in the vicinity of a municipal incineration plant. *Atmospheric Environment* **1986,** *20*, (11), 2279-2282.
38. Jensen, T. E.; Hites, R. A., Aromatic diesel emissions as a function of engine conditions. *Analytical Chemistry* **1983,** *55*, (4), 594-599.
39. Venkatesan, M. I., Occurrence and possible sources of perylene in marine sediments-a review. *Marine Chemistry* **1988,** *25*, (1), 1-27.
40. Davies, I. W.; Harrison, R. M.; Perry, R.; Ratnayaka, D.; Wellings, R. A., Municipal incinerator as a source of PAH in the environment. *Environmental Science & Technology* **1976,** *10*, (5), 451-453.
41. Mandalakis, M.; Gustafsson, O.; Reddy, C. M.; Xu, L., Radiocarbon Apportionment of Fossil versus Biofuel Combustion Sources of Polycyclic Aromatic Hydrocarbons in the Stockholm Metropolitan Area. *Environmental Science and Technology* **2004,** *38*, (20), 5344-5349.
42. Reddy, C. M.; Pearson, A.; Xu, L.; McNichol, A. P.; Benner, B. A.; Wise, S. A.; Klouda, G. A.; Currie, L. A.; Eglinton, T. I., Radiocarbon as a tool to apportion the sources of polycyclic aromatic hydrocarbons and black carbon in environmental samples. *Environmental Science & Technology* **2002,** *36*, (8), 1774-1782.
43. Silliman, J. E.; Meyers, P. A.; Eadie, B. J., Perylene: an indicator of alteration processes or precursor materials? *Organic Geochemistry* **1998,** *29*, (5-7), 1737-1744.
44. Gschwend, P. M.; Chen, P. H.; Hites, R. A., On the formation of perylene in recent sediments- kinetic models. *Geochimica Et Cosmochimica Acta* **1983,** *47*, (12), 2115-2119.

45. Soma, Y.; Tanaka, A.; Soma, M.; Kawai, T., Photosynthetic pigments and perylene in the sediments of southern basin of Lake Baikal. *Organic Geochemistry* **1996,** *24*, (5), 553-561.
46. Silliman, J. E.; Meyers, P. A.; Ostrom, P. H.; Ostrom, N. E.; Eadie, B. J., Insights into the origin of perylene from isotopic analyses of sediments from Saanich Inlet, British Columbia. *Organic Geochemistry* **2000,** *31*, (11), 1133-1142.
47. Silliman, J. E.; Meyers, P. A.; Eadie, B. J.; Klump, J. V., A hypothesis for the origin of perylene based on its low abundance in sediments of Green Bay, Wisconsin. *Chemical Geology* **2001,** *177*, (3-4), 309-322.
48. Fraser, M. P.; Grosjean, D.; Grosjean, E.; Rasmussen, R. A.; Cass, G. R., Air quality model evaluation data for organics .1. Bulk chemical composition and gas/particle distribution factors. *Environmental Science & Technology* **1996,** *30*, (5), 1731-1743.
49. Oanh, N. T. K.; Reutergardh, L. B.; Dung, N. T., Emission of polycyclic aromatic hydrocarbons and particulate matter from domestic combustion of selected fuels. *Environmental Science & Technology* **1999,** *33*, (16), 2703-2709.
50. Schauer, C.; Niessner, R.; Poschl, U., Polycyclic aromatic hydrocarbons in urban air particulate matter: Decadal and seasonal trends, chemical degradation, and sampling artifacts. *Environmental Science & Technology* **2003,** *37*, (13), 2861-2868.
51. Windsor, J. G.; Hites, R. A., PAH in Gulf of Maine sediments and Nova Scotia soils. *Geochimica Et Cosmochimica Acta* **1979,** *43*, (1), 27-33.
52. Offenberg, J. H.; Baker, J. E., Aerosol size distributions of polycyclic aromatic hydrocarbons in urban and over water atmospheres. *Environmental Science & Technology* **1999,** *33*, (19), 3324-3331.
53. Offenberg, J. H.; Baker, J. E., Precipitation scavenging of polychlorinated biphenyls and polycyclic aromatic hydrocarbons along an urban to over-water transect. *Environmental Science & Technology* **2002,** *36*, (17), 3763-3771.
54. Golomb, D.; Barry, E.; Fisher, G.; Varanusupakul, P.; Koleda, M.; Rooney, T., Atmospheric deposition of polycyclic aromatic hydrocarbons near New England coastal waters. *Atmospheric Environment* **2001,** *35*, (36), 6245-6258.
55. McVeety, B. D.; Hites, R. A., Atmospheric deposition of Polycyclic Aromatic Hydrocarbons to water surfaces: A mass balance approach. *Atmospheric Environment* **1988,** *22*, (3), 511-536.
56. Baek, S. O.; Field, R. A.; Goldstone, M. E.; Kirk, P. W.; Lester, J. N.; Perry, R., A review of atmospheric PAH- sources, fate and behavior. *Water Air and Soil Pollution* **1991,** *60*, (3-4), 279-300.
57. Kamens, R. M.; Karam, H.; Guo, J. H.; Perry, J. M.; Stockburger, L., The behavior of oxygenated PAH on atmospheric soot particles. *Environmental Science & Technology* **1989,** *23*, (7), 801-806.
58. Farrington, J. W.; Frew, N. M.; Gschwend, P. M.; Tripp, B. W., Hydrocarbons in cores of northwestern atlantic coastal and continental margin sediments. *Estuarine and Coastal Marine Science* **1977,** *5*, (6), 793-808.
59. Rothermich, M. M.; Hayes, L. A.; Lovley, D. R., Anaerobic, sulfate-dependent degradation of polycyclic aromatic hydrocarbons in petroleum-contaminated harbor sediment. *Environmental Science & Technology* **2002,** *36*, (22), 4811-4817.

60. Jones, K. D.; Tiller, C. L., Effect of solution chemistry on the extent of binding of phenanthrene by a soil humic acid: A comparison of dissolved and clay bound humic. *Environmental Science & Technology* **1999,** *33*, (4), 580-587.
61. Talley, J. W.; Ghosh, U.; Tucker, S. G.; Furey, J. S.; Luthy, R. G., Particle-scale understanding of the bioavailability of PAHs in sediment. *Environmental Science & Technology* **2002,** *36*, (3), 477-483.
62. MacRae, J. D.; Hall, K. J. In *Biodegradation of Polycyclic Aromatic Hydrocarbons (PAH) in marine sediment under denitrifying conditions*, 1998; 1998; pp 177-185.
63. Heitkamp, M. A.; Cerniglia, C. E., Effects of chemical structures and exposure on the microbial degradation of PAH in fresh water and estuarine ecosystems. *Environmental Toxicology and Chemistry* **1987,** *6*, (7), 535-546.
64. White, H. K.; Xu, L.; Lima, A. L. C.; Eglinton, T. I.; Reddy, C. M., Abundance, composition, and vertical transport of PAHs in marsh sediments. *Environmental Science & Technology* **2005,** *39*, (21), 8273-8280.
65. Chiou, C. T.; McGroddy, S. E.; Kile, D. E., Partition characteristics of polycyclic aromatic hydrocarbons on soils and sediments. *Environmental Science & Technology* **1998,** *32*, (2), 264-269.
66. Reiser, R.; Toljander, H.; Albrecht, A.; Giger, W., Alkylbenzenesulfonates in recent lake sediments as molecular markers for the environmental behavior of detergent-derived chemicals. In *Molecular markers in environmental geochemistry*, Eganhouse, R. P., Ed. American Chemical Society: Washington, D.C., U.S.A., 1997; pp 196-212.
67. Müller, G.; Grimmer, G.; Böhnke, H., Sedimentary record of heavy metals and polycyclic aromatic hydrocarbons in lake constance. *Naturwissenschaften* **1977,** *64*, (8), 427-431.
68. Lee, R. F.; Gardner, W. S.; Anderson, J. W.; Blaylock, J. W.; Barwellclarke, J., Fate of PAH in controlled ecosystem enclosures. *Environmental Science & Technology* **1978,** *12*, (7), 832-838.
69. Schneider, A. R.; Stapleton, H. M.; Cornwell, J.; Baker, J. E., Recent declines in PAH, PCB, and toxaphene levels in the northern Great Lakes as determined from high resolution sediment cores. *Environmental Science & Technology* **2001,** *35*, (19), 3809-3815.
70. Elmquist, M.; Zencak, Z.; Gustafsson, O., A 700 Year Sediment Record of Black Carbon and Polycyclic Aromatic Hydrocarbons near the EMEP Air Monitoring Station in Aspvreten, Sweden. *Environmental Science and Technology* **2007**.
71. Schneider, A.; Stapleton, H.; Cornwell, J.; Baker, J., Recent declines in PAH, PCB and toxaphene levels in the northern Great Lakes as determined from high resolution sediment cores. *Environ. Sci. Technol.* **2001,** *35*, (19), 3809-3815.
72. Blumer, M.; Youngblood, W. W., Polycyclic Aromatic Hydrocarbons in Soils and Recent Sediments. *Science* **1975,** *188*, (4183), 53-55.
73. Yunker, M. B.; Macdonald, R. W.; Vingarzan, R.; Mitchell, R. H.; Goyette, D.; Sylvestre, S., PAHs in the Fraser River basin: a critical appraisal of PAH ratios as indicators of PAH source and composition. *Organic Geochemistry* **2002,** *33*, (4), 489-515.

74. Simoneit, B. R. T., Biomass burning - A review of organic tracers for smoke from incomplete combustion. *Applied Geochemistry* **2002,** *17*, (3), 129-162.
75. O'Malley, V. P.; Abrajano, T. A.; Hellou, J., Determination of the 13C/12c ratios of individual PAH from environmental samples: can PAH sources be apportioned? *Organic Geochemistry* **1994,** *21*, (6-7), 809-822.
76. O'Malley, V. P.; Abrajano, T. A.; Hellou, J., Stable Carbon Isotopic Apportionment of Individual Polycyclic Aromatic Hydrocarbons in St. John's Harbour, Newfoundland. *Environmental Science and Technology* **1996,** *30*, (2), 634-639.
77. McRae, C.; Sun, C. G.; Snape, C. E.; Fallick, A. E.; Taylor, D. In *delta C-13 values of coal-derived PAHs from different processes and their application to source apportionment*, 1999; 1999; pp 881-889.
78. Sofowote, U. M.; McCarry, B. E.; Marvin, C. H., Source Apportionment of PAH in Hamilton Harbour Suspended Sediments: Comparison of Two Factor Analysis Methods. *Environ. Sci. Technol.* **2008,** *42*, (16), 6007-6014.
79. Dickhut, R. M.; Gustafson, K. E., Atmospheric washout of PAH in southern Chesapeake Bay region. *Environmental Science & Technology* **1995,** *29*, (6), 1518-1525.
80. Simcik, M. F.; Eisenreich, S. J.; Lioy, P. J., Source apportionment and source/sink relationships of PAHs in the coastal atmosphere of Chicago and Lake Michigan. *Atmospheric Environment* **1999,** *33*, (30), 5071-5079.
81. Powell, H.; Doucette, J. Tuesday morning: Stepping stones for red tide and New England's jump on coal burning. http://www.whoi.edu/sbl/liteSite.do?litesiteid=6894&articleId=10666 (February 28, 2009)

CHAPTER 2

Recent trends in PAH fluxes and perylene production in the sediments of Siskiwit Lake, Michigan, U.S.A.

A.A. Benson[1], G.F. Slater[1], F. Yang[2], C.H. Marvin[2], D.C.G. Muir[2]

1. School of Geography and Earth Sciences, McMaster University, Hamilton, Ontario, Canada

2. National Water Research Institute, Environment Canada, Burlington, Ontario, Canada

Abstract

PAH deposition in North America had been declining since the mid-1950's due primarily to changes in the predominant fuels for industry and energy production. Stricter emission guidelines as well as development of cleaner combustion technology were expected to continue to reduce PAH deposition. However, recent research has documented either stable or increasing PAH deposition in urban/sub-urban areas in the last 20 years. Atmospheric PAH fluxes to Siskiwit Lake in northern Michigan, a remote lake isolated from local sources such as traffic, were determined in order to characterize the recent trends in PAH deposition over the since PAH deposition to this location was last characterized [1]. The observation of a continuing decrease in pyrogenic PAH deposition to Siskiwit Lake over the last 20 years indicated ongoing decreases in atmospheric PAH transport to this location, and therefore was consistent with the hypothesis that recent increases observed in urban or sub-urban areas are related to vehicular sources. In contrast to pyrogenic PAH, perylene concentrations have been found to increase with depth in many sedimentary environments, suggesting in situ production. Perylene concentrations in Siskiwit Lake followed similar trends to other studies; however, comparison to the previous study by McVeety and Hites [1] directly demonstrated significant perylene production over the past 20 years. The kinetics of perylene production in Siskiwit Lake sediments was also explored to determine whether the reaction follows a simple concentration dependant kinetic model.

1. Introduction

Polycyclic Aromatic Hydrocarbons (PAH) are persistent organic pollutants (POP) consisting of two or more fused aromatic rings. Several PAH have been implicated in the formation of dangerous DNA-adducts and thus have been classified as known or suspected carcinogens or mutagens [2]. Because of their association with particulate aerosols they are also implicated in air quality and have been strongly linked to many respiratory problems [3, 4]. The primary type of PAH released to the environment is pyrogenic PAH which are a result of incomplete combustion of organic material including fossil fuels (e.g. coal) and modern biomass (e.g. wood) [5-8]. Most of these PAH are deposited close to the combustion source; however a fraction of the fine particulate can be transported over large distances [9]. Profiles of atmospherically deposited PAH in lake sediments provide a record of this deposition and thereby a historical profile of combustion related impacts [8, 10-14].

Profiles of atmospheric PAH deposition observed in several studies have been attributed to emissions from energy production and industry [6-8]. In these studies, PAH deposition generally peaks circa 1960 and begins to decrease steadily afterward [1, 8]. It was assumed that this decline would continue, however, studies by Lima et al [8] and Van Metre et al [10] have shown that PAH fluxes at 11 urban/sub-urban sites in the United States began increasing again in the 1990's. Van Metre et al [10] correlated increased PAH fluxes to increased use of passenger vehicles in these areas and hypothesized that the recent increases

in PAH fluxes are due to increases in local sources as a result of increased traffic. Lima et al [8] likewise related increased PAH fluxes in Rhode Island to increases in local sources, however specifically correlated increased PAH deposition to increased diesel fuel consumption and thus increased use of heavy vehicles. In addition, Schnieder et al [11] demonstrated a constant atmospheric PAH flux from Lake Michigan over a similar time period and Elmquist et al [12] also noted constant PAH fluxes after 1990 in Aspverten, Sweden during the same time period as the studies discussed above.

If the hypothesis that these recent increases are due to local traffic sources is correct, then it is expected that, in contrast to these sites, PAH fluxes at a remote location where the primary source is regional scale atmospheric transport and deposition should show continuing decreases in PAH fluxes in the past 20 years. Siskiwit Lake, on Isle Royale, in northern Michigan is located less than 50 km offshore of Thunder Bay, Ontario, Canada in Lake Superior. The prohibition of powered vehicles on the island means that there are no local sources of PAHs. The only potential sources of PAHs to Siskiwit are atmospheric deposition from sources that could be transported by the prevailing west to east, and northwest to southeast wind directions [15, 16]. These potential sources include the city of Thunder Bay urban/industrial area, and coal power generating plants in Thunder Bay and Atikokan Ontario. PAH fluxes to the sediments of Siskiwit Lake on Isle Royale in Michigan were previously characterized by McVeety et al [1] based on a core taken in 1984. The goal of the present study

was to revisit this site 20 years later and test the hypothesis that the lack of local traffic sources would result in decreasing recent trends, which would be in contrast to the observations of other research suggesting constant or increasing recent deposition [8, 10, 11].

In contrast to pyrogenic PAH, the origin of perylene (a five ring PAH) observed in sediments is not well constrained [19-23]. Perylene has been identified as a component of emissions from incinerators and vehicle exhaust [24, 25] and has been found adsorbed to atmospheric particulate [26]. Natural abundance radiocarbon analysis of PAH in several reference sediments demonstrated that perylene was the most modern PAH, however fossil sources also make contributions to perylene loadings [27]. This was further demonstrated by Mandalakis et al [27] who showed that the Δ14C of perylene in surface sediments from Stockholm, Sweden had values of -916 to -812‰ indicating that perylene is predominantly derived from fossil fuel combustion at this site. The correlation of perylene concentrations with profiles of other pyrogenic PAH in other cores is further evidence that this perylene is in some way related to combustion [28]. However, in contrast to these studies, several studies have found perylene to be disproportionately higher in concentration when compared to other pyrogenic PAH. Furthermore, in these sediments concentrations of perylene are low at the sediment-water interface and generally increase with depth, often by over an order of magnitude [8, 23, 19]. These observations have been interpreted to imply that perylene is being produced in situ when the

sediment becomes anoxic [22, 23] however, the reaction by which this process is occurring, and the chemical precursor for it, are still not known [20, 21]. Gschwend et al [23] suggested a terrestrial precursor, while Soma et al [30] found correlations between perylene concentrations and several terrestrial and aquatic photosynthetic pigments; the highest correlation being 0.851 (n=20) for chlorophyll-A which has both aquatic and terrestrial sources. Silliman et al [20] have suggested that perylene concentrations are not linked to any specific precursor but are instead controlled by the efficiency of anoxic diagenesis as a result of microbial activity. It was hypothesized that microbes that produce perylene are unable to compete for labile carbon in oxic conditions; thus perylene production begins when anoxia sets in allowing perylene producing microbes a chance to compete for the carbon pool [20].

There has been little discussion of perylene production kinetics in the literature. Gschwend et al [23] estimated first order and second order rate constants for this process of 0.012 yr-1 and 0.0013 nmol yr-1 respectively; and suggested that detrital inputs may be related to variations in perylene observed in other cores. However other researchers (e.g. [22]) have since discovered perylene at sites where there would be little or no terrestrial input. Thus, the secondary goal of this study was to investigate perylene production in Siskiwit lake sediments and to compare the current concentrations of perylene to those observed 20 years ago by McVeety and Hites [1]. Moreover, this study will model

perylene curves as 1st and 2nd order reactions similar to Gschwend et al [23] to investigate the possibility that perylene production follows a simple kinetic model.

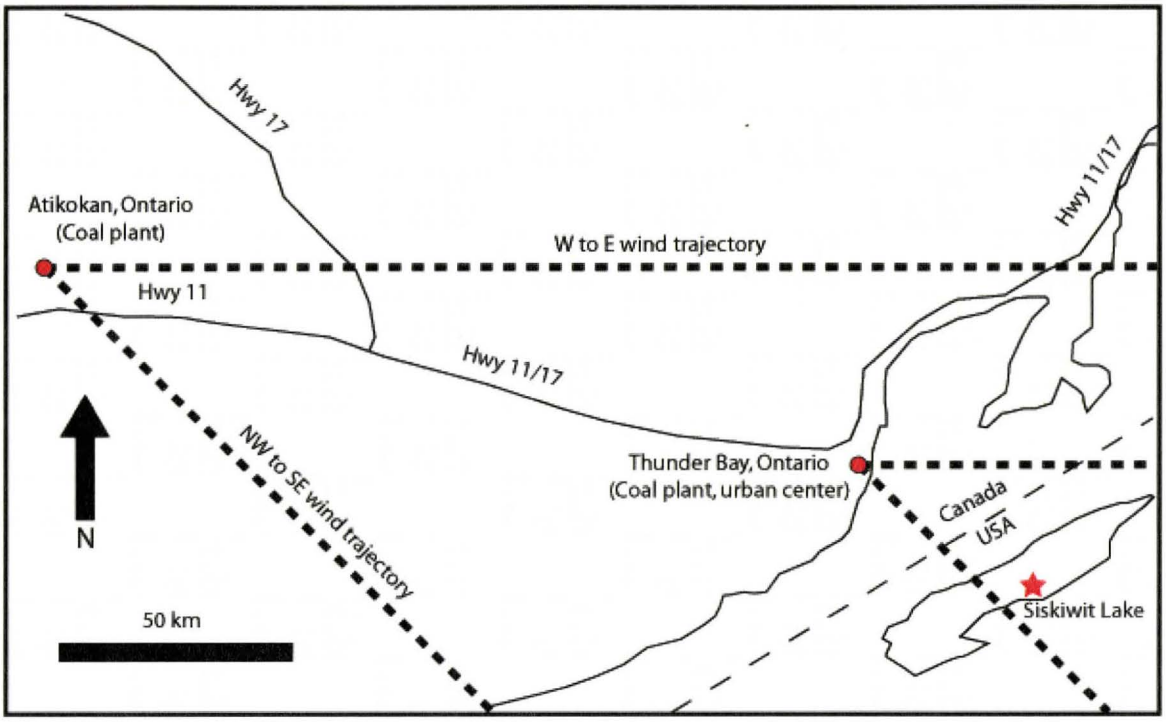

Figure 2-1: A map showing the location of Siskiwit Lake (red star) as well as the location of regional combustion sources (red dots). Dotted lines are dominant and secondary wind trajectories.

2. Experimental Section

2.1 Study Area and Sediment Sampling

Siskiwit Lake is located on Isle Royale, Michigan, U.S.A (figure 2-1). The lake is surrounded by the protected land of Isle Royal National Park and Isle Royale and is entirely surrounded by Lake Superior. Thus Siskiwit Lake is sheltered from shoreline development which may introduce point sources of PAH. Consistent with the previous assumption by McVeety and Hites [1] we feel it is reasonable to assume that all pyrogenic PAH loadings are derived from

atmospheric deposition of particulate to the surface of the lake. Piston cores were collected from the deepest section of the lake. The cores were sliced directly after coring into 1 cm intervals, placed into plastic Ziploc bags and kept cool and dark until they could be frozen upon return to the laboratory where they were stored at -20 degrees Celsius until further processing. Sediment was dried at 50 degrees Celsius in solvent rinsed and pre-combusted aluminum pans. Dried sediment was ground with an agate mortar and pestle and stored in the dark in pre-combusted 500 ml glass vials.

2.2 Quantification of PAH

PAH analysis was performed using modified EPA methods 8100, 3051A and 3630C. In short, 50 g of sediment was spiked with 5 ppm surrogate standards (9,10-dihydrophenanthrene and m-terphenyl) then microwave extracted (MarsX) in 1:1 hexane/acetone at 115 degrees celsius for 15 mins. Extracts were allowed to cool to approximately 30 degrees then filtered with hexane and dichloromethane through glass fiber filter paper (Whatman) to remove solid sediment portion. Filtered extracts were treated with activated copper pellets to remove elemental sulphur, reduced in volume to approximately 1 ml and fractionated on fully activated silica gel. A total of four fractions were collected: F1: hexane (aliphatic hydrocarbons), F2: 2:1 hexane/dichloromethane (aromatic hydrocarbons), F3: dichloromethane, F4: methanol. All fractions were archived except for the F2 containing the aromatic hydrocarbons. The F2 fraction

was reduced in volume and solvent exchanged into 100% hexane then transferred to 1 ml amber vials and spiked with an internal standard (o-terphenyl).

PAH quantification was performed on a GC/MS (Agilent 6890 GC, Agilent 5973n MS) equipped with a split/splitless injector kept in splitless mode and a 0.25 mm I.D. 30 m DB-XLB column (Jackson and White). The oven was programmed to 65 degrees celsius and ramped at 4 degrees per minute to 320 degrees and held for 10 mlnutes. The following 16 EPA priority PAH were quantified: naphthalene, acenapthylene, acenapthene, fluorene, phenanthrene, anthracene, fluoranthene, pyrene, benz(a)anthracene, chrysene, benzo(b)fluoranthene, benzo(k)fluoranthene, benzo(a)pyrene, benzo(g,h,i)perylene, dibenz(a,h)anthracene and ideno(1,2,3-cd)pyrene. Perylene is not an EPA priority pollutant, however was also quantified. All PAH were quantified in scan mode with 5-point calibration curve ($R2 > 0.999$).

2.3 Quality Control

Accuracy of the PAH method was determined using three samples of standard reference material EC-1 (Environment Canada, lacustrine sediment). The results were all within 15% of the reference values. Precision (average relative standard deviation <6%) was measured by triplicate injections of standards (2 ppm and 8 ppm) as well as triplicate injections of two samples during each instrumental sequence. The limit of quantification for parent PAH compounds was 1 ppm in solution or 19.4 ng/g dw. PAH extraction took place in

batches, procedural blanks (n=6) were run with each batch, there were no detectable PAH concentrations in any of the blanks.

2.3 Sedimentation rates and sediment dating

^{210}Pb analysis was performed by Environment Canada's National Water Research Institute (NWRI, Burlington, Ontario) on a separate core taken from the site on the same date as cores used for PAH analysis. Briefly, sediment was dried then acid treated and prepared using a ^{210}Po enrichment method; ^{210}Po is analyzed as it is assumed to be in secular equilibrium with ^{210}Pb. The final ^{210}Po was plated on highly polished Ag discs and the activity of each sample was measured with an alpha counting device in disintegrations per minute (dpm). Sedimentation rates were calculated as an average over the core. Focusing factors were calculated by integrating the total amount of excess ^{210}Pb over the core and dividing by the expected amount based on atmospheric ^{210}Pb flux at the surface.

3. Results

3.1 ^{210}Pb dating

Both the constant initial concentration (CIC) and the constant rate of supply (CRS) models were applied to the ^{210}Pb data [31]. Although all models agreed well with each other, the CIC2 model was used for the calculation of ages for this core as it was the closest to matching the dating from McVeety and Hites [1]. Furthermore, focusing factors calculated from ^{210}Pb fluxes for this study were

identical to those reported by McVeety and Hites [1]. For more information on the ^{210}Pb dating of the cores please see appendix B.

3.2 Pyrogenic PAH fluxes

While concentrations are commonly compared in the literature PAH fluxes take into consideration sedimentation rate and sediment focusing factor and will be used to describe PAH deposition in this study. Flux is calculated using the following equation after McVeety and Hites [1].

$$F= (C*p*s)/y \quad (1)$$

Where:

F= flux (ng cm-2 yr-1)

C= Concentration (ng g-1 dw)

p= in-situ density (g dry sed/cm3 wet sed)

s= sedimentation rate (cm yr-1)

y= focusing factor as determined by ^{210}Pb (dimensionless)

The total pyrogenic PAH flux (not including Perylene) versus year of deposition as determined by ^{210}Pb dating is shown in Figure 2-2. The total PAH curve can be divided into two sections, from 1911 to 1955 fluxes increased by 378% from 6.4 +/- 0.32 ng cm-2 yr -1 to a maximum in 1955 of 24.2 +/- 1.2 ng cm-2 yr -1. This increase occurred at a constant linear rate of approximately 0.43 ng cm-2 yr-1 (n=6, r2= 0.990). After the maximum in 1955, PAH fluxes steadily declined to 8.5 +/- 0.42 ng cm-2 yr -1 in 2001 at a constant linear rate of 0.33 ng cm-2 yr-2 (n=6, r2=0.963).

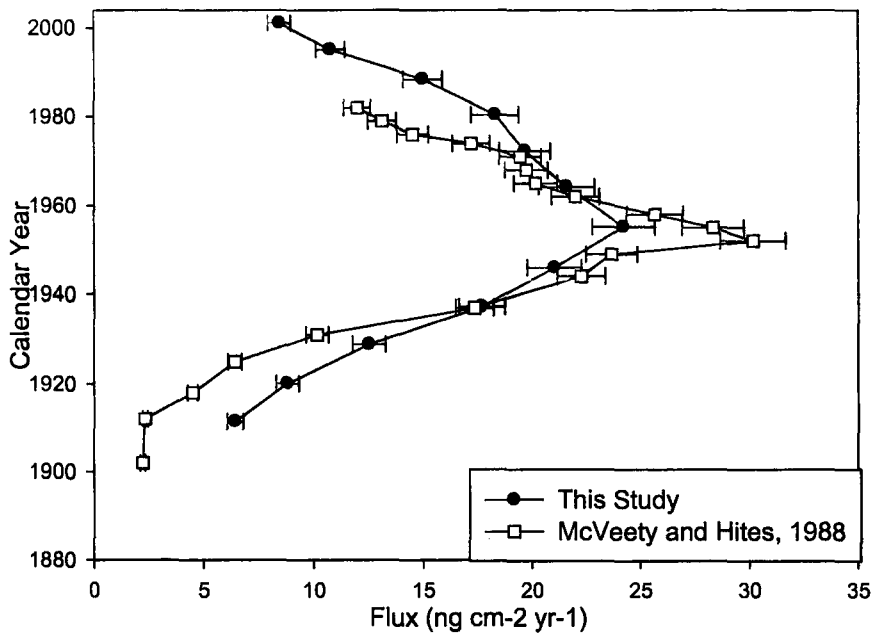

Figure 2-2: Plots of total PAH flux versus calendar year for this study as well as McVeety and Hites [1]. Error bars are 6% analytical error.

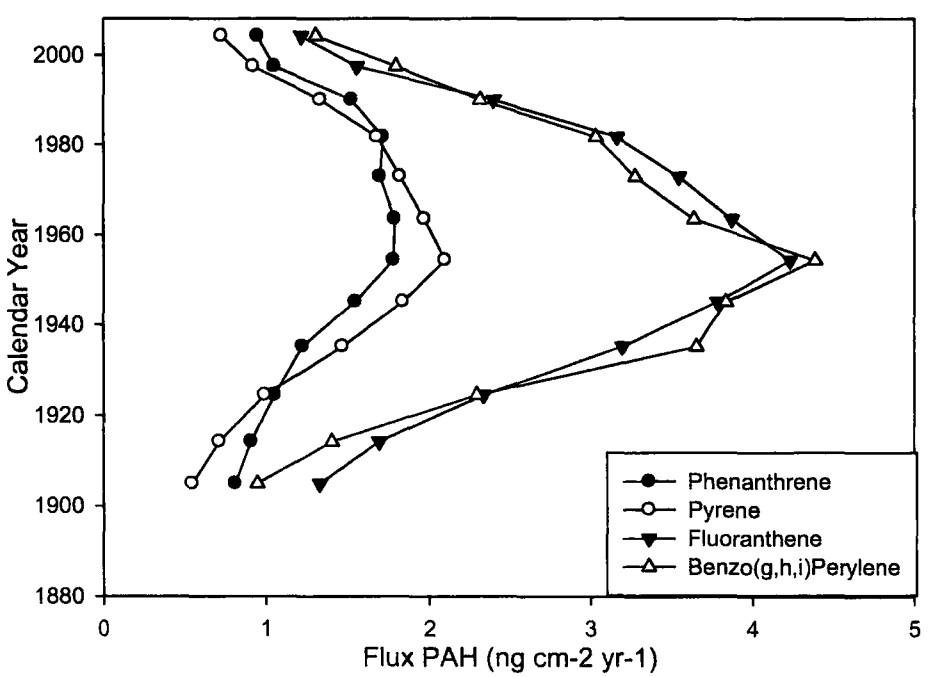

Figure 2-3: Plots of representative single parent PAH demonstrating that single PAH fluxes and total PAH observe similar trends. Error bars are approximately the size of symbols.

Representative plots of single PAH phen, py and flua fluxes are shown in figure 2-3. Phen, Py and Flua fluxes increased by 222%, 401% and 332% respectively during the period from 1911 to 1955. After 1955, all individual PAH observed a continuous decline in flux. As is expected, the trends in these plots are similar to the total PAH curve. With the exception of perylene, all individual PAH exhibit similar trends over the length of the core.

3.3 Perylene concentrations

Perylene concentrations in the uppermost sample are 194 ng g-1 in 2001 and increase by an order of magnitude to 2000 ng g-1 at 1955 (figure 2-4). This increase occurs at a linear rate of 26 ng g-1 yr-1 (n=9 r2=0.96). After this point perylene concentrations become somewhat variable however remain circa 2000 ng g-1 with the exception of an anomalous low value at the bottom of the core.

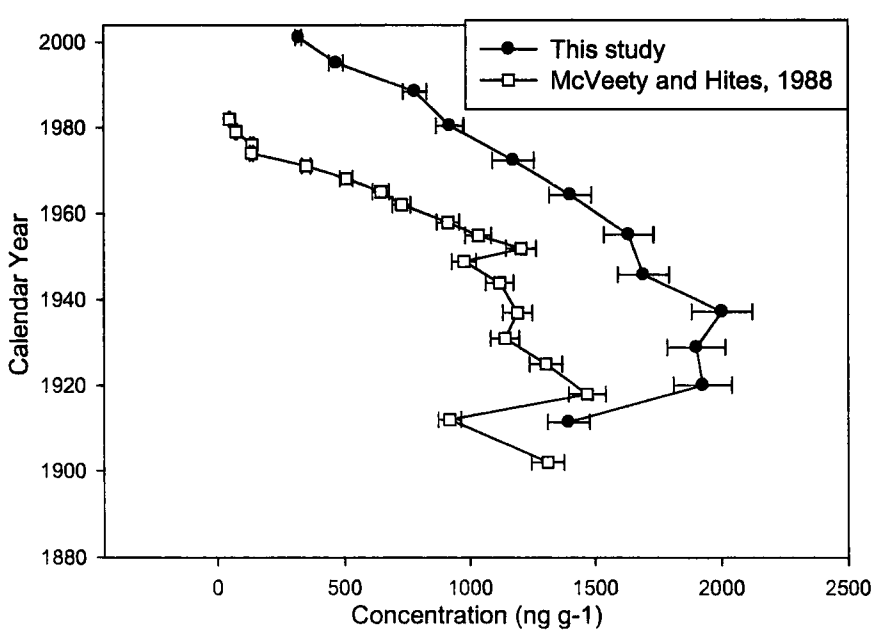

Figure 2-4: Plots of perylene concentrations from this study as well as McVeety and Hites [1]. Error bars are 6% analytical error.

4. Discussion

4.1 Pyrogenic PAH fluxes

The PAH flux profile from this study agrees well with McVeety and Hites [1] for the period between 1920 and 1980. Furthermore, the timing of the maximum PAH deposition and the overall shape of the profile are also consistent with profiles from the Pettaquamscut River in Rhode Island [8] and Lake Erie [11]. This PAH deposition profile has previously been correlated with the amount and type of fuel used for energy production in the United States [8, 10].

4.2 Recent declining PAH trends

The recent trends in pyrogenic PAH deposition seen in this study clearly demonstrate that long range PAH deposition to Siskiwit Lake has continued to decrease in recent sediments (figure 2-2); and in fact current deposition is approaching levels observed in the early stages of industrialization. This contrasts to the observations of Lima et al [8], Van Metre et al [10] and Schneider et al [11] who observed constant or increasing PAH deposition over a similar time period. Because Siskiwit Lake is isolated from major traffic sources, it is not likely to be impacted by the elevated traffic emissions hypothesized to be the cause of the increases observed by these researchers. Thus, corroborating the hypothesis [10] that increasing PAH deposition in urban and sub-urban areas is a result of increased local vehicular traffic. Rather, the most likely source of atmospheric PAH deposition to Siskiwit Lake are regional sources originating from industrial activities in the urban center of Thunder Bay, Ontario as well as two coal power

generation plants in Atikokan, Ontario and Thunder Bay, Ontario. Based on prevailing and secondary wind directions [15, 16], these sources are often upwind of Siskiwit Lake and thus are potentially contributing to the PAH loadings (Figure 2-1). The observation of continuing decreases in PAH fluxes to Siskiwit Lake is therefore consistent with implementation of emissions guidelines on industry, and further, that emission from vehicular sources in nearby Thunder Bay are in fact a relatively minor input of PAH. This suggests that legislation has been effective in reducing industrial PAH emissions to the atmosphere and perhaps any renewed efforts should be focused on mitigating local vehicular emissions.

4.3 Perylene

The fact that the core from this study was obtained from the same location as a core reported on by McVeety and Hites [1] but 20 years later provides an excellent opportunity to investigate the potential production of perylene. Perylene production in these sediments is directly demonstrated by the offset between the curve from this study and the curve from McVeety and Hites [1] (Figure 4). In contrast, this offset is not observed for the pyrogenic PAH. A 158% to 1300% increase in perylene concentrations was observed over concentrations observed by McVeety and Hites [1] with the increase being greatest at the top of the core and diminishing with depth in the core. From circa 1955 to the bottom of the core the offset between the two cores appears to be relatively constant although perylene concentrations vary somewhat. It is important to note, however, that perylene concentrations increased over the entire length of the core relative to

concentrations recorded by McVeety and Hites [1]. This indicates that perylene production is ongoing even in sediments deposited near the beginning of the 1900's.

4.4 Kinetic model for perylene production

Similar to Gschwend et al [23], this study modeled the perylene production curves as 1st and 2nd order reactions to obtain rate constants and estimate precursor concentrations. An iterative computer program similar to the one used by Gschwend et al [23] was used to fit reaction curves to the data sets. To ensure the programs were comparable, we re-plotted data from Gschwend et al [23] and produced the same rate constants and precursor concentrations that were found by their program.

In both the work by Gschwend et al [23] and this study, the reactions were assumed to be unimolecular for 1st order or a bi-molecular for 2nd order with a precursor being transformed into perylene [23]. It is possible for this to be a multiple step reaction but requires only that the rate limiting step is the prescribed 1st or 2nd order reaction [23]. It is also possible that the reaction is a pseudo-first order reaction and thus one of the 2nd order reactants is in vast excess of the other. In this case, it is impossible to distinguish 1st and 2nd order reactions using this method.

Table 2-1 summarizes information from the kinetic modeling in this study as well as modeled data from McVeety and Hites [1]. A comparison of the kinetic curve fit for the profiles from this study with the profile from McVeety and Hites [1]

reveal few differences aside from increased concentration (Figure 2-5). Both curves fit well with r^2 values of at least 0.89 although the top of the profile from McVeety and Hites [1] appears to deviate slightly from the predicted reaction curve. While it is not possible to exactly determine the cause of this, it is likely due at least in part to the different sampling resolutions. However, the overall trends in the curves match well including the anomalous low perylene concentration seen at approximately 1911. The fact that this low concentration interval is observed in both cores suggests that it, as well as some of the variability in the lower part of the core, may represent changes in the conditions of reaction such as precursor concentration changes as was suggested by Gschwend et al [23].

Table 2-1: A summary of the kinetic model results

1st order reactions

Study	**Site**	**r2**	**k** yr-1	**Co** nmol g-1	**Std Error** nmol g-1
This Study	Siskiwit Lake, Michigan	0.91	0.043	7.2	0.43
McVeety and Hites, 1988	Siskiwit Lake, Michigan	0.92	0.048	3.2	0.3
Gschwend et al, 1983	Mountain Pond, Maine	0.97	0.012	4.9	0.29

2nd order reactions

Study	**Site**	**r2**	**k** nmol yr-1	**Co** nmol g-1	**Std Error** nmol g-1
This study	Siskiwit Lake, Michigan	0.89	0.0076	9.1	0.46
McVeety and Hites, 1988	Siskiwit Lake, Michigan	0.91	0.012	4	0.32
Gschwend et al, 1983	Mountain Pond, Maine	0.96	0.0013	7.1	0.31

4.5 Rate constants and precursor concentrations

Data sets from Siskiwit Lake produced very similar rate constants of 0.043 and 0.048 yr-1 for 1st order and 0.0076 and 0.012 nmol yr-1 for this study and McVeety and Hites [1] respectively. However, the calculated precursor concentrations were different with the current profile from Siskiwit Lake yielding higher precursor concentrations of 7.2 nmol g-1 for 1st order and 9.1 nmol g-1 for 2nd order and the profile from McVeety and Hites [1] yielding precursor concentrations of 3.2 nmol g-1 for 1st order and 4 nmol g-1 for 2nd order. This is expected as the program back-calculates precursor concentration based on maximum amount of perylene produced and thus assumes a mass balance. Because this study demonstrates that production occurred over the entire core maximum perylene concentrations were higher for this study, and thus back-calculated precursor concentrations are also higher. This demonstrates that mass balance is in fact not achieved as would be expected for a reaction that has gone to completion.

4.6 Can Perylene Production be explained by simple kinetics?

The fact that the curve fits and rate constants are similar for both cores demonstrates the similarity in the overall shapes of the two curves which suggests that perylene production is similar in pattern. However this pattern cannot be explained by simple concentration dependant kinetics. Using the similar rate constants and taking into consideration the 20 year interval between the two data sets, it was not possible to predict the observed concentration

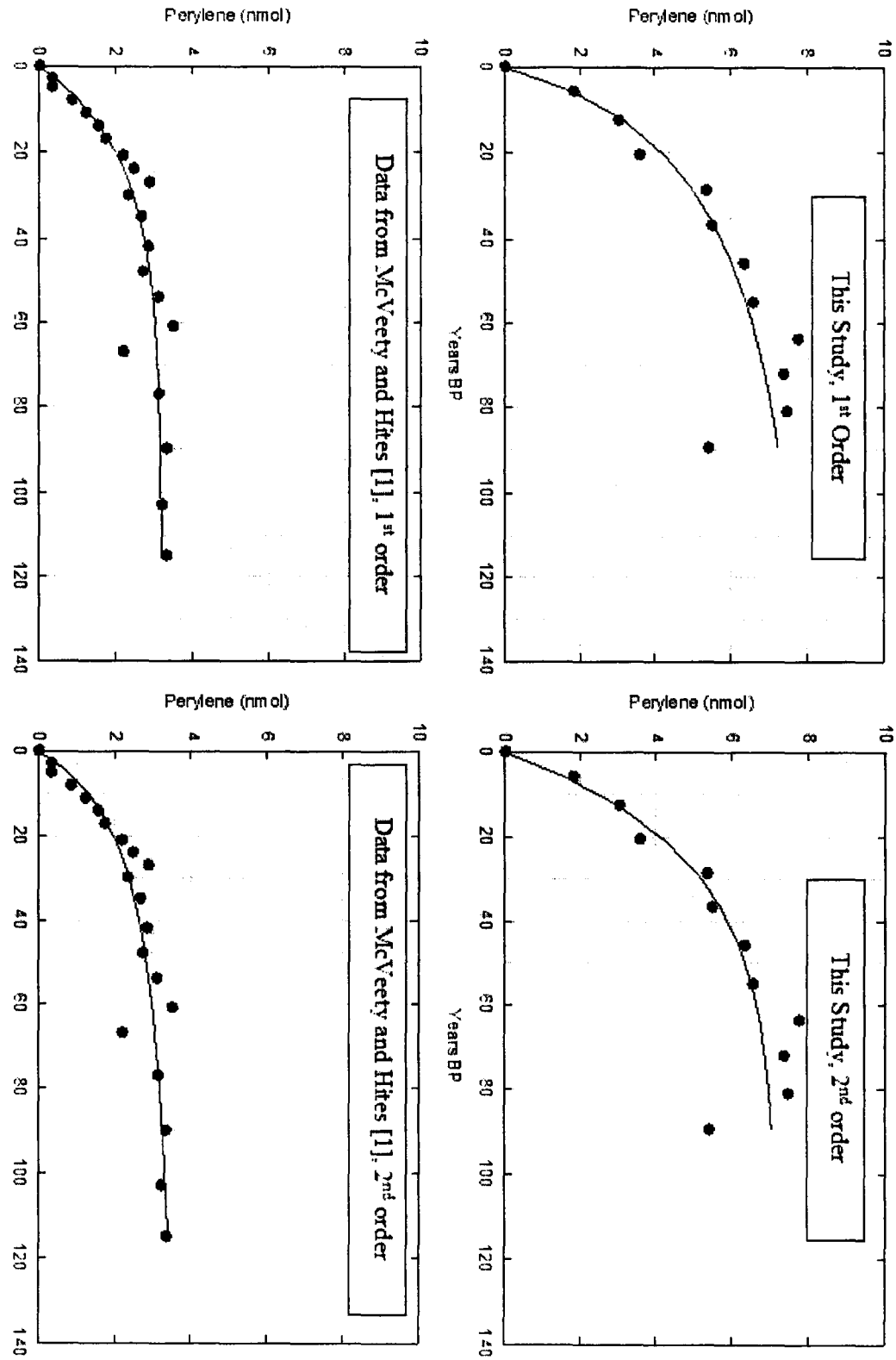

Figure 2-5: Plots of 1st and 2nd order curve fits for data from this study (top 2 graphs) and data from McVeety and Hites [1] from the same site (bottom graphs).

changes using 1st or 2nd order rate equations. A 1st or 2nd order reaction in a closed system as was assumed here and in Gschwend et al [23] would produce two curves that converge at a maximum concentration indicating that the reaction has gone to completion and the precursor chemical reservoir has been exhausted. This is not observed in the two data sets from Siskiwit Lake and instead considerable perylene production occurs over the entire core. This suggests either that there is a sustained supply of precursor which means the reaction is in fact not in a closed system or that perylene production is controlled by more complex kinetics perhaps involving biology as is suggested by Silliman et al [32]. Furthermore, it may also be possible that convergence of the two profiles indicating completion of the reaction occurs deeper in the sediments and is not captured by this study or McVeety and Hites [1]. In all cases, significant perylene production does occur, as demonstrated in this study, but cannot be described using simple kinetic modeling techniques employed here and in Gschwend et al [23].

5. Summary of Findings

Recent pyrogenic PAH fluxes have continued to decrease through the 1990s and are approaching background levels at this remote site. This is in contrast to increasing PAH fluxes in the late 1990's and early 2000's seen by other investigators (e.g.[8, 10]) and corroborates the subsequent hypothesis [10] that recent PAH increases are due to overprinting of long-range transport by emissions from vehicular sources. Furthermore, it can be inferred that industrial

restrictions that have been enacted are effective in reducing atmospheric PAH emissions.

The perylene profile shows increasing perylene concentrations with increasing core depth and thus reinforces the general paradigm of the literature that, while some perylene has been found in combustion emissions, perylene is predominantly produced in-situ. Moreover, the profile from this study shows increases in perylene concentrations over the entire core when compared with the profile from McVeety and Hites [1]. This demonstrates that a non-trivial amount of perylene has been produced over the 20 year interval between samplings and conclusively demonstrates that perylene is produced in-situ at this site. Attempts to model perylene production using the two profiles from Siskiwit Lake as 1st and 2nd order kinetic reactions demonstrated that perylene production in this data set cannot be explained by simple concentration dependant kinetic reactions. Furthermore, precursor concentrations predicted based on maximum perylene concentrations by the modeling were different because production occurred in all sediments thus higher maximum perylene concentrations were observed in this study. The inability of simple rate laws to predict the observed changes in perylene production combined with perylene production occurring over the entire core length suggests that perylene production does occur but is not controlled by simple concentration dependant kinetics. Instead, perylene production may be controlled by a more complex set of kinetics perhaps involving biology as is suggested by Silliman et al [32].

Alternatively, perhaps perylene production occurs over longer time scales then analyzed here and convergence of perylene concentrations and thus completion of the reaction is observed deeper in the sediments.

Citations

1. McVeety, B. D.; Hites, R. A., Atmospheric deposition of Polycyclic Aromatic Hydrocarbons to water surfaces: A mass balance approach. Atmospheric Environment 1988, 22, (3), 511-536.
2. Courter, L. A.; Pereira, C.; Baird, W. M., Diesel exhaust influences carcinogenic PAH-induced genotoxicity and gene expression in human breast epithelial cells in culture. Mutation Research-Fundamental and Molecular Mechanisms of Mutagenesis 2007, 625, (1-2), 72-82.
3. Billet, S.; Garcon, G.; Dagher, Z.; Verdin, A.; Ledoux, F.; Cazier, F.; Courcot, D.; Aboukais, A.; Shirali, P., Ambient particulate matter (PM2.5): Physicochemical characterization and metabolic activation of the organic fraction in human lung epithelial cells (A549). Environmental Research 2007, 105, (2), 212-223.
4. Mazzarella, G.; Ferraraccio, F.; Prati, M. V.; Annunziata, S.; Bianco, A.; Mezzogiorno, A.; Liguori, G.; Angelillo, I. F.; Cazzola, M., Effects of diesel exhaust particles on human lung epithelial cells: An in vitro study. Respiratory Medicine 2007, 101, (6), 1155-1162.
5. Blumer, M.; Youngblood, W. W., Polycyclic Aromatic Hydrocarbons in Soils and Recent Sediments. Science 1975, 188, (4183), 53-55.
6. Laflamme, R. E.; Hites, R. A., Global distribution of polycyclic aromatic hydrocarbons in recent sediments. Geochimica Et Cosmochimica Acta 1978, 42, (3), 289-303.
7. Gschwend, P. M.; Hites, R. A., Fluxes of polycyclic aromatic hydrocarbons to marine and lacustrine sediments in the northeastern United States. Geochimica Et Cosmochimica Acta 1981, 45, (12), 2359-2367.
8. Lima, A. L.; Eglinton, T. I.; Reddy, C. M., High-resolution record of pyrogenic polycyclic aromatic hydrocarbon deposition during the 20th century. Environmental Science and Technology 2003, 37, 53-61.
9. Windsor, J. G.; Hites, R. A., Polycyclic aromatic hydrocarbons in Gulf of Maine sediments and Nova Scotia soils. Geochimica Et Cosmochimica Acta 1979, 43, (1), 27-33.
10. Van Metre, P. C.; Mahler, B. J.; Furlong, E. T., Urban Sprawl Leaves Its PAH Signature. Environmental Science and Technology 2000, 34, (19), 4064-4070.
11. Schneider, A.; Stapleton, H.; Cornwell, J.; Baker, J., Recent declines in PAH, PCB and toxaphene levels in the northern Great Lakes as determined from high resolution sediment cores. Environ. Sci. Technol. 2001, 35, (19), 3809-3815.
12. Elmquist, M.; Zencak, Z.; Gustafsson, O., A 700 Year Sediment Record of Black Carbon and Polycyclic Aromatic Hydrocarbons near the EMEP Air Monitoring Station in Aspvreten, Sweden. Environmental Science and Technology 2007.

13. Fernandez, P.; Vilanova, R. M.; Grimalt, J. O., Sediment fluxes of polycyclic aromatic hydrocarbons in European high altitude mountain lakes. Environmental Science & Technology 1999, 33, (21), 3716-3722.
14. Yunker, M. B.; Macdonald, R. W., Alkane and PAH depositional history, sources and fluxes in sediments from the Fraser River Basin and Strait of Georgia, Canada. Organic Geochemistry 2003, 34, (10), 1429-1454.
15. Canada, E. Climate Normals. http://www.climate.weatheroffice.ec.gc.ca/climate_normals/index_e.html (February 18), 2009
16. Canada, N. R. The Atlas of Canada. http://atlas.nrcan.gc.ca/site/english/maps/archives/3rdedition/environment/climate/020 (February 18), 2009
17. Lima, A. L.; Farrington, J. W.; Reddy, C. M., Combustion-derived Polycyclic Aromatic Hydrocarbons in the environment- a review. Environmental Forensics 2005, 6, 109-131.
18. Kawamura, K.; Suzuki, I.; Fuji, Y.; Watanabe, O., Ice core record of polycyclic aromatic hydrocarbons over the past 400 years. Naturwissenschaften 1994, 81, (11), 502-505.
19. Silliman, J. E.; Meyers, P. A.; Eadie, B. J. In Perylene: an indicator of alteration processes or precursor materials?, 1998; 1998; pp 1737-1744.
20. Silliman, J. E.; Meyers, P. A.; Eadie, B. J.; Klump, J. V., A hypothesis for the origin of perylene based on its low abundance in sediments of Green Bay, Wisconsin. Chemical Geology 2001, 177, (3-4), 309-322.
21. Venkatesan, M. I., Occurrence and possible sources of perylene in marine sediments-a review. Marine Chemistry 1988, 25, (1), 1-27.
22. Wakeham, S. G.; Schaffner, C.; Giger, W.; Boon, J. J.; Deleeuw, J. W., Perylene in sediments from the Namibian shelf.. Geochimica Et Cosmochimica Acta 1979, 43, (7), 1141-1144.
23. Gschwend, P. M.; Chen, P. H.; Hites, R. A., On the formation of perylene in recent sediments- kinetic models. Geochimica Et Cosmochimica Acta 1983, 47, (12), 2115-2119.
24. Blumer, M.; Blumer, W.; Reich, T., Polycyclic aromatic hydrocarbons in soils of a mountain valley- correlation with highway traffic and cancer incidence. Environmental Science & Technology 1977, 11, (12), 1082-1084.
25. Davies, I. W.; Harrison, R. M.; Perry, R.; Ratnayaka, D.; Wellings, R. A., Municipal incinerator as a source of polynuclear aromatic hydrocarbons in the environment. Environmental Science & Technology 1976, 10, (5), 451-453.
26. Lunde, G.; Bjorseth, A., Polycyclic aromatic hydrocarbons in long-range transported aerosols. Nature 1977, 268, 518-519.
27. Mandalakis, M.; Gustafsson, O.; Reddy, C. M.; Li, X., Radiocarbon apportionment of fossil versus biofuel combustion sources of polycyclic aromatic hydrocarbons in the Stockholm metropolitan area. Environmental Science & Technology 2004, 38, (20), 5344-5349.

28. Simcik, M. F.; Eisenreich, S. J.; Golden, K. A.; Liu, S. P.; Lipiatou, E.; Swackhamer, D. L.; Long, D. T., Atmospheric Loading of Polycyclic Aromatic Hydrocarbons to Lake Michigan as Recorded in the Sediments. Environ. Sci. Technol. 1996, 30, (10), 3039-3046.
30. Soma, Y.; Tanaka, A.; Soma, M.; Kawai, T., Photosynthetic pigments and perylene in the sediments of southern basin of Lake Baikal. Organic Geochemistry 1996, 24, (5), 553-561.
31. Appleby, P. G.; Oldfield, F., The calculation of lead-210 dates assuming a constant rate of supply of unsupported ^{210}Pb to the sediment. CATENA 1978, 5, (1), 1-8.
32. Silliman, J. E.; Meyers, P. A.; Eadie, B. J.; Val Klump, J., A hypothesis for the origin of perylene based on its low abundance in sediments of Green Bay, Wisconsin. Chemical Geology 2001, 177, (3-4), 309-322.

CHAPTER 3

Sediment core profiling as an essential tool in site assessment

A.A. Benson[1], S. Desrocher[2], T. Nelson[2], B.A. Bergquist[3], G.F. Slater[1]

1. School of Geography and Earth Sciences, McMaster University, Hamilton, Ontario, Canada

2. Environ (EC) Canada Consulting, Mississauga, Ontario, Canada

3. Department of Geology, University of Toronto, Toronto, Ontario, Canada

Abstract

Differentiating between point source industrial contamination and regional atmospheric deposition is integral to accurately implementing effective monitoring, mitigation and remediation programs. This study evaluates polycyclic aromatic hydrocarbon (PAH), lead (Pb) and mercury (Hg) profiles in sediment cores retrieved from two northern Ontario lakes. One lake has an industrial facility located close to the shore, while the other lake, 3 km away does not. The goal of this study was to demonstrate the use of contaminant concentration profiling in sediment cores as a tool for differentiating atmospheric versus point source industrial inputs in remote areas. Profiles for Pb, Hg and PAH from both lakes were consistent with atmospheric deposition as observed in other remote lakes. Further, differences between the PAH concentration profiles in these lakes and nearby Siskiwit Lake revealed the configuration of regional combustion sources and prevailing wind patterns may have an impact on atmospheric deposition. Comparison of cores collected proximal to the industrial site and in the middle of the lake revealed no relationship regarding increasing concentrations with proximity to the industry. Comparison of the concentrations observed in this study with Canadian Sediment Quality guidelines further showed that the atmospheric deposition occurring in these lakes was sufficient to result in concentrations that are equivalent to or exceed guidelines. The potential for atmospheric deposition to result in concentrations exceeding guidelines was shown to increase in the future. The use of sediment contaminant concentration profiling overcomes the

potential for such atmospherically derived contaminant concentrations to be interpreted as resulting from local industry allowing more effective mitigation and remediation decisions.

1. Introduction

Quantification and source apportionment of contaminants observed in lake sediments in isolated "pristine" environments is becoming increasingly important as negative effects on ecosystem health are being demonstrated [1, 2]. Industrial facilities located in these areas can represent a potential point source of contaminants; however long-range transport of both organic and inorganic contaminants has also been demonstrated to play a significant role in contaminant concentrations [3-5]. Differentiating between point and atmospheric sources then has important implications for monitoring and remediation efforts. If contaminants are found to be related to an industrial site, then point source focussed remediation may represent an effective approach. However, if regional atmospheric deposition is found to be the source of contaminants, remediation efforts and responsibility for these efforts may need to be focussed elsewhere entirely. Many atmospherically derived contaminants such as mercury (Hg), lead (Pb) and polycyclic aromatic hydrocarbons (PAH) are by-products associated with anthropogenic processes, such as combustion, and can travel large distances in the atmosphere before being deposited [6-8]. If such a process is

responsible for contaminants observed in a particular location, then remediation efforts should focus on the source of these atmospheric chemicals.

1.1 Atmospheric Sources

Atmospherically deposited Hg has natural sources including volcanic eruptions and biomass fires as well as anthropogenic sources such as coal combustion, waste incineration and other types of industrial activity [5, 9, 10]. Hg associated with combustion derived particulate is often deposited relatively close to the source [8]; however the fraction associated with very fine particulate can be transported over 1000's of km [11]. Fitzgerald et al [10] note that over the last century anthropogenic emissions of Hg have become more dominant than natural sources. This trend is particularly evident when assessing concentration profiles in sediments from remote lakes [10]. Studies regarding Hg profiles in sediments of remote lakes in Northern Quebec and Ontario indicate that regional atmospheric deposition increases steadily from the background levels beginning around the industrial revolution (circa 1900) [5, 9]. Modern levels of Hg deposition at these sites have been found to be greater than 2 times the natural background [5, 10]. Similar signals have been observed on a global scale suggesting that Hg contamination can be an indicator of both regional atmospheric deposition as well as global atmospheric deposition [8, 10, 12].

Atmospheric deposition of Pb has been greatly affected by anthropogenic activities [4, 13, 14]. Generally Pb deposition at urbanized sites in the United States has been found to correlate with the consumption of leaded gasoline [13,

15]. Lima et al [13] found Pb concentrations in the Pettequamscutt River increased sharply with the implementation of tetraethyl lead (TEL) as a gasoline additive in the 1920s. Concentrations peaked in the 1970s and began decreasing as leaded gasoline was phased out of North American fuels [13, 14]. However this correlation is not as clear in remote areas. Outridge et al [4] found that anthropogenic Pb concentrations from two sub-arctic lakes increased steadily from the early 1900s until the late 1990s while other lakes in the high arctic exhibited constant Pb deposition over the same time period [4]. Several other mid-latitude remote lakes were found to have a similar increasing pattern [5, 14, 16] as sub-arctic lakes from Outridge et al [4]. It was hypothesized that the differences in Pb deposition was due to latitudinal differences in precipitation which significantly affects the rate of atmospheric Pb scavenging [4].

Atmospheric deposition of PAH has been shown to correlate well with industrialization and energy generation [3, 17-19]. Profiles of PAH deposition increase with industrialization beginning circa 1900 to a peak in the late 1950s which is coincident with peak coal consumption in North America [3, 7, 18]. PAH deposition has been shown to decrease after this primarily due to the conversion of industry and power generation to cleaner burning fuels such as oil and/or natural gas [3, 7, 18]. This decline was expected to continue as combustion technology continued to develop and legislation required controlled emissions [3, 7, 18]. In chapter 2 of this thesis, this was shown to be true of Siskiwit Lake on Isle Royale in northern Michigan. However, recent work has found that in some

sub-urban or urban areas PAH deposition became constant or began increasing again in the 1990s [7, 20]. Increased PAH deposition in these areas has been correlated to increased use of passenger vehicles [20] or increased diesel consumption [7].

1.2 Point sources

Point source release of Hg to the environment is typically associated with anthropogenic activities and can be a result of processes such as mining [21] or sewage and septic system outflows [22]. Sediment profiles have been shown to preserve the occurrence of point source Hg releases to rivers and lakes in the past [23]. Typically these events are associated with high sedimentary Hg concentrations and manifest as a peak or abrupt increase in sediment cores [23]. These events clearly overprint any atmospheric signal and thus are recognizable in sediment core Hg profiles.

Point source release of Pb can also be associated with anthropogenic activities such as mining runoff and urban storm runoff [14]. Similar to Hg, it is expected that sediment core profiles will record changes in magnitude of Pb point sources thus overprinting the comparatively low concentrations of atmospheric deposition.

Point source releases of PAH are typically associated with events such as petroleum spills or creosote/coal tar spills [24]. These release large quantities of PAH in a single event at concentrations which can overprint atmospheric deposition in a sediment core PAH profile. Changes in sustained point source

release such as urban or roadway runoff containing crankcase oil will also be recognized as a shift in PAH concentrations in sediment cores [25]. Such petroleum based PAH are often observed in association with the presence of an unresolved complex mixture (UCM) associated with petroleum product biodegradation. The presence of this UCM can be quantified to assess the degree of point source petroleum contamination [26].

1.3 Source differentiation

Differentiating between local industrial and atmospheric deposition sources in lake sediments requires an unambiguous signal. Identifying such a signal is particularly important to environmental monitoring and remediation as accurate differentiation is crucial to appropriate remediation activities as well as apportionment of responsibility. Current practices in site assessment however, do not have sufficient resolution to achieve such differentiation. Standard sampling guidelines define sediment samples as the 15 cm of sediment below the water column [27]. Typically these 15 cm of sediments are sampled using a dredge or grab sampler after which the sediment is homogenized and analyzed as a bulk sample; thus no temporal information regarding the deposition of the observed contaminant concentrations is retained. This provides a one-dimensional assessment that cannot identify characteristics of atmospheric deposition and effectively assumes any exceedences of regulatory guidelines is a result of point source industrial contamination. In contrast, measurement of contaminant concentration profiles deposited in dated sediment cores preserves

the temporal information necessary to identify changes in sources over time, including recognition of characteristic patterns representing atmospheric deposition and the ability identify any abrupt peaks or changes in deposition related to historical point source releases. Thus, contaminant concentration profiling in sediments allows a much more effective assessment of the sources of contaminants at a given site.

The goal of this study was to demonstrate the efficacy of sediment core contaminant profiles over current dredge or grab sampling procedures. Cores were retrieved from two nearby lakes in northern Ontario. One of the lakes, defined as Lake A, has a shoreline industrial facility which was constructed in the 1960s (figure 3-1). The second lake is defined as Lake B and is similar in environmental setting to Lake A, the exception being that there is no industrial facility near Lake B. Organic (PAH and UCM) and inorganic (Pb and Hg) contaminants were profiled in both lakes historically up to circa 100 years as determined by ^{210}Pb dating. Direct comparison of the contaminant concentration profiles from Lakes A and B as well as a comparison to previously published sediment concentration profiles was used to assess the source of contamination. Subsequently, the extent to which atmospheric deposition could be responsible for exceedences of current Canadian sediment quality guidelines was assessed

as well as the implications this may have for assessments at other sites.

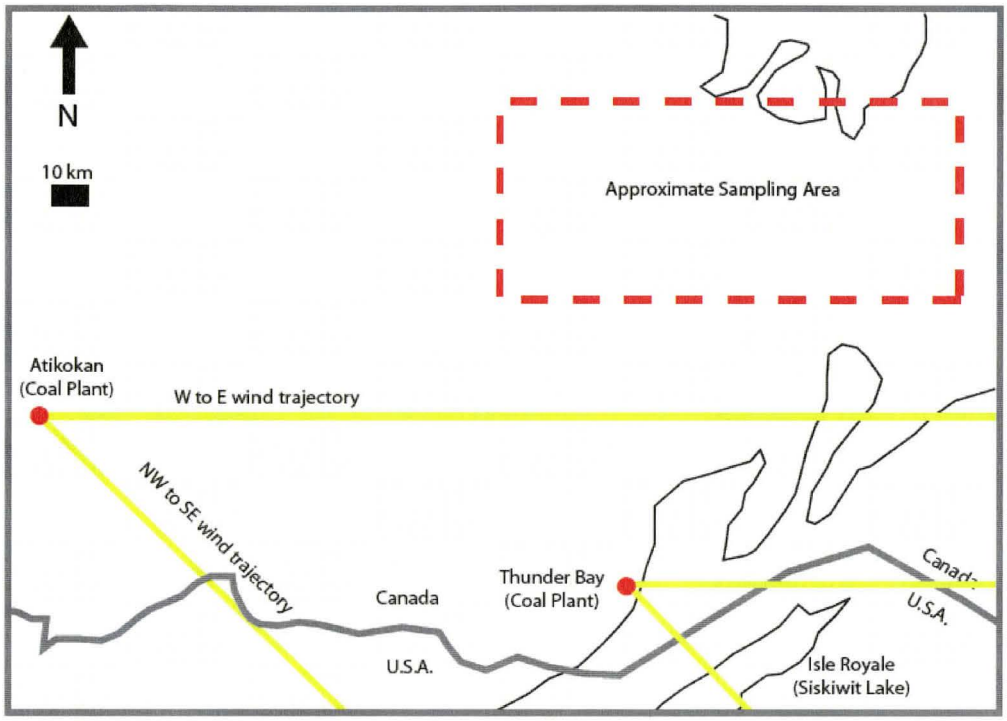

Figure 3-1: A map showing the approximate location of sampling as well as the location of nearby regional coal powered generating stations and major centers (Red dots). Yellow lines mark the dominant wind directions for the area. Location of Siskiwit is noted near the bottom of the figure.

2. Sampling and Methodology

Piston cores were taken from the center of both lakes for comparative analysis. A second core was taken from Lake A proximal to the industrial facility to provide further assessment of the potential role of this industrial point source. Cores were sectioned on-site into 1 cm intervals using cleaned metal spatulas for PAH samples and cleaned plastic spatulas for Pb and Hg samples. Samples were placed either in Ziploc bags for PAH analysis or metal-clean 125 ml HDPE bottles and kept cool or in the dark until they were frozen at -20 °C upon return to the laboratory.

Samples for metals analysis were freeze dried while samples for PAH analysis were dried at 45 °C. All samples were homogenized using an agate mortar and pestle and subsequently kept at -20 °C until further analysis.

2.1 PAH and UCM quantification

PAH and UCM analysis were performed in parallel; briefly, between 6 and 20 g of sediment was spiked with 5 ppm surrogate standards (9,10-dihydrophenanthrene and m-terphenyl) then microwave extracted (MarsX) in 1:1 hexane/acetone at 115 °C for 20 minutes. Extracts were allowed to cool to approximately 30 degrees then filtered with hexane and dichloromethane through glass fibre filter paper (Whatman) to remove solid sediment portion. Filtered extracts were treated with activated copper pellets to remove elemental sulphur, reduced to approximately 1 ml and fractionated on fully activated silica gel. A total of two fractions were collected: F_1: 1:1 hexane/dichloromethane (non-polar hydrocarbons) and F_2: methanol (remaining polar compounds), which was archived. The F1 fraction was reduced to 100 - 300 ul spiked with an internal standard (o-terphenyl) and transferred to amber vials for analysis.

PAH quantification was performed on a GC/MS (Agilent 6890 GC, Agilent 5973n MS) equipped with a split/splitless injector kept in splitless mode and a 0.25 mm I.D. 30 m DB-XLB column (Jackson and White). The oven was programmed to 65 °C and ramped at 5 degrees per minute to 310 degrees and held for 10 minutes then ramped at 15 degrees per minute to 325 degrees and held for 20 minutes. The following 16 EPA priority PAH were quantified:

naphthalene (Napth), acenapthylene (Acey), acenapthene (Ace), fluorene (Flu), phenanthrene (Phen), anthracene (Anth), fluoranthene (Flua), pyrene (Py), benz(a)anthracene (B(a)A), chrysene (Chry), benzo(b)fluoranthene (B(b)F), benzo(k)fluoranthene (B(k)F), benzo(a)pyrene (B(a)P), benzo(g,h,i)perylene(B(ghi)P), dibenz(a,h)anthracene D(ah)A and ideno(1,2,3-cd)pyrene (Ideno). All PAH were quantified with a 4-point calibration curve ($R2 > 0.995$) and corrected to the recovery of 9,10-dihydrophenanthrene or m-terphenyl.

UCM was quantified by integrating the UCM hump from 12 minutes to 55 minutes in TIC mode. These areas were divided by the internal standard o-terphenyl to correct for volume changes. Estimated concentrations were determined using a 4 point calibration curve of 5α-cholestane. All concentrations were corrected to the recovery of m-terphenyl.

2.2 Pb quantification

The leachable Pb fraction was extracted via dilute acid leach using 3N hydrochloric acid and 1.75N nitric acid [14]. Between 10 and 12 mg of dried homogenized sediment was weighed into polypropylene centrifuge tubes. 1 ml of dilute acid solution was added to each sample using a micropipette. The samples were sonicated for 90 minutes and allowed to cool overnight. The mixture was centrifuged at 13,000 rpm for 10 minutes and the extract was siphoned from the sediment using a micropipette. The extract was diluted to 10 ml using 2% nitric

acid and analyzed via ICP-MS (Perkin Elmer Elan 6100). Pb was quantified using a 4 point standard curve (R2>0.999).

2.3 Hg quantification

Total Hg was quantified after freeze-drying and homogenizing sediments. Between 60 and 150 mg of sediment was weighed into pre-cleaned Nickel vessels. The vessels were inserted directly into the analytical instrument (Hydra-C) and combusted at 850 °C to vaporize all labile elements. Hg vapour is retained by sorption to gold coated sand while all other elements are purged. The Hg is removed from the sand using progressive heating and analyzed by exposure to an Hg lamp. Hg concentrations were determined via a 5 point calibration curve (R2>0.999).

2.4 ^{210}Pb Analysis

Total ^{210}Pb activity was analyzed in 1 cm sections from cores taken from the middle of both Lakes A and B. Approximately 1 g of sediment was dried then acid treated and prepared using a ^{210}Po enrichment method. The final ^{210}Po was plated on highly polished Ag discs and the activity of each sample was measured with an alpha counting device in disintegrations per minute (dpm). Sedimentation rates were determined using two versions of the constant initial concentration model (CIC1 and CIC2). For a more complete discussion of this please see appendix B.

2.5 Quality Control

Accuracy of the PAH method was determined using three samples of standard reference material EC-1 (Environment Canada, lacustrine sediment). Our results were all within 16% of the reference values. Precision (average relative standard deviation <6%) was measured by triplicate injections of standards and samples. The limits of quantification are as follows: for parent PAH compounds 0.5 ppm in solution, for Pb 2 ppm in solution and for Hg 10 ng g-1 sediment.

PAH extraction took place in batches, procedural blanks (n=3) were run with each batch, there were no detectable PAH concentrations in any of the blanks. Precision of Pb analysis (<3%) was completed by triplicate injections of standards instrument drift was monitored using repeated injections of known standards. Procedural blanks for metals analysis indicated no significant contamination from the method. Accuracy of Hg analysis was determined by analysis of NIST 1944 Standard New Jersey/New York waterway sediment reference; all concentrations were within 10% of certified values. Precision of Hg analysis (<6%) was determined using triplicate injections of standards and a sample.

3. Results

3.1 ^{210}Pb dating

The CIC2 model was used to calculate final sedimentation rates and subsequent dates for both sites. The average sedimentation rate in Lake A was

0.096 cm yr-1 which is approximately double the average sedimentation rate of 0.054 cm yr-1 in Lake B. Thus 10 cm depth in Lake A sediments, and 6 cm depth in Lake B, represented 100 years respectively. ^{210}Pb analysis was not directly performed on the industry proximal core from Lake A and was instead inferred from the middle core. Sedimentation rates are not expected to change drastically due to the relative closeness of the cores within the small sedimentary basin. For more information regarding dating methods please see appendix B.

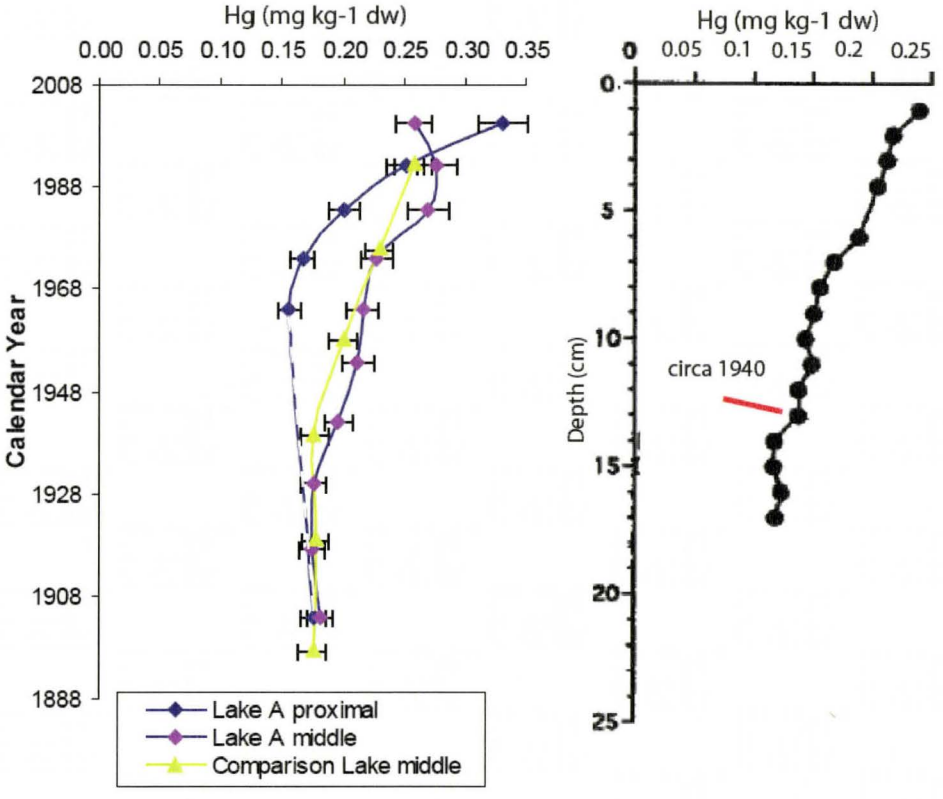

Figure 3-2: Left image is a plot of all Hg data from this study; each point represents a 1 cm core slice. Right image is a plot of Hg data from an unnamed lake in northern Quebec (Lucotte et al, 1995). Error bars are 6% analytical error.

3.2 Hg Concentrations

Hg concentrations from all cores are plotted in mg kg-1 dry weight (dw) versus calendar year as determined by ^{210}Pb dating to a maximum of 100 years as shown in figure 3-2. Hg concentration profiles were very similar for all three cores. Concentrations in the bottom samples for all cores, representing circa 1900 were 0.18 mg kg, while concentrations in the most recent sediments were 0.26 +/- 0.07. Concentration increases over the sediment cores had overall very similar shapes. The concentration change was somewhat more abrupt in the industry proximal core from Lake A but in general deposition profiles agreed with each other.

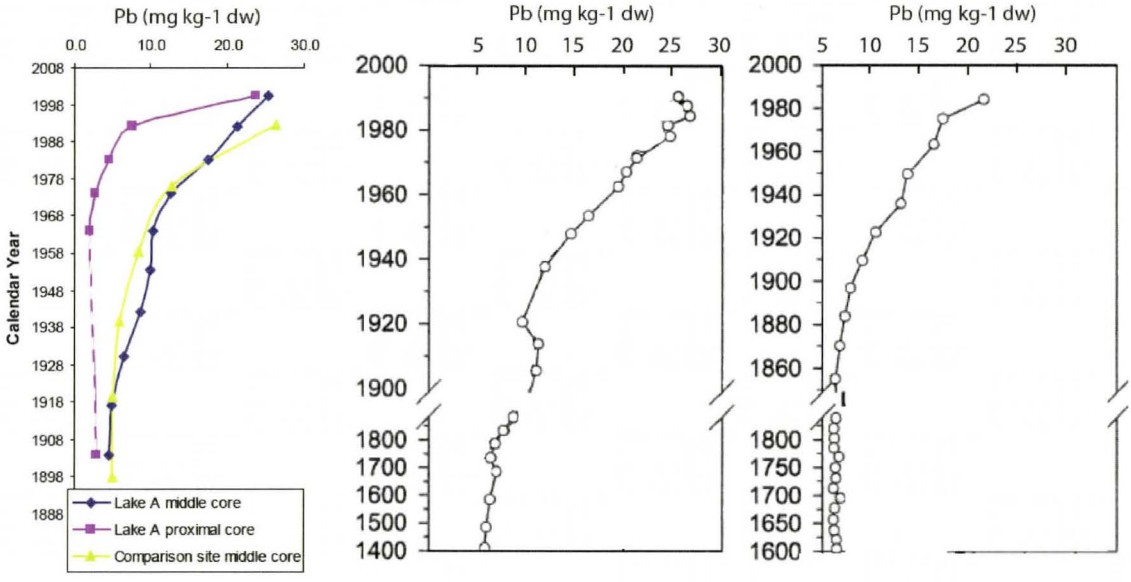

Figure 3-3: Left image is a plot of Pb data from all cores in this study; each data point represents a single 1 cm core slice. Center image is a plot of Pb concentrations from sub-arctic Imitavik Lake (Outridge et al, 2002) and right image is a plot of Pb concentrations sub-arctic Far Lake (Outridge et al, 2002). Error bars are less than the size of the plot symbols.

3.3 Lead (Pb)

Pb concentrations (mg kg-1 dw) are plotted versus calendar year as determined by ^{210}Pb dating in figure 3-3. As observed for Hg, Pb concentrations and trends for all cores were very similar. Concentrations of circa 0.5 mg kg-1 dw were found in the bottom sediments representing deposition around 1900. Concentrations increased to circa 0.25 mg kg-1 dw in the most recent sediments from all cores. Similar to Hg, the increase occurred somewhat more abruptly in the Lake A proximal core however the change is still comparable to the other cores.

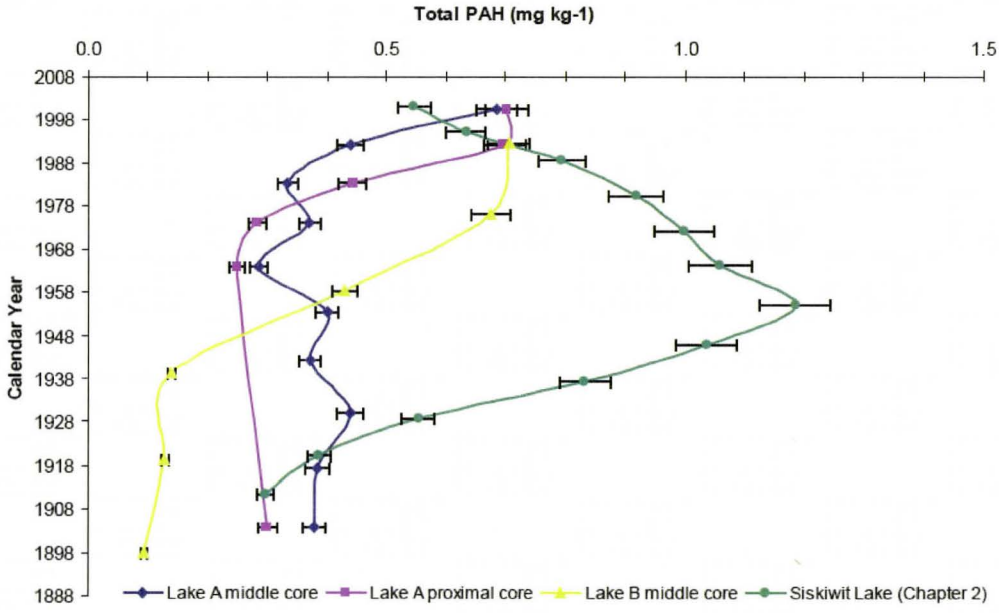

Figure 3-4: A graph showing total PAH data from all cores in this study as well as data from Siskiwit Lake in chapter 2 of this thesis. Each data point represents a 1 cm core slice. Error bars are 6% analytical error.

3.4 Pyrogenic PAH Concentrations

Concentrations of total pyrogenic PAH in mg kg-1 dw are plotted versus calendar year as determined by ^{210}Pb dating in figure 3-4. PAH concentrations and trends were similar for the cores in Lake A. Bottom sediments of the Lake A cores representing the early 1900's were circa 0.3 mg kg-1 dw and were variable circa 0.4 mg kg-1 dw until 1988 then increased steadily to concentrations of 0.7 mg kg-1 dw in the most recent sediments. Concentrations from the bottom of the Lake B core were circa 0.1 mg kg-1 dw and increased beginning approximately 1940 to concentrations of 0.7 mg kg-1 dw, the same concentration as observed in upper sediments in Lake A.

3.5 UCM detection

There was no significant indication of UCM found in the cores (figure 3-5) indicating minimal impact from petroleum derived point sources. Several large n-alkane peaks ranging from C17 to C31 were identified in the chromatograms via comparison with a known alkane standard. While this study did not directly quantify n-alkanes, these peaks show an odd over even amplitude preference consistent with terrestrial plant waxes as an origin rather than petroleum hydrocarbons [28].

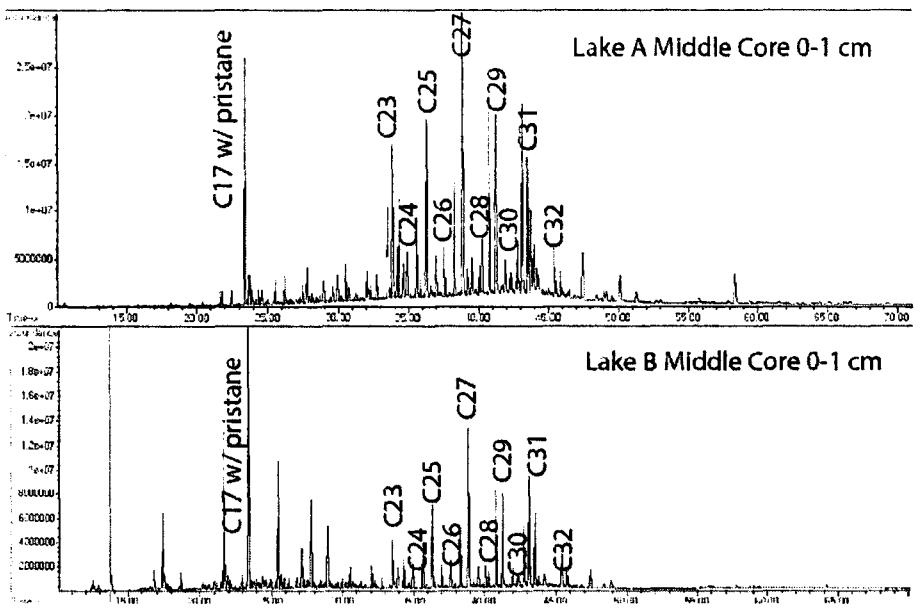

Figure 3-5: Example of chromatograms from this study showing the lack of UCM in both Lake A and Lake B. Large alkane peaks (see text) are marked with their respective carbon number.

4. Discussion

4.1 Sediment Core Profiles of Hg and Pb

Profiles of Hg and Pb from this study strongly suggest that atmospheric deposition rather than local industrial activity is the dominant source of these metals. The middle cores of Lake A and Lake B (figures 3-2 and 3-3) demonstrate that trends and concentrations are similar at both sites despite the lack of industry at Lake B. There are also no sudden changes in Hg or Pb concentration concurrent with the industrial facility's construction in the 1960s, suggesting that the lake sediments were not impacted by this event or the subsequent industrial operations. Moreover, the core proximal to the industrial shoreline from Lake A does not record significantly higher concentrations for Pb or Hg than the middle core suggesting that there is no spatial relationship

between proximity to industry and concentration of contaminant as would be expected if the industry was a point source of contamination.

Comparison of Hg and Pb profiles from Lake A and Lake B to similar sites in the literature corroborates atmospheric deposition as the source of contamination in Lake A (figures 3-2 and 3-3). The increasing trends and concentrations found in Lake A and B are consistent with Hg and Pb deposition demonstrated in several lakes in northern Quebec [5] and Pb deposition for two sub-arctic lakes near James Bay [4]. The literature sites chosen for comparison are similar in latitude and entirely isolated from industry thus previous studies have found that the only plausible source of contamination to the these lakes is atmospheric deposition [4, 5]. Given the similarity of the profiles from Lakes A and B, it is very likely that atmospheric deposition is responsible for Pb and Hg loadings in this study thus the industrial facility located on Lake A is not a significant source of Pb and Hg to the sediments.

4.2 Sediment core profiles of PAH

PAH profiles also suggest that the industrial facility is not a point source of contamination to sediments in Lake A (figure 3-4). The similarity in observed maximum PAH concentrations occurring in the most recent sediments from Lake A and B PAH profiles suggest that recent input sources are similar. Moreover, as observed for Pb and Hg, there is also no change in PAH concentration in Lake A that is coincident with the construction of the industrial facility in the 1960s indicating that the facility did not affect PAH deposition. In addition, if the industry

was a point source of PAH to the sediment, there would be an increase in sediment PAH concentrations expected for the core taken in closer proximity to the industrial facility. Both of the cores from Lake A, proximal and middle, demonstrate very similar PAH profile trends and concentrations suggesting that there is no spatial relationship between PAH concentrations and industry proximity. Finally, there was no UCM detected in any of the cores, notably including the core closest to the industrial site, indicating that the likelihood of PAH deposition associated with a petroleum spill or runoff resulting from industrial activities is minimal.

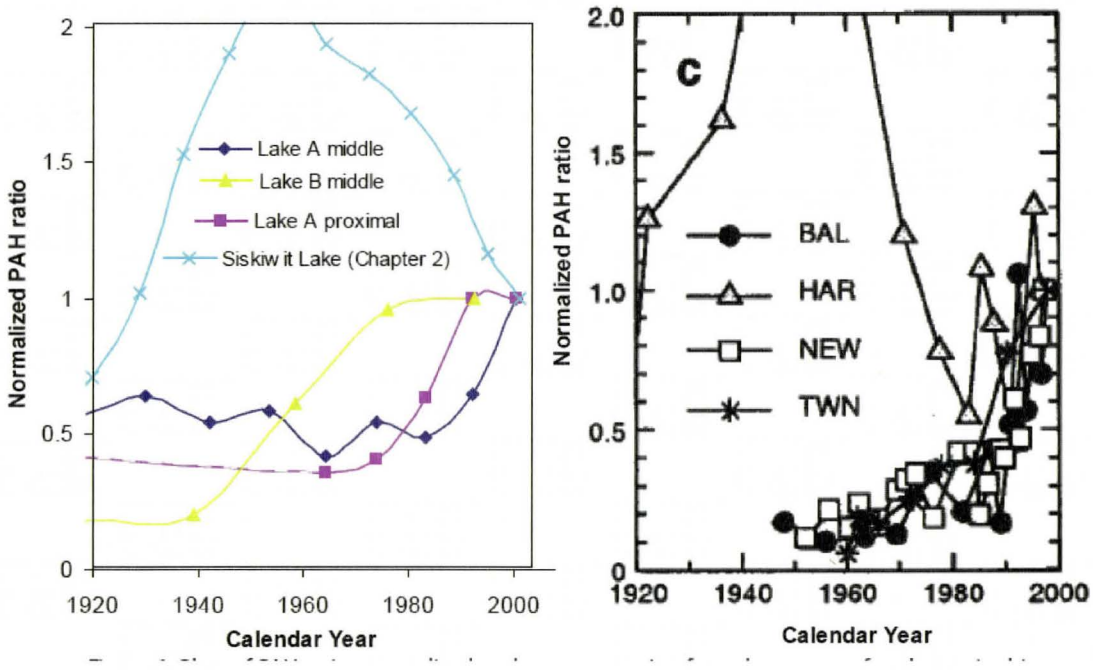

Figure 3-6: Left image are plots of PAH normalized to the concentration from the top centimetre of each core in this study as well as data from Siskiwit Lake (chapter 2 of this thesis). Right image are normalized plots from Van Metre et al (2000). Abbreviations are as follows: BAL= Lake Ballinger, WA, USA; HAR=Lake Harriet, MN, USA; NEW=Newbridge Pond, NY, USA; TWN=Town Lake, TX, USA.

The profiles of PAH concentrations observed in this study were very similar in trends to those observed by Van Metre et al (2000) at several sub-urban sites in the United States (figure 3-6). Van Metre et al attributed the recent increases they observed to various non-point sources such as increases in urbanization of watersheds or, at sites where land-use indicated that urbanization was constant, to increased local traffic [20]. The timing of recent increases in PAH concentrations that were found in Lake A are similar to those of Van Metre [20] but are of lesser magnitude. However, these increases occur in Lakes A and B despite there being no urbanization of the watershed. There is, however, a two-lane highway adjacent to the lake which receives substantial heavy truck traffic as well as an adjacent rail line which are potential sources for both Lake A and Lake B.

4.3 Absence of PAH atmospheric deposition curve found at other sites

Interestingly, PAH profiles from this study do not show the long range atmospheric transport and deposition profiles found in both urbanized watersheds [7, 20] and isolated watersheds [3, 29, 30], including nearby Siskiwit Lake as demonstrated in chapter 2 of this thesis. As noted, the lack of this characteristic profile is however consistent with results at several sites sampled by Van Metre et al [20] where deposition was related to vehicular traffic. However, the proximity of these lakes to Siskiwit Lake where this atmospheric profile was observed both by McVeety et al and in Chapter 2 of this thesis raises the question as to why these differences in atmospheric PAH sources between these two relatively

closely located study sites are observed. The data attributed to long-range transport and deposition data from Siskiwit Lake in chapter 2 of this thesis is plotted with the data from Lakes A and B in figure 4. Siskiwit Lake shows substantially higher maximum PAH concentrations of 1.2 mg kg-1 dw compared to 0.7 mg kg-1 dw from Lakes A and B. Furthermore, maximum concentrations in Siskiwit Lake occur in a distinct peak circa 1960 whereas they occur in the most recent sediment in Lakes A and B.

The explanation for the absence of these features in this study may relate to regional wind patterns and the relative configuration of nearby sources. Data from Environment Canada and Natural Resources Canada shows that predominant wind patterns in this area are west to east with a secondary direction of northwest to southeast (Figure 1)[31, 32]. The largest potential regional sources of PAH in this area are the coal power generating plants in Atikokan, Ontario and Thunder Bay, Ontario as well as the urban industrial sources from Thunder Bay itself. As can be seen in Figure 3-1, Siskiwit Lake falls within the area expected to be impacted by atmospheric deposition from these sources based on wind directions. In contrast, Lakes A and B are north of the dominant wind trajectories from these sources. The prevailing wind trajectories and the relative configuration of source shown in figure 3-1 suggests that in fact, Siskiwit lake may not be as isolated from impacts as has been indicated previously [3], rather that it is receiving ongoing deposition from these regional sources. The two lakes in this study appear to be more isolated from

local and regional atmospheric sources based on both wind direction and PAH deposition concentration profiles. As such, the lower PAH concentrations observed in this study appear to be closer to levels that would be expected for a remote system. However, in contrast to the indication that these lakes are more isolated than Siskiwit from regional PAH sources, the similarity in depositional patterns to the work of Van Metre et al [20] suggests that even these locations are being impacted by recently increasing sources such as transportation related combustion due to increased traffic on the highway.

4.4 PAH and Hg exceedences of CCME guidelines

Despite the evidence that PAH, Hg, and Pb are being atmospherically deposited in Lakes A and B, Napth, Anth, Py, B(a)A, B(a)P and Hg concentrations in several of the upper one centimetre intervals of sediments in both lakes A and B are equal to or greater than Canada Sediment Quality Guidelines for the Protection of Aquatic Life as set by the Canadian Council of the Ministers of the Environment (table 3-1; CCME) [33]. This observation suggests that atmospheric deposition alone has the potential to result in sedimentary concentrations exceeding CCME guidelines. The potential for a long range or regional source to result in concentrations exceeding guidelines has significant implications to the assessment of contaminated sites, and in particular to our ability to accurately apportion responsibility for such exceedences.

However, comparison of the concentrations observed in these lakes to CCME guidelines requires the differences in sampling protocols to be addressed.

While academic investigations routinely measure profiles of contaminant concentrations in sediments, sediment sampling associated with site assessment generally involves dredge or grab sampling of this upper 15 cm of material directly below the water column [27] with subsequent homogenization and bulk analysis of the sample. Using this methodology, a previous assessment of the Lake A site found exceedences for Napth and Hg. In order to compare the results of our study to this previous report, the sediment core profiles from Lake A and B

Table 3-1: Concentration data tables. Unless otherwise specified, all concentrations are in mg kg-1

Sample	Year	mid pt	Napth	Acey	Ace	Flu	Phen	Anth	Flua	Py	B(a)A	Chry	B(b)F and	B(a)P	Pery	B(ghi)P	D(ah)A	Ideno	Lead (Pb)	Mercury (Hg)
CCME guidline			0.03	0.06	0.07	0.02	0.04	0.05	0.11	0.05	0.03	0.06	N.V.	0.03	N.V.	N.V.	0.06	N.V.	35	0.17
Lake A Middle Core																				
LAM 0-1	2000	0.5	0.04	0.02	N.D.	0.02	0.02	0.07	0.11	0.08	0.06	0.03	0.07	0.05	0.87	0.07	N.D.	0.07	25	0.26
LAM 1-2	1992	1.5	0.02	N.Q.	N.D.	0.02	0.02	0.04	0.07	0.05	0.04	0.02	0.05	0.03	0.58	0.05	N.D.	0.05	21	0.25
LAM 2-3	1983	2.5	'0.02	N.Q.	N.D.	N.Q.	0.01	0.03	0.05	0.04	0.04	0.02	0.05	0.03	0.87	0.05	N.D.	0.04	18	0.27
LAM 3-4	1974	3.5	'0.02	N.Q.	N.D.	N.D.	0.02	0.04	0.08	0.04	0.04	0.02	0.05	0.03	0.90	0.05	N.D.	0.04	13	0.23
LAM 4-5	1964	4.5	'0.02	N.Q.	N.D.	N.D.	0.02	0.03	0.04	0.03	0.04	0.02	0.04	0.03	1.14	0.03	N.D.	0.03	10	0.22
LAM 5-6	1953	5.5	0.02	N.Q.	N.D.	N.D.	0.02	0.05	0.05	0.03	0.05	0.02	0.05	0.04	2.33	0.05	N.D.	0.04	10	0.21
LAM 6-7	1942	6.5	0.03	N.Q.	N.D.	N.D.	'0.02	0.05	0.05	0.03	0.05	0.02	0.05	0.04	2.17	0.05	N.D.	0.03	9	0.20
LAM 7-8	1930	7.5	0.03	N.Q.	N.D.	N.D.	'0.02	0.06	0.05	0.04	0.06	'0.02	0.05	0.05	3.44	0.05	N.D.	0.04	7	0.18
LAM 8-9	1917	8.5	0.04	N.Q.	N.D.	N.D.	'0.02	0.05	0.04	0.03	0.05	'0.02	0.05	0.04	2.87	0.05	N.D.	0.03	5	0.17
LAM 9-10	1904	9.5	0.03	N.Q.	N.D.	N.D.	0.02	0.05	0.04	0.03	0.05	'0.02	0.04	0.04	2.16	0.04	N.D.	0.03	5	0.18
15 cm dredge			0.03	N.Q.	N.D.	N.Q.	0.02	0.05	0.05	0.04	0.05	0.02	N.V.	0.04	N.V.	N.V.	N.D.	N.V.	10	0.21
15 cm dredge in 50 yrs			0.04	N.Q.	N.D.	N.Q.	0.02	0.06	0.06	0.05	0.05	0.02	N.V.	0.05	N.V.	N.V.	N.D.	N.V.	17	0.23
Lake B Middle Core																				
LBM 0-1	1993	0.5	0.05	N.Q.	N.D.	N.Q.	N.Q.	0.08	0.13	0.09	0.07	0.03	0.08	0.05	2.22	0.07	N.D.	0.07	26	0.26
LBM 1-2	1978	1.5	0.04	N.Q.	N.D.	N.Q.	N.Q.	0.08	0.13	0.09	0.07	0.02	0.08	0.05	2.96	0.07	N.D.	0.07	13	0.23
LBM 2-3	1958	2.5	0.03	N.Q.	N.D.	N.Q.	N.Q.	0.06	0.08	0.06	0.04	0.02	0.05	0.03	2.82	0.04	N.D.	0.04	9	0.20
LBM 3-4	1939	3.5	'0.02	N.Q.	N.D.	N.Q.	N.Q.	0.05	0.04	0.03	0.03	'0.02	N.Q.	'0.02	3.16	N.Q.	N.D.	N.Q	6	0.18
LBM 4-5	1919	4.5	'0.02	N.Q.	N.D.	N.Q.	N.Q.	0.04	0.03	0.02	0.03	'0.02	N.Q.	'0.02	3.74	N.Q.	N.D.	N.Q	5	0.18
LBM 5-6	1898	5.5	'0.02	N.Q.	N.D.	N.Q.	N.Q.	0.04	0.03	'0.02	0.02	'0.02	N.Q.	'0.02	4.22	N.Q.	N.D	N.Q	5	0.18
15 cm dredge			0.02	N.Q.	N.D.	N.Q.	N.Q.	0.05	0.05	0.03	0.03	0.02	N.V.	0.02	N.V.	N.V.	N.D	N.V	7	0.19
15 cm dredge in 50 yrs			0.03	N.Q.	N.D.	N.Q.	N.Q.	0.06	0.07	0.06	0.04	0.02	N.V.	0.03	N.V.	N.V.	N.D	N.V	12	0.21

* Concentration below quantification limit value is an estimate
N.Q. Concentration below quantification limit no estimate was produced
N.D. Compound not detected
N.V No CCME value for compound

were modeled to estimate concentrations in a homogenized 15 cm dredge sample (table 3-1). In order to do this, the contribution of sediments below the bottom of the core profiles in this study had to be included. This was done by assuming the concentration in the bottom sample from each core was representative of the concentration for the number of centimetres required to reach a sediment depth of 15 cm. Thus in addition to the 10 cm analyzed in the Lake A core, 5 cm was added and the concentrations in these sediments were assumed to be the same concentration as the lower most interval analyzed. Similarly, for Lake B of which 6 cm were analyzed, an additional 9 cm was added with an assumed concentration equivalent to the lower most concentration analyzed. This assumption is reasonable as studies show that PAH and Hg deposition in this region prior to 1900 (approximately the bottom of each core) represent essentially background pre-industrial sources and does not vary considerably [3-5, 34]. In Lake A the modeled concentrations of the Napth, Anth, Py, B(a)A, B(a)P and Hg were at or above CCME guidelines, whereas in Lake B Anth, B(a)A and Hg were above guidelines. Thus, though contaminant deposition to these lakes is consistent with an atmospheric source, the resultant sedimentary concentrations can still exceed CCME guideline levels. This result has significant implications to site assessment and remediation. Without using the sediment concentration profile and comparison approach of this study, observations of contaminant concentrations exceeding guidelines would likely

have been attributed to the local industry on Lake A. This industry may have then been determined to be responsible for the remediation of these sediments, though all available evidence in this study indicates that these contaminants had an atmospheric source and thus that this facility was not responsible for the observed contamination. These results demonstrate that accurate differentiation and demonstration of local or point source impacts is essential when assessing contaminated sites.

4.5 Future Implications

The potential for atmospheric deposition to cause exceedences of CCME sediment quality guidelines using current dredge sampling protocols is expected to increase in the future assuming that ongoing sediment deposition contains contaminant concentrations consistent with current levels. In order to assess the impact of future sediment accumulation in Lake A, the expected concentrations for a 15 cm dredge sample were modelled using the measured core concentrations and adding 5 cm of new sediment to the top of the core, the equivalent of 50 years of deposition. The contaminant concentrations in this new sediment were assumed to the same as the current upper sediment concentrations. Based on these assumptions the modeled concentrations of several contaminants increased indicating that ongoing deposition at current levels will result in a greater number of contaminants exceeding standards than currently observed.

A similar process was performed using the middle core from Lake B, in this case however due to the lower average sedimentation rate, only three centimetres of upper sediment at current concentrations were added to represent the same 50 year period used in Lake A. Nonetheless, when modeled concentrations for the upper 15 cm were calculated including this additional 3 cm of additional sediment Napth, Anth, Py, B(a)A, B(a)P and Hg all increased to levels above CCME guidelines.

It is worth noting that these modeled concentrations assumed a steady state deposition of contaminants at current rates. Based on the shape of the deposition curves, this assumption is likely close to a best case scenario. If sediment concentrations of contaminants increase then greater exceedences of guidelines can be expected.

4.6 Effect of sedimentation rate on bulk samples

In addition to trends in contaminant concentrations in deposited sediments, sedimentation rate also has an effect on concentrations found in dredge samples. Currently at Lake B, 15 cm of sediment represents approximately 278 years at an average sedimentation rate of 0.054 cm yr-1. At Lake A however, with an average sedimentation rate of 0.096 cm yr-1, 15 cm represents approximately 156 years; a difference of 122 years. Atmospheric deposition of combustion derived pollutants, such as Hg, Pb and PAH, was low prior to the industrial revolution circa 1900 [3-5]. Thus, 15 cm at Lake B includes 9 cm (178 years) of the comparatively low pre-industrialized atmospheric

deposition while Lake A includes only 5 cm (56 years). This effect will inevitably result in observed concentrations being lower in lakes with low sedimentation rates. This further demonstrates that the assessment of sedimentation rate and sediment contaminant concentrations via core profiling and dating is essential in assessing current trends. This observation also raises several questions: Does including sediments deposited long before the industrial revolution accurately represent current industrial sediment impacts? And potentially more importantly, what sediment concentrations should we be concerned about. If bioturbation is relatively low, contaminant concentrations in surface sediments will be far more important in controlling biological exposure.

5. Implications to site assessment

The relative contributions of atmospheric deposition to contaminant concentrations observed in lake sediments is often not effectively assessed or is underestimated using current dredge or grab sampling techniques. This is especially relevant because, as demonstrated in this study, atmospheric deposition alone may have the potential to produce concentrations of some contaminants that are at or above current CCME guidelines using these methods. This may result in inaccurate apportionment of responsibility for observed contaminant concentrations and/or ineffective mitigation and remediation efforts.

Sediment core profiling can effectively differentiate atmospheric deposition and point source contamination. Sediment core profiles include a temporal component which allows assessment of contaminant deposition through history

thereby providing the ability to recognize atmospheric deposition curves as well as other notable changes in concentration potentially including previous point source releases. This ability is invaluable to site assessment and thus sediment core contaminant profiling is a superior sampling and analysis method in comparison to dredge sampling and bulk analysis.

Differentiation of atmospheric deposition versus point source contamination can become even more important for sites exhibiting higher sedimentary PAH concentration such as those at urban or sub-urban sites described by Lima et al {Lima} and Van Metre et al {Van Metre}. At these site atmospheric deposition can produce sedimentary concentrations that are orders of magnitude above those found in Lakes A and B in this study. Thus the potential is even greater to observe concentrations exceeding guideline that are the result of atmospheric deposition alone. Alternatively, atmospheric deposition has the potential to mask the existence of point sources contributing to sedimentary systems. In either case, the apportionment of responsibility and effectiveness of mitigation and remediation efforts would be compromised by the lack of accurate understanding of contaminant sources. The implementation of a method such as sediment core contaminant profiles which can differentiate atmospheric from point sources is thus integral in future environmental monitoring efforts in urban, sub-urban and remote settings.

Citations

1. Hung, H.; Blanchard, P.; Halsall, C. J.; Bidleman, T. F.; Stern, G. A.; Fellin, P.; Muir, D. C. G.; Barrie, L. A.; Jantunen, L. M.; Helm, P. A.; Ma, J.; Konoplev, A., Temporal and spatial variabilities of atmospheric polychlorinated biphenyls (PCBs), organochlorine (OC) pesticides and polycyclic aromatic hydrocarbons (PAHs) in the Canadian Arctic: Results from a decade of monitoring. *Science of the Total Environment* **2005,** *342*, (1-3), 119-144.
2. McDonald, J. D.; White, R. K.; Barr, E. B.; Zielinska, B.; Chow, J. C.; Grosjean, E., Generation and characterization of hardwood smoke inhalation exposure atmospheres. *Aerosol Science and Technology* **2006,** *40*, (8), 573-584.
3. McVeety, B. D.; Hites, R. A., Atmospheric deposition of Polycyclic Aromatic Hydrocarbons to water surfaces: A mass balance approach. *Atmospheric Environment* **1988,** *22*, (3), 511-536.
4. Outridge, P. M.; Hermanson, M. H.; Lockhart, W. L., Regional variations in atmospheric deposition and sources of anthropogenic lead in lake sediments across the Canadian Arctic. *Geochimica Et Cosmochimica Acta* **2002,** *66*, (20), 3521-3531.
5. Lucotte, M.; Mucci, A.; Hillairemarcel, C.; Pichet, P.; Grondin, A. In *Anthropogenic Mercury enrichment in remote lakes of northern Quebec (Canada)*, 1995; Kluwer Academic Publ: 1995; pp 467-476.
6. Windsor, J. G.; Hites, R. A., Polycyclic aromatic hydrocarbons in gulf of Maine sediments and Nova Scotia soils. *Geochimica Et Cosmochimica Acta* **1979,** *43*, (1), 27-33.
7. Lima, A. L.; Eglinton, T. I.; Reddy, C. M., High-resolution record of pyrogenic polycyclic aromatic hydrocarbon deposition during the 20th century. *Environmental Science and Technology* **2003,** *37*, 53-61.
8. Iverfeldt, A., Occurrence and turnover of atmospheric mercury over the nordic countries. *Water Air and Soil Pollution* **1991,** *56*, 251-265.
9. Mukherji, S.; Swain, A. K.; Venkataraman, C., Comparative mutagenicity assessment of aerosols in emissions from biofuel combustion. *Atmospheric Environment* **2002,** *36*, (36-37), 5627-5635.
10. Fitzgerald, W. F.; Engstrom, D. R.; Mason, R. P.; Nater, E. A., The Case for Atmospheric Mercury Contamination in Remote Areas. *Environmental Science & Technology* **1998,** *32*, (1), 1-7.
11. Glass, G. E.; Leonard, E. N.; Chan, W. H.; Orr, D. B., Airborne mercury in precipitation in the Lake Superior region. *Journal of Great Lakes Research* **1986,** *12*, (1), 37-51.
12. Slemr, F.; Langer, E., Increase in global atmospheric concentrations of mercury inferred from measurements over the Atlantic Ocean. *Nature* **1992,** *355*, (6359), 434-437.
13. Lima, A. L.; Bergquist, B. A.; Boyle, E. A.; Reuer, M. K.; Dudas, F. O.; Reddy, C. M.; Eglinton, T. I., High-resolution historical records from Pettaquamscutt River basin sediments: 2. Pb isotopes reveal a potential new

stratigraphic marker. *Geochimica Et Cosmochimica Acta* **2005,** *69*, (7), 1813-1824.
14. Graney, J. R.; Halliday, A. N.; Keeler, G. J.; Nriagu, J. O.; Robbins, J. A.; Norton, S. A., Isotopic record of lead pollution in lake sediments from the northeastern United States. *Geochimica Et Cosmochimica Acta* **1995,** *59*, (9), 1715-1728.
15. Nriagu, J. O.; Kemp, A. L. W.; Wong, H. K. T.; Harper, N., Sedimentary record of heavy metal pollution in Lake Erie. *Geochimica Et Cosmochimica Acta* **1979,** *43*, (2), 247-258.
16. Lockhart, W. L.; Wilkinson, P.; Billeck, B. N.; Brunskill, G. J.; Hunt, R. V.; Wagemann, R., Polycyclic aromatic hydrocarbons and mercury in sediments from 2 isolated lakes in central and northern Canada. *Water Science and Technology* **1993,** *28*, (8-9), 43-52.
17. Lima, A. L.; Farrington, J. W.; Reddy, C. M., Combustion-derived Polycyclic Aromatic Hydrocarbons in the environment- a review. *Environmental Forensics* **2005,** *6*, 109-131.
18. Gschwend, P. M.; Hites, R. A., Fluxes of polycyclic aromatic hydrocarbons to marine and lacustrine sediments in the northeastern United States.. *Geochimica Et Cosmochimica Acta* **1981,** *45*, (12), 2359-2367.
19. Laflamme, R. E.; Hites, R. A., Global distribution of polycyclic aromatic hydrocarbons in recent sediments. *Geochimica Et Cosmochimica Acta* **1978,** *42*, (3), 289-303.
20. Van Metre, P. C.; Mahler, B. J.; Furlong, E. T., Urban Sprawl Leaves Its PAH Signature. *Environmental Science and Technology* **2000,** *34*, (19), 4064-4070.
21. Park, J. G.; Curtis, L. R., Mercury Distribution in Sediments and Bioaccumulation by Fish in Two Oregon Reservoirs: Point-Source and Nonpoint-Source Impacted Systems. *Archives of Environmental Contamination and Toxicology* **1997,** *33*, (4), 423-429.
22. Barringer, J. L.; Szabo, Z.; Schneider, D.; Atkinson, W. D.; Gallagher, R. A., Mercury in ground water, septage, leach-field effluent, and soils in residential areas, New Jersey coastal plain. *Science of the Total Environment* **2006,** *361*, (1-3), 144-162.
23. Smith, J. N.; Loring, D. H., Geochronology for mercury pollution in the sediments of the Saguenay Fjord, Quebec. *Environmental Science & Technology* **1981,** *15*, (8), 944-951.
24. Sun, C.; Snape, C. E.; McRae, C.; Fallick, A. E., Resolving coal and petroleum-derived polycyclic aromatic hydrocarbons (PAHs) in some contaminated land samples using compound-specific stable carbon isotope ratio measurements in conjunction with molecular fingerprints*. *Fuel* **2003,** *82*, (15-17), 2017-2023.

25. Latimer, J. S.; Hoffman, E. J.; Hoffman, G.; Fasching, J. L.; Quinn, J. G., Sources of petroleum hydrocarbons in urban runoff. *Water, Air, & Soil Pollution* **1990,** *52*, (1), 1-21.
26. Frysinger, G. S.; Gaines, R. B.; Xu, L.; Reddy, C. M., Resolving the unresolved complex mixture in petroleum-contaminated sediments. *Environmental Science & Technology* **2003,** *37*, (8), 1653-1662.
27. Ministry of the Environment. E-Laws. http://www.e-laws.gov.on.ca/navigation?file=home&lang=en (February 18, 2009),
28. Eglinton, G.; Hamilton, R. J., Leaf Epicuticular Waxes. *Science* **1967,** *156*, (3780), 1322-1335.
29. Fernandez, P.; Vilanova, R. M.; Grimalt, J. O., Sediment fluxes of polycyclic aromatic hydrocarbons in European high altitude mountain lakes. *Environmental Science & Technology* **1999,** *33*, (21), 3716-3722.
30. Elmquist, M.; Zencak, Z.; Gustafsson, O., A 700 Year Sediment Record of Black Carbon and Polycyclic Aromatic Hydrocarbons near the EMEP Air Monitoring Station in Aspvreten, Sweden. *Environmental Science and Technology* **2007**.
31. Natural Resources Canada (NRCAN). The Atlas of Canada, 3rd edition. http://atlas.nrcan.gc.ca/site/english/maps/archives/3rdedition/environment/climate/020 (February 18, 2009),
32. Environment Canada. Climate Normals. http://www.climate.weatheroffice.ec.gc.ca/climate_normals/index_e.html (February 18, 2009)
33. Canadian Environmental Protection Act (CEPA). Interim Sediment Quality Guidelines as defined by the Canadian Council of Ministers of the Environment (CCME). http://www.ec.gc.ca/CEPARegistry/the_act/ (February 18),
34. Lockhart, W. L.; Wilkinson, P.; Billeck, B. N.; Brunskill, G. J.; Hunt, R. V.; Wagemann, R., Polycyclic aromatic hydrocarbons and mercury in sediments from 2 isolated lakes in central and northern Canada. *Water Science and Technology* **1993,** *28*, (8-9), 43-52.

CHAPTER 4

SUMMARY AND CONCLUSIONS

This thesis contributed to the overall understanding of PAH in remote environments as well as how combustion derived contaminants versus local point sources are assessed in these environments. This has implications for any new potential legislation involving combustion emissions and sediment quality guidelines as well as development of site assessment techniques which can more accurately account for the role of regional atmospheric deposition in sediment contamination.

Pyrogenic polycyclic aromatic hydrocarbon (PAH) profiles in sediment cores have been used in many other studies to elucidate the trends in atmospheric deposition of combustion derived contaminants over time. PAH deposition since the mid-1950's had been decreasing primarily due to the use of cleaner burning fuels as well as advances in combustion technology [1-3]. It was assumed that this trend would continue, however several studies have found that recent PAH deposition in several urban or sub-urban area has recently begun increasing or has become constant [1, 4-6]. The recent increases have been correlated to local traffic sources [1, 4] and thus it was hypothesized [4] that local traffic sources are beginning to overprint regional PAH deposition in some areas.

In chapter 2 it was demonstrated that recent PAH deposition to Siskiwit Lake has continued to decrease towards levels observed early in industrialization. Due to the isolation of Siskiwit Lake from traffic sources, the decreasing trends in PAH deposition observed supports the hypothesis that local traffic sources in urban or sub-urban areas are overprinting regional atmospheric deposition [1, 4]. Furthermore, since the most likely regional PAH emission sources to Siskiwit Lake are predominantly industry or power generation, decreasing PAH concentrations in recent sediments of Siskiwit Lake also suggest that current restrictions on industry do in fact appear to be effective in reducing PAH emissions to the atmosphere. This indicates that any further mitigation may need to be directed to traffic sources. Future work at this site involves natural abundance radiocarbon analysis of recent pyrogenic PAH. This will investigate changes in the relative source (i.e. fossil fuel combustion or biomass combustion) over time which is expected to further corroborate the decreasing emissions from industrial and power generation sources.

Chapter 2 also demonstrated conclusively that perylene production has occurred in sediments from Siskiwit Lake over the past 20 years. This was done by directly comparing the profile obtained during this study with a profile created in 1984 from the same site. Perylene concentrations from this study are noticeably higher than those from McVeety and Hites [7] which is in contrast to pyrogenic PAH profiles that agree well with each other; this consistent increase in perylene concentrations must then represent in-situ production. 1st and 2nd order

kinetic reaction curves were fit to the perylene profiles in order to assess the possibility that the reaction fits a simple concentration dependant process. The reaction models fit well to the concentration profiles and reaction constants were similar for both profiles from Siskiwit Lake indicating that the pattern of perylene production in the cores, and thus the shapes of the profiles, are similar. However, the models were unable to accurately predict the observed increases in perylene concentrations over the 20 year period suggesting that perylene production cannot be described by a simple kinetic model. If perylene production was governed by simple concentration dependant kinetics, it would be expected that the two concentration profiles would converge at some point as the reactants were used up and the reaction goes to completion. This however, was not seen and instead perylene production occurred over the entire core. This suggests that either convergence occurs deeper in the core or that perylene production is controlled by complex kinetics which may involve biology as was suggested by Silliman et al [9].

In chapter 3 profiles of contaminants in sediment cores from two lakes, Lake A and Lake B, in northern Ontario were effectively used to demonstrate that an adjacent industrial facility is not acting as a point source of contamination to Lake A. Instead it was found that concentrations were consistent with regional atmospheric deposition. The current standard sampling methods in site assessment involve dredge sampling of the upper 15 cm of sediment and the subsequent homogenization of the sample before analysis. This bulk analysis

approach does not preserve any temporal component and thus changes in contaminant concentrations over time cannot be recognized. Thus the role of atmospheric deposition in contaminant loadings to sediment is often not considered or may be underestimated. Contaminant concentration profiles on the other hand preserve changes in concentrations over time. Subsequent comparison of the profiles to literature data, as was done in chapter 3, can allow for the recognition of trends representing regional atmospheric deposition as well as recognition of abrupt large changes in concentration that are associated with point source release of contaminants. This becomes more significant as it was also shown in Chapter 3 that current atmospheric deposition (top 1 or 2 cm of the cores) alone produces contaminant concentrations above the CCME guidelines. The cores from this study were then modeled to compare to 15 cm dredge samples taken for a previous site assessment. It was found that atmospheric deposition to Lake A can produce exceedences in these samples as well. Thus, using solely dredge sampling, these exceedences could be falsely attributed to be the result of local industrial operations. Moreover, if atmospheric deposition continues to produce concentrations at or above those found in the top centimetre of the cores, future dredge samples will show increasing contamination. This highlights the suggestion that differentiation of atmospheric deposition from other contamination is integral when apportioning the source of contaminants. As such, analyzing contaminant profiles in sediment cores is an essential tool in site assessment.

This thesis contributes to the overall understanding of the fate and behaviour of PAH in remote lake sediments and how PAH concentrations can be accurately assessed. This includes PAH derived from anthropogenic sources as well as PAH derived from natural sources. This information can be integral in revising current policies or environmental quality guidelines that protect human and environmental health thus making them more representative of the types of environmental contamination that are occurring.

CITATIONS

1. Lima, A. L.; Eglinton, T. I.; Reddy, C. M., High-resolution record of pyrogenic polycyclic aromatic hydrocarbon deposition during the 20th century. *Environmental Science and Technology* **2003,** *37*, 53-61.
2. Gschwend, P. M.; Hites, R. A., Fluxes of PAH to marine and lacustrine sediments in the northeastern United States. *Geochimica Et Cosmochimica Acta* **1981,** *45*, (12), 2359-2367.
3. Hites, R. A.; Laflamme, R. E.; Windsor, J. G.; Farrington, J. W.; Deuser, W. G.,) PAH in an anoxic sediment core from the Pettaquamscut River (Rhode Island, USA). *Geochimica Et Cosmochimica Acta* **1980,** *44*, (6), 873-878.
4. Van Metre, P. C.; Mahler, B. J.; Furlong, E. T., Urban Sprawl Leaves Its PAH Signature. *Environmental Science and Technology* **2000,** *34*, (19), 4064-4070.
5. Schneider, A.; Stapleton, H.; Cornwell, J.; Baker, J., Recent declines in PAH, PCB and toxaphene levels in the northern Great Lakes as determined from high resolution sediment cores. *Environ. Sci. Technol.* **2001,** *35*, (19), 3809-3815.
6. Elmquist, M.; Zencak, Z.; Gustafsson, O., A 700 Year Sediment Record of Black Carbon and Polycyclic Aromatic Hydrocarbons near the EMEP Air Monitoring Station in Aspvreten, Sweden. *Environmental Science and Technology* **2007**.
7. McVeety, B. D.; Hites, R. A., Atmospheric deposition of Polycyclic Aromatic Hydrocarbons to water surfaces: A mass balance approach. *Atmospheric Environment* **1988,** *22*, (3), 511-536.
8. Gschwend, P. M.; Chen, P. H.; Hites, R. A., On the formation of perylene in recent sediments- kinetic models. *Geochimica Et Cosmochimica Acta* **1983,** *47*, (12), 2115-2119.
9. Silliman, J. E.; Meyers, P. A.; Eadie, B. J.; Klump, J. V., A hypothesis for the origin of perylene based on its low abundance in sediments of Green Bay, Wisconsin. *Chemical Geology* **2001,** *177*, (3-4), 309-322.

APPENDIX A

Raw data concentration charts

Appendix A: Concentration Data Tables
(Unless otherwise specified, all concentrations are in ppm or mg kg-1)

Sample	% Recovery Front	% Recovery Back	Napth	Acey	Ace	Flu	Phen	Anth	Flua	Py	B(a)A	Chry	B(b)F and B(k)F	B(a)P	Pery	B(ghi)P	D(ah)A	Ideno
Siskiwit Lake																		
Sisk 0-1	72.6	97.1	0.04	N.Q	N.D.	N.Q.	0.06	0.01	0.08	0.05	0.02	0.05	0.08	0.03	0.19	0.08	N.D.	0.05
Sisk 1-2	71.1	81.8	0.04	N.Q	N.D.	N.Q.	0.06	0.02	0.09	0.05	0.03	0.05	0.09	0.03	0.47	0.10	N.D.	0.07
Sisk 2-3	72.3	84.3	0.06	N.Q	N.D.	N.Q.	0.08	0.01	0.12	0.07	0.03	0.07	0.11	0.03	0.78	0.12	N.D.	0.08
Sisk 3-4	62.9	73.0	0.05	N.Q	N.D.	N.Q.	0.08	0.02	0.16	0.08	0.04	0.08	0.13	0.03	0.92	0.15	N.D.	0.10
Sisk 4-5	84.7	103.2	0.05	N.Q	N.D.	N.Q.	0.08	0.01	0.18	0.09	0.04	0.09	0.15	0.03	1.38	0.16	N.D.	0.11
Sisk 5-6	77.0	93.0	0.04	N.Q	N.D.	N.Q.	0.09	0.02	0.19	0.10	0.04	0.10	0.17	0.04	1.42	0.18	N.D.	0.11
Sisk 6-7	77.7	92.0	0.05	N.Q	N.D.	N.Q.	0.09	0.02	0.20	0.10	0.05	0.10	0.19	0.04	1.63	0.21	N.D.	0.14
Sisk 7-8	83.9	97.5	0.04	N.Q	N.D.	N.Q.	0.07	0.01	0.18	0.09	0.04	0.09	0.16	0.03	1.69	0.19	N.D.	0.13
Sisk 8-9	81.1	93.1	0.03	N.Q	N.D.	N.Q.	0.06	N.Q.	0.15	0.07	0.05	0.04	0.13	0.03	2.00	0.17	N.D.	0.11
Sisk 9-10	88.2	97.8	0.04	N.Q	N.D.	N.Q.	0.05	N.Q.	0.11	0.05	0.04	0.02	0.08	N.Q.	1.90	0.10	N.D.	0.06
Sisk 10-11	92.8	105.7	0.04	N.Q	N.D.	N.Q.	0.04	N.Q.	0.08	0.03	0.03	0.00	0.06	N.Q.	1.93	0.06	N.D.	0.04
Sisk 11-12	93.2	104.4	0.03	N.Q	N.D.	N.Q.	0.04	N.Q.	0.06	0.03	0.03	0.00	0.04	N.Q.	1.39	0.04	N.D.	0.03

* Concentration below quantification limit, value is an estimate
N.Q. Concentration below quantification limit, no estimate was produced
N.D. Compound not detected

Appendix A continued: Concentration Data Tables
(Unless otherwise specified, all concentrations are in ppm or mg kg-1)

Sample	% Recovery Front	% Recovery Back	Napth	Acey	Ace	Flu	Phen	Anth	Flua	Py	B(a)A	Chry	B(b)F and B(k)F	B(a)P	Pery	B(ghi)P	D(ah)A	Ideno	Lead (Pb)	Mercury (Hg)
Lake A Middle Core																				
LAM 0-1	92.8	95.2	0.04	N.Q.	N.D.	N.Q.	0.02	0.07	0.11	0.08	0.06	0.03	0.07	0.05	0.87	0.07	N.D.	0.07	25	0.26
LAM 1-2	94.0	100.6	0.02	N.Q.	N.D.	N.Q.	0.02	0.04	0.07	0.05	0.04	0.02	0.05	0.03	0.58	0.05	N.D.	0.05	21	0.28
LAM 2-3	88.3	99.1	*0.02	N.Q.	N.D.	N.Q.	0.01	0.03	0.05	0.04	0.04	0.02	0.05	0.03	0.87	0.05	N.D.	0.04	18	0.27
LAM 3-4	85.5	99.7	*0.02	N.Q.	N.D.	N.D.	0.02	0.04	0.06	0.04	0.04	0.02	0.05	0.03	0.90	0.05	N.D.	0.04	13	0.23
LAM 4-5	88.5	92.5	*0.02	N.Q.	N.D.	N.D.	0.02	0.03	0.04	0.03	0.04	0.02	0.04	0.03	1.14	0.03	N.D.	0.03	10	0.22
LAM 5-6	86.3	99.8	0.02	N.Q.	N.D.	N.D.	0.02	0.05	0.05	0.03	0.05	0.02	0.05	0.04	2.33	0.05	N.D.	0.04	10	0.21
LAM 6-7	91.5	102.0	0.03	N.Q.	N.D.	N.D.	*0.02	0.05	0.05	0.03	0.05	0.02	0.05	0.04	2.17	0.05	N.D.	0.03	9	0.20
LAM 7-8	92.2	100.9	0.03	N.Q.	N.D.	N.D.	*0.02	0.06	0.05	0.04	0.06	*0.02	0.05	0.05	3.44	0.05	N.D.	0.04	7	0.18
LAM 8-9	90.6	100.7	0.04	N.Q.	N.D.	N.D.	*0.02	0.05	0.04	0.03	0.05	*0.02	0.05	0.04	2.87	0.05	N.D.	0.03	5	0.17
LAM 9-10	89.2	99.6	0.03	N.Q.	N.D.	N.D.	0.02	0.05	0.04	0.03	0.05	*0.02	0.04	0.04	2.16	0.04	N.D.	0.03	5	0.18
Lake A Proximal Core																				
LAP 0-1	81.4	81.7	0.06	0.01	N.D.	0.01	0.02	0.09	0.17	0.09	0.05	0.03	0.06	0.03	0.27	0.05	N.D.	0.05	24	0.33
LAP 1-2	85.9	79.5	0.06	0.01	N.D.	0.01	0.01	0.09	0.17	0.09	0.05	0.02	0.07	0.03	0.4	0.05	N.D.	0.05	8	0.25
LAP 2-3	94.3	85.3	0.05	N.Q.	N.D.	0.01	0.01	0.06	0.09	0.05	0.04	0.02	0.04	0.03	0.5	0.04	N.D.	0.04	5	0.20
LAP 3-4	68.3	60.4	0.04	N.Q.	N.D.	0.01	N.Q.	0.04	0.04	0.02	0.03	*0.02	0.03	0.02	0.6	0.03	N.D.	0.02	3	0.17
LAP 4-5	82.8	86.7	0.02	N.Q.	N.D.	0.01	0.01	0.05	0.04	0.02	0.02	*0.02	0.02	0.02	0.6	0.02	N.D.	0.01	2	0.16
LAP 9-10	78.0	73.6	0.04	N.Q.	N.D.	0.02	0.01	0.05	0.04	0.02	0.02	*0.02	0.03	0.02	2.2	0.02	N.D.	0.02	3	0.18

* Concentration below quantification limit, value is an estimate
N.Q. Concentration below quantification limit, no estimate was produced
N.D. Compound not detected

Appendix A continued: Concentration Data Tables
(Unless otherwise specified, all concentrations are in ppm or mg kg-1)

Sample	% Recovery Front	% Recovery Back	Napth	Acey	Ace	Flu	Phen	Anth	Flua	Py	B(a)A	Chry	B(b)F and B(k)F	B(a)P	Pery	B(ghi)P	D(ah)A	Ideno	Lead (Pb)	Mercury (Hg)
Lake B Middle Core																				
LBM 0-1	84.7	102.8	0.05	N.Q.	N.D.	N.Q.	N.Q.	0.08	0.13	0.09	0.07	0.03	0.083	0.05	2.2	0.07	N.D.	0.07	26	0.26
LBM 1-2	85.1	102.6	0.04	N.Q.	N.D.	N.Q.	N.Q.	0.08	0.13	0.09	0.07	0.02	0.082	0.05	3	0.07	N.D.	0.07	13	0.23
LBM 2-3	82.4	98.9	0.03	N.Q.	N.D.	N.Q.	N.Q.	0.06	0.08	0.05	0.04	0.02	0.05	0.03	2.8	0.04	N.D.	0.04	9	0.20
LBM 3-4	81.9	102.9	*0.02	N.Q.	N.D.	N.Q.	N.Q.	0.05	0.04	0.03	0.03	*0.02	N.Q.	*0.02	3.2	N.Q.	N.D.	N.Q.	6	0.18
LBM 4-5	84.3	103.2	*0.02	N.Q.	N.D.	N.Q.	N.Q.	0.04	0.03	0.02	0.03	*0.02	N.Q.	*0.02	3.7	N.Q.	N.D.	N.Q.	5	0.18
LBM 5-6	85.3	93.5	*0.02	N.Q.	N.D.	N.Q.	N.Q.	0.04	0.03	*0.02	0.02	*0.02	N.Q.	*0.02	4.2	N.Q.	N.D.	N.Q.	5	0.18

* Concentration below quantification limit, value is an estimate
N.Q. Concentration below quantification limit, no estimate was produced
N.D. Compound not detected

APPENDIX B:

^{210}Pb dating

This appendix is divided into two parts. Part 1 is a report completed by Fan Yang at the National Water Research Institute (NWRI) and provides the background about ^{210}Pb dating and modeling as well as the results for the Siskiwit Lake site. Part 2 is the calculations and charts regarding ^{210}Pb analysis in Lakes A and B for chapter 3 of this thesis.

^{210}Pb Dating of Lacustrine Sediments from Lake Siskiwit, site 4, (Core 295), Isle Royal National Park Michigan, USA

Fan Yang

Report 06-04
June 2006

National Water Research Institute
Canada Centre for Inland Waters
Burlington, Ontario L7R 4A6

Yang, Fan, 2006. ^{210}Pb Dating of Lacustrine Sediments from Lake Siskiwit (Core 295), Province. National Water Research Institute, Burlington, Ontario. NWRI Report 06-04.

SUMMARY

A lacustrine sediment core was dated from Lake Siskiwit (site4). The ^{210}Pb activity profile of the sediment core was used to determine the chronological age of the sediment as well as the sedimentation rate. The mean specific gravity was determined to be 2.302 $g \cdot cm^{-3}$. Data were analysed using two types of models: the Constant Initial Concentration (CIC) model and the Constant Rate of Supply (CRS) model.

The sedimentation rate was calculated to be 0.172 $cm \cdot yr^{-1}$ for core 295 using the CIC1 model. The average mass sedimentation rate was determined to be 0.015 $g \cdot cm^{-2} \cdot yr^{-1}$ using the CIC1 model, 0.010 $g \cdot cm^{-2} \cdot yr^{-1}$ using the CIC2 model, and 0.009 ± 0.003 $g \cdot cm^{-2} \cdot yr^{-1}$ using the CRS model. Porosity and density analyses indicate slight changes in sediment composition which may be accompanied by varying accumulation rate. CRS results also indicate the variability in sedimentation rate in this core.

INTRODUCTION

In this study, a core (295) taken from Lake Siskiwit in Michigan, was dated using a ^{210}Pb method (Eakins and Morrison, 1978). The core was collected and submitted by Dr. Derek Muir of Aquatic Ecosystem Protection Research Division in Burlington, Ontario.

LOCATION AND CORE PREPARATION

The sample site from which the core was taken ($48^{0}00'13''N$, $88^{0}47'40"W$) is located in Michigan. On September 7, 2005, Lake Siskiwit was cored using a 6.7 cm inner diameter corer. The core was subsectioned into 1/2 to 1-cm intervals giving thirty-three samples. The samples were weighed, freeze-dried, and then re-weighed. These weights were used to calculate porosity and the uncompacted depth (see Appendix A, Delorme, 1991).

A plot of porosity versus cumulative dry weight for core 295 is shown in Figure 1a.

Specific Gravity was determined using an automated Accupyc pycnometer (Micromeritics, 1992). Figure 1b is a plot of specific gravity (or density) versus cumulative dry weight. Mean specific gravity for the sediments of core 295 is 2.302 $\pm$ 0.031 $g{\cdot}cm^{-3}$ based on 5 samples and 25 determinations (see Appendix B this report).

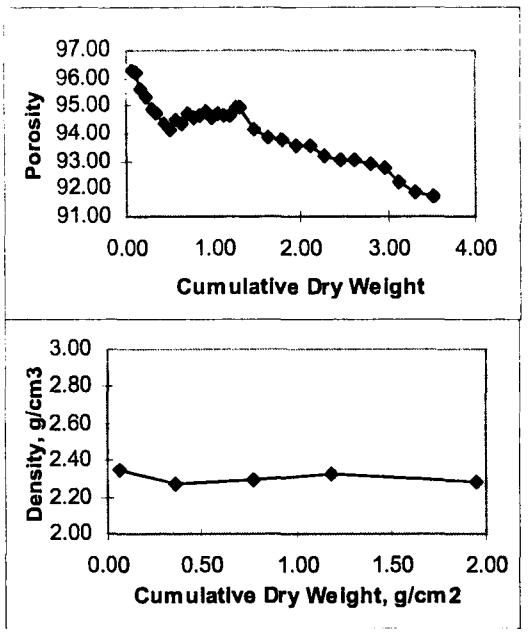

Figure 1. Relationship between cumulative dry weight and (a) porosity, (b) density.

METHOD

Laboratory Procedures

Homogeneous portions of 11 samples (Table 1) from core 295 were treated using a variation on the Eakins and Morrison (1978) polonium distillation procedure. Details of the laboratory procedure are found in a laboratory manual (Turner, 1990).

Following grinding and homogenizing, 0.5 g of sediment waas treated with concentrated HCl to remove carbonate materials, then mixed with approximately 10 dpm of ^{209}Po spike in a test tube. The ^{209}Po spike was prepared on September 6, 1991 at 6.07 dpm ml^{-1} activity. The test tube and contents were then placed in an oven at 110°C until dry.

After cooling, glass wool plugs (one to hold the sediment at the bottom of the tube, one dampened to catch polonium at the opening of the tube) were inserted, then the tubes were placed into a tube furnace and heated to 700°C for 2 hr to distil the polonium from the sediments. At this temperature, polonium passes easily from the sediment, through

the dry wool plug and does not condense until reaching the wet wool plug outside the furnace.

After cooling, the tube was cut, and the upper part containing the damp glass wool (condenser) was digested in concentrated HNO_3 under reflux (to destroy organic material). The residue was then filtered and the filtrate boiled down and digested with two HCl treatments to remove any remaining traces of HNO_3.

The polonium was then plated from the remaining solution onto a finely polished silver disk. The disk was counted in an alpha spectrometer. ^{209}Po was identified by its 4.88 MeV alpha particle, and ^{210}Po by its 5.305 MeV alpha particle. The ^{210}Po counts obtained from the spectrometer were compared to the ^{209}Po counts (of known activity) to determine the activity of ^{210}Po in the sediment sample.

Sediment Dating Theory

Dating of lacustrine sediments has been actively pursued for several decades (Robbins and Edgington, 1975; Matsumoto, 1975; Appleby and Oldfield, 1978; and Farmer, 1978). Sedimentation rates are derived using either the CIC (constant initial concentration of unsupported ^{210}Pb; Robbins and Edgington, 1975; Matsumoto, 1975) or the CRS (constant rate of supply; Appleby and Oldfield, 1978) model. The CIC model assumes a constant sedimentation rate over the time period in which unsupported ^{210}Pb is measured. The CRS model assumes a variable sedimentation rate. Both models assume a constant flux of unsupported ^{210}Pb to the sediment/water interface. Depth can be corrected for sediment compaction in the CIC model using sediment porosity measurements (CIC1), otherwise cumulative dry weight is used (CIC2). Sediment compaction is accounted for in the CRS model by dealing with cumulative dry weight instead of sediment depth.

The profile of ^{210}Pb in a sediment core can be described as follows:

$$A_{tx} = (A_{Uo})e^{-\lambda t} + A' \quad (1a)$$

where A_{Tx} is the total activity of ^{210}Pb in the sample in $pCi \cdot g^{-1}$ dry wt at depth x, and of age t.

A' is the activity of ^{210}Pb supported by ^{226}Ra in $pCi \cdot g^{-1}$ dry wt (represented by constant ^{210}Po activities attained at depth),

A_{Uo} is the unsupported activity of ^{210}Pb at the sediment/water interface in $pCi \cdot g^{-1}$ dry wt,

λ is the radioactive decay constant for ^{210}Pb ($0.693/22.26\ yr^{-1} = 0.0311\ yr^{-1}$),

And since $A_{Ux} = A_{Tx} - A'$ then $A_{Ux} = (A_{Uo})e^{-\lambda t}$ (1b)

where A_{Ux} is the unsupported activity of ^{210}Pb in the sample in $pCi \cdot g^{-1}$ dry wt at depth x.

The Constant Initial Concentration (CIC) Model:

In the following derivations, equations which refer to the usage of cumulative dry weight instead of uncompacted depth in the CIC model are designated with an 'a'.

In the CIC model, uncompacted mid-depth, z, can be used instead of natural depth, x, to compensate for sediment compaction (CIC1 model). Otherwise cumulative dry weight is used (CIC2 model). The uncompacted mid-depth is calculated from uncompacted thickness (Delorme 1991).

$$t_{ui} = \{(\phi_o - \phi_i)/(1 - \phi_o)\} + (TV_i * V_q) \quad (2)$$

where t_{ui} is the uncompacted thickness of the i^{th} sample,

ϕ_i is the porosity of the i^{th} sample expressed as a percentage,

ϕ_o is the porosity at the sediment-water interface calculated by regressing the top

eight sample porosities (ϕ_i) against natural mid-depth, and ϕ_o = y intercept,

TV_i is the total volume of the i^{th} sample,

V_q is the volume of a cylinder 1 cm high and surface area equal to either the inside of the core tube or the stainless steel extrusion ring, whichever is appropriate.

The CIC model assumes a constant sedimentation rate (or mass sedimentation rate) over the time period in which unsupported ^{210}Pb is measured, thus

$$t = z/S_o \quad (3)$$

$$t = c/\omega \quad (3a)$$

where S_o is the sedimentation rate in $cm \cdot yr^{-1}$ at the sediment/ water interface,

z is uncompacted mid-depth,

c is cumulative dry weight in $g \cdot cm^{-2}$,

ω is the mass sedimentation rate in $g \cdot cm^{-2} \cdot yr^{-1}$.

The total ^{210}Pb activity at the sediment water interface is:

$$A_{to} = (P/\omega) \quad (4)$$

where P is the flux of ^{210}Pb at the sediment water interface in $pCi \cdot cm^{-2} \cdot yr^{-1}$, (assumed constant).

Substituting equations (3) [and (3a)] and (4) into equation (1a) gives:

$$A_{tz} = (P/\omega)e^{-z\lambda/S_o} + A' \quad (5)$$

or

$$A_{Tx} = (P/\omega)e^{-c\lambda/\omega} + A' \quad (5a)$$

Equation (5) or [5(a)] can be simplified using natural logarithms:

$$\ln(A_{Tz} - A') = \ln(P/\omega) - (\lambda/S_o)z \quad (6)$$

$$\ln(A_{Tx} - A') = \ln(P/\omega) - (\lambda/\omega)c \quad (6a)$$

The form of the equation is $y = b + (m)\,x$

A graphical solution for P/ω (the y-intercept) and λ/S_o [or (λ/ω)] (the slope of the line) is possible from a plot of x and y {z vs $\ln(A_z - A')$} [or c vs $\ln(A_x - A')$] (see Figure 3). As λ is known, then S_o [or ω] can be calculated.

$$S_o = \lambda/\text{slope} = \lambda/(m) \quad (7)$$

$$\omega = \lambda/\text{slope} = \lambda/(m) \quad (7a)$$

When using uncompacted depth, the mass sedimentation rate ($g \cdot cm^{-2} \cdot yr^{-1}$) is represented by:

$$\omega = S_o\,(1 - \phi_o)\,\rho_s = S_i\,(1 - \phi_i)\,\rho_s \quad (8)$$

where ρ_s is the density of the solid phase of the sample (assumed constant),

S_i is the sedimentation rate ($cm \cdot yr^{-1}$) at a given uncompacted mid-depth z.

The flux at the sediment/water interface P ($pCi \cdot cm^{-2} \cdot yr^{-1}$) can be calculated from the y-intercept and mass sedimentation rate.

$$P = \omega\,(e^b) \quad (9)$$

Using equation (6) [or (6a)] the time 't' in years since the sample was deposited is given by:

$$t = \frac{\ln(A_{Tz} - A') - \ln(P/\omega)}{(-\lambda)} = \frac{z}{S_o} \quad \text{CIC1} \quad (10)$$

or $t = \frac{\ln (A_{Tx} - A') - \ln(P/\omega)}{(-\lambda)} = \frac{c}{\omega}$ CIC2 (10ai)

which can be written as:

$$t = -\frac{1}{\lambda} \ln \frac{(A_{Tz}-A')}{A_{to}} = \frac{z}{S_o} \text{ or } = \frac{c}{\omega} \quad (10aii)$$

The uncompacted mid-depth (cm) divided by the sedimentation rate ($cm \cdot yr^{-1}$) [or cumulative dry weight, ($g \cdot cm^{-2}$) divided by mass sedimentation rate ($g \cdot cm^{-2} \cdot yr^{-1}$)] gives t.

The Constant Rate of Supply (CRS) Model:

Since the CRS model assumes a constant rate of supply, then

$$P = A_{Ui} * \omega_t \quad (11)$$

where P is the flux of ^{210}Pb at the sediment water interface in $pCi \cdot cm^{-2} \cdot yr^{-1}$, (assumed constant)

A_{Ui} is the initial activity of unsupported ^{210}Pb in sediment of age t

ω_t is the dry Mass Sedimentation Rate ($g \cdot cm^{-2} \cdot yr^{-1}$) at time t.

Sediment laid down during time period δt occupies a layer of thickness (δx):

$$\delta x = \frac{\omega_t}{\rho_x} \delta t \quad (12)$$

were ρ_x is the dry mass/unit wet volume of the sample ($g \cdot cm^{-3}$) at depth x.

$$\rho_x = \frac{d\omega}{dx} \quad (13)$$

The rate of change of depth is

$$x' = \frac{\omega}{} \quad (14)$$

ρ_x

where ' denotes differentiation with regards to t.

and $x' \rho_x = \omega = x'_o \rho_o$ (15)

Equation (15) combines with (1b) to give

$$x' \rho_x A_{Ux} = x'_o \rho_o (A_{Uo}) e^{-\lambda t} \quad (16)$$

Let $B(x) = \int_x^\infty \rho_x * A_{Ux}\, dx = \int_x^\infty A_{Ux}\, d\omega$ (17)

represent the total residual or cumulative unsupported ^{210}Pb beneath sediments of depth x,

and $B(0) = \int_0^\infty \rho_o * A_{Uo}\, dx = \int_0^\infty A_{Uo}\, d\omega$ (18)

represent the total residual unsupported ^{210}Pb in the sediment column, then

$$B(x) = B(0) e^{-\lambda t} \quad (19)$$

The age of layer at depth x is thus:

$$t = -\frac{1}{\lambda} \ln \frac{B(x)}{B(0)} \quad (20)$$

where B(x) and B(0) are calculated by direct numerical integration of the ^{210}Pb profile (the plot of unsupported activity versus cumulative dry weight).

The mass sedimentation rate is calculated by dividing the change in the mid-sample cumulative dry weight by the difference of time in years for the sample analysed.

The mean ^{210}Pb supply rate (flux) is calculated from

$$P = \lambda B(0) \qquad (21)$$

RESULTS

Table 1 lists the ^{210}Po activities for the 11 samples prepared for core 295. Figure 2 depicts the ^{210}Po activity profile with depth and cumulative dry weight.

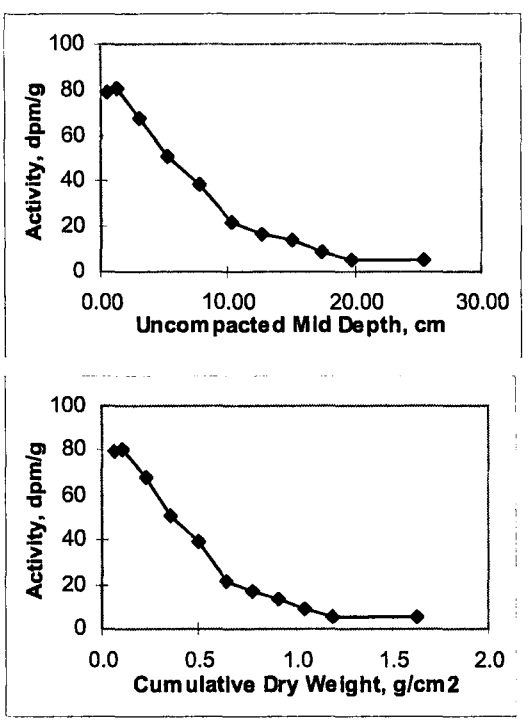

Figure 2. Distribution of Total ^{210}Po activity in dpm·g^{-1} in relation to uncompacted mid-depth and cumulative dry weight for core 295.

Table 1. Activity of ^{210}Po in Core 295 Sediment.

Sample	Cum. Dry Wt., g·cm^{-2}	Uncompacted Mid Depth, cm	^{210}Po, dpm·g^{-1}		Sample	Cum. Dry Wt., g·cm^{-2}	Uncompacted Mid Depth, cm	^{210}Po, dpm·g^{-1}

1	0.06	0.42	79.09	12	0.77	12.60	16.97
2	0.11	1.20	80.41	14	0.92	15.03	13.82
4	0.23	2.96	67.92	16	1.05	17.30	8.96
6	0.35	5.18	50.79	18	1.19	19.76	5.54
8	0.50	7.69	38.98	22	1.62	25.45	5.23
10	0.64	10.21	21.77				

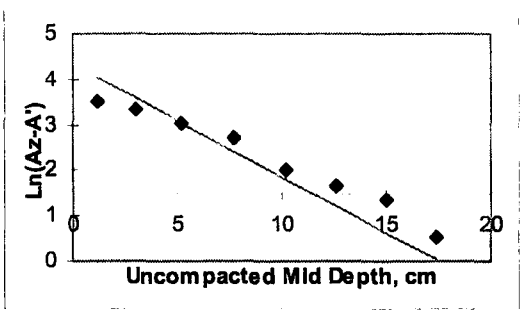

Figure 3. The distribution of uncompacted mid-depth against $\ln(A_z - A')$ for core 295. The y intercept of the regression line = 3.901, the slope = -0.181, $r^2 = 0.978$.

^{210}Pb Analysis of core295 using the CIC model.

For the first CIC model (CIC1), the unsupported activity is plotted against uncompacted mid-depth (Figure 3) using the expanded equation (6). Based on the graphical solution, the y-intercept is $\ln(P/\omega) = 3.901$ and the slope of the line (λ/S_o) is -0.181 (see Appendix C). Samples 2 to 9 were used to calculate an average sedimentation rate of 0.172 $cm \cdot yr^{-1}$, an average mass sedimentation rate of 0.015 $g \cdot cm^{-2} \cdot yr^{-1}$ and a flux of 0.759 $pCi \cdot cm^{-2} \cdot yr^{-1}$. The mean dates calculated for each core section, based on a division of the uncompacted mid-depth by the sedimentation rate (equation 3), are given in Appendix F. The '±' values are two standard deviations based on data calculated for the top, bottom, and mid-depth of the sample.

For the second CIC model (CIC2), the unsupported activity is plotted against cumulative dry weight (Figure 4) using the expanded equation (6a). Based on the graphical solution, the y-intercept is $\ln(P/\omega) = 3.970$ and the slope of the line (λ/ω) is -3.153 (see Appendix D). Samples 2 to 9 were used to calculate an average mass sedimentation rate of 0.010 $g \cdot cm^{-2} \cdot yr^{-1}$ and a flux of 0.523 $pCi \cdot cm^{-2} \cdot yr^{-1}$. The dates calculated for each core section, based on a division of the cumulative dry weight by the mass sedimentation rate (equation 3a) are given in Appendix F. The '±' values are two standard deviations based on data calculated for the top, bottom, and mid-section of the sample.

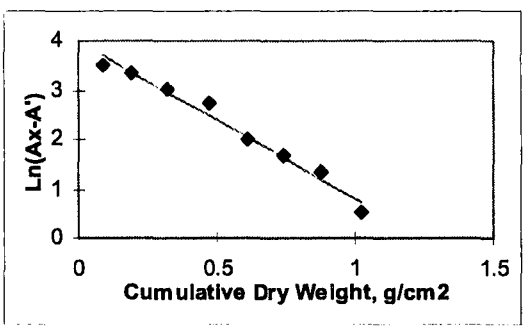

Figure 4. The distribution of cumulative dry weight against $\ln(A_x - A')$ for core 295. The y intercept of the regression line = 3.970, the slope = -3.152, $r^2 = 0.978$.

Ideally, the CIC1 and CIC2 models should give almost identical results. A difference in the mass sedimentation rates or calculated fluxes determined from the CIC1 and CIC2 models may indicate a problem in the calculation of uncompacted mid-depth. It may indicate a change in lithology that was not completely accounted for by porosity or specific gravity measurements.

^{210}Pb Analysis of core295 using the CRS model.

For the CRS model, the unsupported activity is plotted against cumulative dry weight (Figure 2). The profile is integrated to determine B(0) and B(x) and calculate time (see Appendix E) according to equation 20. Since not all samples were analysed for ^{210}Pb activity, a multiple regression analysis was performed to obtain the dates for each core

section as given in Appendix F. Samples 1 to 10 were used in this example to calculate a mass sedimentation rate of 0.009 ± 0.003 $g \cdot cm^{-2} \cdot yr^{-1}$ and flux of 0.484 $pCi \cdot cm^{-2} \cdot yr^{-1}$. The variation in mass sedimentation rate in core 295 is illustrated in figure 5.

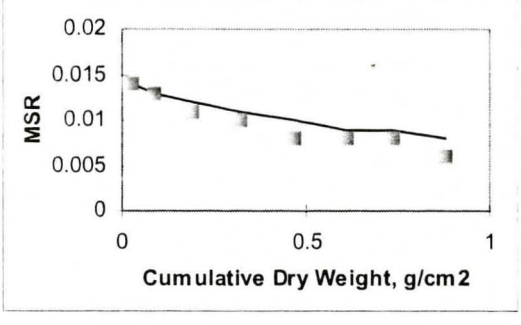

Figure 5. Plot of mass sedimentation rate (MSR) versus cumulative dry weight for core 295. Points represent mass sedimentation rates determined from integrated area defined by activity and cumulative dry weight for the sample, the line represents the running mean of the mass sedimentation rate.

Comparison of CIC and CRS ^{210}Pb Analysis of Core295.

Table 2 lists mass sedimentation rates and flux rates as calculated from the CIC and CRS models. The rates are very low. The mass sedimentation rates are in fair agreement. Although the flux rates of the CRS and CIC2 models agree most closely, all three rates are within the same order of magnitude.

The year corresponding to individual core sections (Appendix F) as determined by the CIC and CRS models are plotted against cumulative dry weight in Figure 6. Figure 6 shows good agreement between the chronology of the two CIC models. CRS model chronology is within error of the CIC model chronologies except for the cumulative dry weight higher than 0.77 g/cm^2.

Table 2. Summary of Mass Sedimentation Rate and Atmospheric Flux.

Model	Average Mass Sedimentation Rate, $g \cdot cm^{-2} \cdot yr^{-1}$	Calculated Flux Rate $pCi \cdot cm^{-2} \cdot yr^{-1}$
CIC1	0.015	0.759

CIC2	0.010	0.523
CRS	0.009 ± 0.003*	0.484

* Based on incremental mass sedimentation rates (Appendix E)

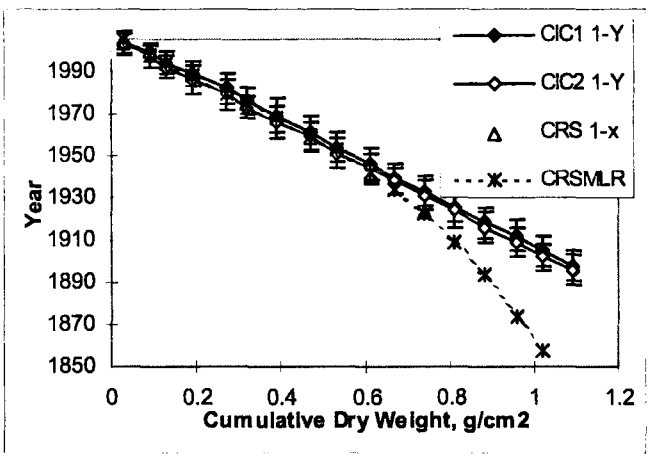

Figure 6. Plot of the Year determined from CIC (squares and circles)/CRS (triangles) models versus cumulative dry weight for core 295.

Due to the variability in sedimentation illustrated in Figure 5, the CRS chronology is considered to be the most accurate chronology for this core and is given more credence.

Comparison with other cores

Baker and Hites (2000) reported a mass sedimentation rate of 0.018 g cm^{-2} yr^{-1} for the first 6.0 cm and 0.007 g $cm^{-2}yr^{-1}$ below 6.0 cm for a core from Site 5. This is slightly higher than the sedimentation rate found for Core 4 or Core 5 (see Yang 2006). The inventory of unsupported ^{210}Pb in the sediment core dated by Baker and HItes (2000) was 23.0 pCi/cm^2. Since the expected inventory in this region is 15.5 pCi/cm2, they calculated a focusing factor of 1.48. This is in good agreement with the focussing factor calculated based on the surface slices from Core 4 and 5 (Appendix G) but lower than the focussing factor calculated based on the average sedimentation rate.

REFERENCES

Appleby, P.G. and F. Oldfield. 1978. The calculation of ^{210}Pb dates assuming a constant rate of supply of unsupported ^{210}Pb to the sediment. Catena 5:1-8

Baker, J. I. and Hites, R. A. 2000. Siskiwit Lake Revisited: Time Trends of PolychlorinatedDibenzo-p-dioxin and Dibenzofuran Deposition at Isle Royale, Michigan. Environ. Sci. Technol. 34, 2887-2891.

Blais, J.M. and J. Kalff. 1995. The influence of lake morphology on sediment focusing. Limnol. Oceanogr. 40(3):582-588.

Delorme, L.D. 1991. The preparation of lacustrine sediment samples from cores for use in dating and paleolimnology. National Water Research Institute, Burlington, Ontario, Contribution 92-188, 18p.

Eakins, J.D. and R.T. Morrison. 1978. A new procedure for determination of lead-210 in lake and marine sediments. International Journal of Applied Radiation and Isotopes 29:531-536.

Farmer, J.G. 1978. The determination of sedimentation rates in Lake Ontario using the ^{210}Pb dating method. Canadian Journal of Earth Sciences 15:431-437.

Graustein, W.C. and K.K. Turekain (1986). ^{210}Pb and ^{137}Cs in air and soils measure the rate and vertical profile of aerosol scavenging. J. Geophys Res 91: 14355-14366.

Hakanson, L. 1977. The influence of wind, fetch and water depth on the distribution of sediments in Lake Vanern, Sweden. Can. J. Earth Sci. 14:397-412.

Hilton, J. 1985. A conceptual framework for predicting the occurrence of sediment focusing and sediment redistribution in small lakes. Limnol. Oceanogr. 30(6):1131-1143.

Hilton, J., J.P. Lishman, and P.V. Allen. 1986. The dominant process of sediment distribution and focusing in a small, eutrophic, monomictic lake. Limnol. Oceanogr. 31(1):125-133.

Matsumoto, E. 1975. ^{210}Pb geochronology of sediments from Lake Shinji. Geochemical Journal 9:167-172.

Micromeritics 1992. Automated Accupyc pycnometer 1330, for determining skeletal density and volume of powders, porous materials, and irregularly shaped solid objects. Operators Manual V2.01, Micromeritics Instrument Corporation, Norcross, Georgia.

Oldfield, F. and P.G. Appleby. 1984. Empirical testing of ^{210}Pb dating models for lake sediments IN Lake Sediments and Environmental History (Eds. E.Y. Harworth and J.W.G. Lund). University of Minnesota Press, Minneapolis. pp 93-124.

Robbins, J.A. and D.N. Edgington. 1975. Determination of recent sedimentation rates in Lake Michigan using Pb-210 and Cs-137. Geochimica et Cosmochimica Acta 39:285-304.

Rowan, D.J., J. Kalff and J.B. Rasmussen. 1992. Estimating the mud deposition boundary depth in lakes from wave theory. Can. J. Fish. Aquat. Sci. 49:2490-2497.

Turner, L.J. 1990. Laboratory determination of ^{210}Pb - ^{210}Po using alpha spectrometry: Second Edition. NWRI Tech. Note LRB-90-TN-07, Burlington, Ontario, 63p.

Wong, C.S., G.Sanders, D.R.Engstrom, D.T.Long, D.L.Swackhamer & S.J.Eisenreich 1995. Accumulation, inventory, and diagenesis of chlorinated hydrocarbons in Lake Ontario sediments. Env.Sci.Technol. 29:2661-2672.

Yang, F. 2006. 210Pb Dating of Lacustrine Sediments (Core 294) from Lake Siskiwit (Site 5),
Isle Royale National Park, Michigan. Report 06-03. April 2006. Environment Canada, Burlington ON. 22 pp.

Appendices

Appendix

A Calculation of porosity and uncompacted depths given sample wet and dry weights, and specific gravity for core295.

B Specific gravity determination.

C Lead sedimentation rate analysis, CIC1 Model.

D Lead sedimentation rate analysis, CIC2 Model.

E Lead sedimentation rate analysis, CRS Model.

F Mean date calculated for each core slice.

G. Focussing factor

Appendix A: Calculation of porosity and uncompacted depths given sample wet and dry weights, (Delorme, 1991) and specific gravity for core295.

Sample Number	Wet Wt. g	Dry Wt. g	Cumm. Dry Wt g/cm2	Water Cont. cm3	Sed. Vol. cm3	Total Vol. cm3	Comp. Thick cm	Comp. Depth cm	Comp. Mid-pt cm	Sample Poros. %	Uncomp Thick. cm	Uncomp Depth cm	Uncomp. Mid-pt cm	Time B.P. Years
1	25.16	2.07	0.06	23.09	0.9	23.98	0.68	0.68	0.34	96.25	0.83	0.83	0.42	2
2	21.33	1.77	0.11	19.57	0.77	20.33	0.58	1.26	0.97	96.23	0.73	1.56	1.2	6
3	20.78	1.98	0.16	18.8	0.86	19.66	0.56	1.81	1.54	95.63	0.9	2.46	2.01	11
4	20.74	2.12	0.23	18.62	0.92	19.54	0.55	2.37	2.09	95.29	1	3.46	2.96	17
5	22.56	2.5	0.3	20.05	1.09	21.14	0.6	2.97	2.67	94.86	1.17	4.63	4.05	23
6	18.23	2.07	0.35	16.15	0.9	17.05	0.48	3.45	3.21	94.72	1.1	5.73	5.18	30
7	22.02	2.67	0.43	19.35	1.16	20.51	0.58	4.03	3.74	94.36	1.31	7.04	6.39	37
8	19.16	2.39	0.5	16.77	1.04	17.81	0.51	4.54	4.29	94.16	1.29	8.33	7.69	44
9	20.07	2.38	0.57	17.68	1.03	18.72	0.53	5.07	4.8	94.48	1.22	9.55	8.94	51
10	22.51	2.71	0.64	19.8	1.17	20.98	0.6	5.67	5.37	94.4	1.31	10.86	10.21	59
11	19.36	2.2	0.7	17.16	0.96	18.11	0.51	6.18	5.92	94.72	1.13	11.99	11.43	66
12	20.98	2.44	0.77	18.54	1.06	19.6	0.56	6.73	6.46	94.59	1.21	13.2	12.6	73
13	22.59	2.6	0.85	19.99	1.13	21.12	0.6	7.33	7.03	94.65	1.24	14.44	13.82	80
14	21.48	2.42	0.92	19.06	1.05	20.11	0.57	7.9	7.62	94.77	1.17	15.61	15.03	87
15	20.81	2.41	0.99	18.39	1.05	19.44	0.55	8.46	8.18	94.61	1.2	16.81	16.21	94
16	20.63	2.33	1.05	18.3	1.01	19.31	0.55	9	8.73	94.76	1.15	17.96	17.39	101
17	21.12	2.44	1.12	18.68	1.06	19.74	0.56	9.56	9.28	94.63	1.2	19.16	18.56	107
18	21.15	2.44	1.19	18.72	1.06	19.77	0.56	10.12	9.84	94.65	1.2	20.36	19.76	114
19	20.71	2.26	1.25	18.45	0.98	19.43	0.55	10.68	10.4	94.96	1.09	21.45	20.91	121
20	20.35	2.23	1.32	18.12	0.97	19.09	0.54	11.22	10.95	94.93	1.09	22.54	22	127
21	42.18	5.29	1.47	36.88	2.3	39.18	1.11	12.33	11.77	94.13	1.91	24.45	23.5	136
22	42.2	5.52	1.62	36.68	2.4	39.07	1.11	13.44	12.88	93.86	1.99	26.44	25.45	147
23	43.39	5.77	1.79	37.61	2.51	40.12	1.14	14.57	14.01	93.75	2.05	28.49	27.47	
24	41.29	5.63	1.95	35.67	2.44	38.11	1.08	15.66	15.11	93.59	2.04	30.53	29.51	
25	44.24	6.06	2.12	38.18	2.63	40.81	1.16	16.81	16.23	93.55	2.13	32.66	31.6	
26	36.67	5.3	2.27	31.37	2.3	33.67	0.95	17.77	17.29	93.16	2.05	34.71	33.69	
27	45.48	6.7	2.46	38.78	2.91	41.69	1.18	18.95	18.36	93.02	2.32	37.03	35.87	
28	41.46	6.06	2.63	35.4	2.63	38.03	1.08	20.03	19.49	93.08	2.2	39.23	38.13	
29	39.85	5.96	2.8	33.89	2.59	36.48	1.03	21.06	20.55	92.9	2.21	41.44	40.34	
30	37.9	5.76	2.96	32.14	2.5	34.64	0.98	22.05	21.55	92.77	2.2	43.64	42.54	
31	37.9	6.13	3.14	31.78	2.66	34.44	0.98	23.02	22.53	92.27	2.34	45.98	44.81	
32	37.71	6.37	3.32	31.34	2.76	34.11	0.97	23.99	23.51	91.89	2.45	48.43	47.21	
33	40.26	6.9	3.51	33.36	3	36.36	1.03	25.02	24.51	91.76	2.55	50.98	49.71	

Appendix B. Specific gravity determination.

The specific gravities ($g \cdot cm^{-3}$) of Core 295 sediments were determined using an automated Accupyc pycnometer (Micromeritics, 1992).

Sample Slice	No. Of Tests	Uncompacted Mid Depth	Specific Gravity	Standard Deviation	Mean	Standard Deviation
1	5	0.42	2.3480	0.0095		
6	5	5.18	2.2743	0.0086		
12	5	12.60	2.2882	0.0090		
18	5	19.76	2.3210	0.0121		
24	5	29.51	2.2806	0.0099	2.3024	0.0312

Appendix C. Lead Sedimentation Rate Analysis, CIC1 Model.

$\ln (A - A') = \ln (49.427) - 0.181 (Z)$ $R = -0.989$

where $(A - A')$ = unsupported ^{210}Pb in $pCi \cdot g^{-1}$,
and Z = uncompacted depth in cm.
based on data from lines 2 to 9

Specific Gravity = 2.302 $g \cdot cm^{-3}$ $P/\omega = 49.427$ $\omega = 0.015$
The initial porosity at the sediment/water interface is 96.13
Atmospheric flux rate at the time of collection 2005.68 is 1.685 $dpm \cdot cm^{-2} \cdot yr^{-1}$
or 0.759 $pCi \cdot cm^{-2} \cdot yr^{-1}$
Supported ^{226}Ra activity = 2.356 $pCi \cdot g^{-1}$ or 5.230 $dpm \cdot g^{-1}$
Sedimentation Rate = 0.172 $cm \cdot yr^{-1}$
Mass Sedimentation Rate = 0.015 $g \cdot cm^{-2} \cdot yr^{-1}$

Summary of 210Pb Analyses							
Uncomp Depth cm	Porosity	Total 210Pb dpm.g-1	Total 210Pb pCi.g-1	Unsupp 210Pb dpm.g-1	Unsupp 210Pb pCi.g-1	Sed.Rate cm.yr-1	Years (*)
1.2	0.9623	80.41	36.221	75.18	33.865	0.2227	2000
2.96	0.9529	67.92	30.595	62.69	28.239	0.2575	1994
5.18	0.9472	50.79	22.878	45.56	20.523	0.2895	1988
7.69	0.9416	38.98	17.559	33.75	15.203	0.2889	1979
10.21	0.944	21.77	9.806	16.54	7.451	0.2601	1966
12.6	0.9459	16.97	7.644	11.74	5.288	0.2664	1958
15.03	0.9477	13.82	6.225	8.59	3.869	0.2618	1948
17.39	0.9476	8.96	4.036	3.73	1.68	0.2662	1940

(*) Year calculated using the sedimentation rate of the sample

Appendix D. Lead Sedimentation Rate Analysis, CIC2 Model.

$\ln (A - A') = \ln (52.963) - 3.153 (X)$ $R = -0.989$

where $(A - A')$ = unsupported ^{210}Pb in $pCi \cdot g^{-1}$,
and X = cumulative dry weight in $g \cdot cm^{-2}$
based on data from lines 2 to 9

Specific Gravity = 2.302 $g \cdot cm^{-3}$ $P/\omega = 52.963$ $\omega = 0.010$
The initial porosity at the sediment/water interface is 96.13
Atmospheric flux rate at the time of collection 2005.68 is 1.161 $dpm \cdot cm^{-2} \cdot yr^{-1}$
or 0.523 $pCi \cdot cm^{-2} \cdot yr^{-1}$
Supported ^{226}Ra activity = 2.356 $pCi \cdot g^{-1}$ or 5.230 $dpm \cdot g^{-1}$
Mass Sedimentation Rate = 0.010 $g \cdot cm^{-2} \cdot yr^{-1}$

Summary of 210Pb Analyses						
Mid-Sample Cum Dry Wt g.cm-2	Porosity	Total 210Pb dpm.g-1	Total 210Pb pCi.g-1	Unsupp 210Pb dpm.g-1	Unsupp 210Pb pCi.g-1	Years (*)
0.09	0.9623	80.41	36.221	75.18	33.865	1997
0.19	0.9529	67.92	30.595	62.69	28.239	1986
0.32	0.9472	50.79	22.878	45.56	20.523	1973
0.47	0.9416	38.98	17.559	33.75	15.203	1959
0.61	0.944	21.77	9.806	16.54	7.451	1944
0.74	0.9459	16.97	7.644	11.74	5.288	1931
0.88	0.9477	13.82	6.225	8.59	3.869	1916
1.02	0.9476	8.96	4.036	3.73	1.68	1902

(*) Year calculated using the mass sedimentation rate of the sample.

Appendix E. Lead Sedimentation Rate Analysis, CRS Model.

Uncomp Mid-Pt cm	Cum Dry Wt g.cm-2	Mid Scn Cum Dry Wt g.cm-2	Unsup Activity pCi.g-1	Area pCi.cm-2	Cum Area pCi.cm-2	Time B.P. Years	Cum Avg Mass Sed Rate g.cm-2.yr-1	Date	Mass Sed Rate g.cm-2.yr-1
0.42	0.06	0.03	33.27	0.998	0.998	2.13	0.014	2003	0.014
1.2	0.11	0.09	33.27	1.846	2.844	6.486	0.013	1999	0.013
2.96	0.23	0.19	33.865	3.416	6.26	16.539	0.012	1989	0.011
5.18	0.35	0.32	28.239	3.169	9.43	29.933	0.011	1975	0.01
7.69	0.5	0.47	20.523	2.501	11.93	46.784	0.01	1958	0.008
10.21	0.64	0.61	15.203	1.586	13.516	65.26	0.009	1940	0.008
12.6	0.77	0.74	7.451	0.828	14.344	81.99	0.009	1923	0.008
15.03	0.92	0.88	5.288	0.687	15.031	108.868	0.008	1896	0.006
17.39	1.05	1.02	3.869	0.375	15.406	149.066	0.007	1856	0.003

Based on data from lines 1 to 10
Total Area equals 15.56
Atmospheric flux rate at the time of collection 2005.68 is 0.484 $pCi \cdot cm^{-2} \cdot yr^{-1}$

Appendix F. Mean date calculated for each core slice.

Sample	Uncompacted Mid Depth cm	Cumulative Dry Weight g.cm-2	Cumulative Dry Weight Mid Sample	CIC1 Year	Std Dev +-	CIC2 Year	Std Dev +-	CRS Year	CRS MLR* Year
1	0.42	0.06	0.03	2003	5	2003	6	2003	2005
2	1.2	0.11	0.09	1999	4	1997	5	1999	1998
3	2.01	0.16	0.13	1994	5	1992	5		1994
4	2.96	0.23	0.19	1989	6	1986	7	1989	1987
5	4.05	0.3	0.27	1982	7	1979	7		1980
6	5.18	0.35	0.32	1976	6	1973	5	1975	1975
7	6.39	0.43	0.39	1969	8	1966	8		1968
8	7.69	0.5	0.47	1961	8	1959	7	1958	1959
9	8.94	0.57	0.53	1954	7	1951	7		1952
10	10.21	0.64	0.61	1946	8	1944	7	1940	1942
11	11.43	0.7	0.67	1939	7	1938	6		1933
12	12.6	0.77	0.74	1933	7	1931	7	1923	1922
13	13.82	0.85	0.81	1925	7	1924	8		1909
14	15.03	0.92	0.88	1918	7	1916	7	1896	1894
15	16.21	0.99	0.96	1912	7	1909	7		1874
16	17.39	1.05	1.02	1905	7	1902	6	1856	1857
17	18.56	1.12	1.09	1898	7	1896	7		

*Calculation based on a Multiple Linear Regression with an R^2 of 0.999 and a Standard Error of 2.000.

Appendix G. Focussing factor

		Core 5	**Core 4**
Latitude		48° 00'18"N	48°00'13"N
Longitude		88° 46'22"W	88° 47'40"W
Year		2005	2005
Core diameter		10	6.7
Avg Pb-210 flux	Bq m^{-2} yr^{-1}	172	179
Avg Pb-210 flux	pCi cm^2 yr^{-1}	0.464	0.484
Background Pb-210 flux	Bq m^{-2} yr^{-1}	175	175
Focusing Factor[1]	using avg Pb-210 flux[1]	0.98	1.02
surface Pb-210 flux	pCi cm^2 yr^{-1}	0.69	0.68
Focusing Factor[2]	using surface Pb-210 flux	1.46	1.43

[1]Using average flux for the entire core

[2] FF calculated using surface flux of excess Pb-210

APPENDIX B, PART 2

^{210}Pb Dating of Lakes A and B

A.A. Benson and G.F. Slater

Total ^{210}Pb activity was analyzed at University of Quebec at Montreal via alpha spectroscopy of ^{210}Po. Unsupported ^{210}Pb activity was determined by subtracting the supported ^{210}Pb activity which is produced through geological sources as opposed to atmospheric flux (figure 1). Wet and dry weights, final dates and core uncompaction modeling was done in the same manner as the previous report by Fan Yang in part 1 of this appendix (Tables 1-4).

Constant Initial Concentration model (CIC1)

In the CIC1 model the natural logarithm of the unsupported ^{210}Pb activity is plotted versus uncompacted mid-point depth as determined in core uncompaction (figure 2). In the CIC2 model the natural logarithm of the unsupported ^{210}Pb activity is plotted versus cumulative dry weight as determined by wet and dry weights of the sediment (figure 2). A linear trend line is fit through the two sets of data and the slopes of these lines are used to solve for the following parameters.

For CIC1 (Ln unsupported vs. uncompacted mid point):

Slope $= \lambda / S_o$

Where:

λ = decay constant for ^{210}Pb = 0.0311 yr-1

S_o = Average sedimentation rate (cm yr-1)

For CIC2 (Ln unsupported vs. cumulative dry weight)

Slope = λ / ω

Where:

ω = Mass sedimentation rate (g cm-2 yr-1)

These parameters can be used to calculate the amount of time (t) the sediments have been buried:

For CIC1:

$t = z / S_o$

Where:

z = the uncompacted mid-point depth

For CIC2:

$t = c/\omega$

Where:

c = the cumulative dry weight

Results

The results of the two models agree well with each other and are in fact within the average error of 8 years. Based on the suggestion from Dr. Bassam Ghaleb at University

of Quebec at Montreal, the CIC2 model was used for the final dates because the use of the cumulative dry weight for calculation generally has less inaccuracies as it is directly measured from wet and dry sediment weights whereas uncompacted mid-point depth is modelled using other assumed parameters.

Table 1- Core uncompaction process for Lake A

Sample #	Wet Wt. g	Dry Wt. g	Cumm. Wt g	Cumm. Dry Wt. g/cm2	Water Cont. g or cm3	Sed. Vol. cm3	Total Vol. cm3	Comp Thick. cm	Comp. Depth cm	Comp. Mid-pt cm	Sample Porosity %	Uncomp. Thick cm	Uncomp Depth cm	Uncomp mid-pt cm
0-1	33.8	4.2	44.5	1.3	29.6	1.8	31.4	0.9	0.9	0.4	94.2	0.9	0.9	0.4
1-2	32.9	3.4	47.9	2.6	29.6	1.5	31.0	0.9	1.8	1.3	95.3	0.9	1.8	1.3
2-3	32.0	3.0	50.9	4.1	29.0	1.3	30.3	0.9	2.6	2.2	95.7	0.9	2.7	2.2
3-4	31.7	2.9	53.8	5.6	28.8	1.3	30.0	0.9	3.5	3.1	95.8	0.9	3.5	3.1
4-5	37.4	3.8	57.6	7.2	33.6	1.7	35.3	1.0	4.5	4.0	95.3	1.0	4.5	4.0
5-6	36.3	4.0	61.6	9.0	32.3	1.8	34.0	1.0	5.4	5.0	94.8	1.0	5.5	5.0
6-7	35.7	4.3	65.9	10.8	31.4	1.9	33.2	0.9	6.4	5.9	94.4	0.9	6.5	6.0
7-8	39.5	4.8	70.6	12.8	34.7	2.1	36.8	1.0	7.4	6.9	94.4	1.0	7.5	7.0
8-9	33.6	3.7	74.4	14.9	29.9	1.6	31.5	0.9	8.3	7.9	94.9	0.9	8.4	7.9
9-10	37.5	3.9	78.3	17.2	33.6	1.7	35.3	1.0	9.3	8.8	95.2	1.0	9.4	8.9

Table 2- Summary of core dates

Depth	Total-Supp Ax-A'	Ln(Total-Supp) (Ln(Ax-A')	Cumm. Dry Wt g cm-2	Uncomp Mid cm	Time (B.P) using CIC2	Calendar Year Using CIC2	Time (B.P) Using CIC1	Calendar Year Using CIC1
0.5	13.04	2.57	1.26	0.89	7.67	2000	9.73	1998
1.5	10.15	2.32	2.62	1.78	15.92	1992	19.48	1989
2.5	9.66	2.27	4.06	2.66	24.69	1983	29.04	1979
3.5	8.20	2.10	5.59	3.53	33.96	1974	38.53	1969
4.5	6.19	1.82	7.22	4.54	43.89	1964	49.59	1958
5.5	4.33	1.47	8.97	5.51	54.51	1953	60.21	1948
6.5	2.94	1.08	10.84	6.45	65.87	1942	70.53	1937
7.5	1.48	0.39	12.84	7.50	78.05	1930	81.96	1926
8.5	1.00	0.00	14.95	8.40	90.87	1917	91.81	1916
9.5	0.76	-0.28	17.17	9.41	104.37	1904	102.86	1905

Table 3- Core uncompaction process for Lake B

Sample #	Wet Wt. g	Dry Wt. g	Cumm. Wt g	Cumm. Dry Wt. g/cm2	Water Cont. g or cm3	Sed. Vol. cm3	Total Vol. cm3	Comp Thick. cm	Comp. Depth cm	Comp. Mid-pt cm	Sample Porosity %	Uncomp. Thick cm	Uncomp Depth cm	Uncomp mid-pt cm
0-1	30.47	2.76	44.49	1.26	27.71	1.20	28.91	0.82	0.82	0.41	95.85	0.82	0.82	0.41
1-2	41.60	3.60	48.09	2.63	38.00	1.57	39.57	1.12	1.94	1.38	96.04	1.12	1.94	1.38
2-3	37.61	3.64	51.73	4.09	33.97	1.58	35.55	1.01	2.95	2.45	95.55	1.00	2.94	2.44
3-4	34.93	3.40	55.13	5.66	31.53	1.48	33.01	0.94	3.89	3.42	95.52	0.93	3.87	3.41
4-5	36.71	3.43	58.56	7.32	33.28	1.49	34.77	0.99	4.87	4.38	95.71	0.98	4.86	4.37
5-6	41.55	3.82	62.38	9.09	37.73	1.66	39.39	1.12	5.99	5.43	95.78	1.11	5.97	5.41

Table 4- Core dating summary

Depth	Total-Supp Ax-A'	Ln(Total-Su (Ln(Ax-A')	Cumm. Dry Wt g cm-2	Uncomp Mid cm	Time (B.P) using CIC2	Calendar Year Using CIC2	Time (B.P) Using CIC1	Calendar Year Using CIC1
0.5	19.04	2.95	1.26	0.41	15.31	1993	7.89	2000
1.5	6.99	1.94	2.63	1.38	31.86	1976	26.62	1981
2.5	3.13	1.14	4.09	2.44	49.67	1958	47.13	1961
3.5	1.32	0.27	5.66	3.41	68.64	1939	65.80	1942
4.5	1.14	0.13	7.32	4.37	88.80	1919	84.27	1924
5.5	1.01	0.01	9.09	5.41	110.27	1898	104.51	1903